NUTRIENT SEPARATION, ENERGY RECOVERY AND WATER REUSE

SUSTAINABLE WASTEWATER TREATMENT: NUTRIENT SEPARATION, ENERGY RECOVERY AND WATER REUSE

By

RYAN C. TICE, B.Eng.

A Thesis

Submitted to the School of Graduate Studies

in Partial Fulfillment of the Requirements

for the Degree

Master of Applied Science

McMaster University

MASTER OF APPLIED SCIENCE (2014) McMaster University

(Civil Engineering) Hamilton, Ontario

TITLE: Sustainable Wastewater Treatment: Nutrient Separation, Energy Recovery and Water Reuse

AUTHOR: Tice, R.C. (McMaster University)

SUPERVISOR: Dr. Younggy Kim

NUMBER OF PAGES: xiv, 118

Abstract

There is a growing awareness of the valuable nutrients (nitrogen and phosphorus) being lost in conventional wastewater treatment systems. Although the removal of these nutrients has been well addressed, efforts for nutrient recovery have seen little development. As the emphasis on sustainability in the wastewater treatment industry increases, conventional wastewater treatment processes are being re-evaluated and new treatment systems developed. A possible nutrient recovery mechanism is the precipitation of magnesium ammonium phosphate hexahydrate ($MgNH_4PO_4 \cdot 6H_2O$), commonly known as struvite. Human urine has been identified as a rich source of nutrients in wastewater; hence the separate collection of urine is considered a viable method of enabling struvite recovery. Since dilution of urine to a certain degree is inevitable, reconcentration of urine beyond the solubility limit of struvite is critical. Currently available methods for reconcentration (e.g., evaporation, freeze-thaw, reverse osmosis and electrodialysis) are relatively expensive with high energy demand. Thus, the research here aims to demonstrate nutrient reconcentration from diluted urine and simultaneous organic removal by using the principles of microbial desalination cells (MDCs), where energy released from organic oxidation is partially used for the separation of nutrient ions. With reduced energy demand, a sustainable method for the utilization of source-separated urine is examined. The performance of bioelectrochemical systems relies on the activity of exoelectrogenic bacteria to transfer electrons to the anode. An examination of exoelectrogen sensitivity at various wastewater treatment conditions (i.e. ammonia and oxygen) is an important component of this research. Methanogenesis is considered the greatest challenge in achieving practical applications in anaerobic bioelectrochemical systems. An electrolytic oxygen production method is suggested for effective control of methanogenesis in a feasible and cost-effective manner.

Acknowledgements

I would like to sincerely thank my parents for their unwavering love and support for me to chase after my dreams. Their unconditional belief in me and timely encouragement make even the toughest challenges conquerable.

I would also like to express my special appreciation and thanks to my supervisor, Dr. Younggy Kim for his endless support and guidance throughout my master's degree. He helped me realize the power of critical reasoning and demonstrated what a brilliant and hard-working researcher can accomplish. I am grateful for my examination committee members, Dr. Sarah Dickson and Dr. Carlos Filipe. They generously gave their time to offer me valuable comments towards improving my work. Special thanks must go to Anna Robertson, for not only showing me the benefits of pursuing a master's degree, but also for being an expert and a continual source of knowledge in the lab. And to Peter Koudys, thanks for all the help constructing and customizing reactors.

Finally, I would like to thank my dearest friends and officemates, Teri Lubianetzky and Ahmed El Ganzouri. They say your real friends aren't the ones you spend the most time with, but the ones you share the most memories with. We had some great memories together and I will miss working with both of you!

Table of Contents

Table of Figures

Table of Tables

Nomenclature

Abbreviations

AEM	anion exchange membrane
AES	air evaporation system
CE	Coulombic efficiency
CEM	cation exchange membrane
COD	chemical oxygen demand
EDS	energy dispersive X-ray spectroscopy
GC	gas chromatography
HALC	high acetate long cycle
HASC	high acetate short cycle
IEM	ion exchange membrane
LASC	low acetate short cycle
MDC	microbial desalination cell
MEC	microbial electrolysis cell
MFC	microbial fuel cell
NSMEC	nutrient separation microbial electrolysis cell
SEM	scanning electron microscopy
SRT	sludge retention time
TAN	total ammonia nitrogen
TIMES	thermoelectric integrated membrane evaporation system
VCD	vapour compression distillation

VSS	volatile suspended solids

Symbols

b	specific microorganism decay rate (d^{-1})
D	diffusivity ($m^2 \cdot s^{-1}$)
E_{ap}	applied electric voltage to NSMEC (V)
F	Faraday constant (96,485 $C \cdot mol^{-1}$)
i	electric current (A)
K_s	half saturation constant (mg $COD \cdot L^{-1}$)
K_{so}	conditional solubility product (-)
K_{sp}	solubility product (-)
μ_{max}	maximum specific growth rate (d^{-1})
n_{O2}	molar amount of O_2 collected (mol)
n_t	molar amount of O_2 produced from water electrolysis (mol)
P	power density ($W \cdot cm^{-2}$)
R	Gas constant (8.314 $J \cdot mol^{-1} \cdot K^{-1}$)
r_{O2}	oxygen recovery (-)
S	substrate concentration (mg $COD \cdot L^{-1}$)
V	volume of solution (L)
$V_{D/C}$	ratio between the diluate and concentrate volumes (-)
Λ	equivalent ionic conductivity ($m^2 \cdot S \cdot mol^{-1}$)
X	methanogen population concentration (mg $COD \cdot L^{-1}$)
z	ionic charge (-)

Subscripts

C	concentrate (solution that gets concentrated in NSMEC)
D	diluate (solution that gets diluted in NSMEC)

Declaration of Academic Achievement

This dissertation consists of previously prepared material that is either published or is currently under review for publication in peer-reviewed scientific journals. The author of this dissertation is the primary author on each of these articles. As the primary author, contributions included: experimental design, literature review, collection and analysis of data, and manuscript preparation. The thesis supervisor is the second author on each of these articles. He offered input and expertise during each phase of the research process and manuscript preparation. Chapter 3 has been submitted to the journal *Water Research* and is currently under review. Chapter 4 is in the submission process to the *Journal of Power Sources*. Chapter 5 has been accepted for publication in the *International Journal of Hydrogen Energy*.

Chapter 1: Introduction

1.1 Research background

In wastewater treatment, there is a growing awareness of the valuable nutrients (i.e. nitrogen and phosphorus) being lost in treatment systems. The removal of these nutrients has been well addressed, largely due to the water quality concerns of discharging nutrient rich effluent into natural water systems. However, there has been little development on efforts to recover these nutrients since conventional wastewater treatment techniques leave little opportunity for effective nutrient recovery. As sustainability is emphasized in the wastewater treatment industry, conventional wastewater treatment techniques are being re-evaluated and new methods developed.

Phosphorus is considered an essential nutrient for life, but it exists at relatively low concentrations within the Earth's crust [1]. It is projected that peak phosphorus production from mining will occur in 2030 [2]. As world reserves of phosphorus diminish, sustainable methods for phosphorus production must be developed. One such renewable source of phosphate is magnesium ammonium phosphate hexahydrate ($MgNH_4PO_4 \cdot 6H_2O$), commonly known as struvite. Struvite can be produced from inorganics in nutrient rich animal and domestic wastewaters. Human urine is a particularly rich source of nutrients; thus, separate collection of urine has been identified as a feasible method of enabling struvite recovery and decreasing the nutrient load to municipal wastewater treatment

facilities [3], [4]. However, some dilution of urine is inevitable, as the dilution of urine below the struvite solubility limit is required to prevent potential clogging problems in collection systems. Currently available methods for reconcentration (e.g., evaporation, freeze-thaw, reverse osmosis and electrodialysis) are relatively expensive with intensive energy demand [3]. Thus, this study aims to demonstrate nutrient reconcentration from diluted urine and simultaneous organic removal by using the principle of microbial desalination cells (MDCs), where energy released from organic oxidation is partially used for the separation of nutrient ions from diluted urine. With reduced energy demand, a sustainable method for the utilization of source-separated urine can be established.

A microbial electrolysis cell (MEC) is an electrically driven hydrogen evolution process (Fig. 1.1) [5]. In MECs, organic substrate is oxidized to CO_2 at the bioanode. The oxidation reaction is driven by exoelectrogenic bacteria, which have the unique ability to transfer electrons extracellularly to the anode. The anode provides a surface for exoelectrogenic bacteria to adhere and transfer electrons creating electric current. Water is reduced to H_2 in water electrolysis at the cathode with a small external voltage application ($E_{ap} > 0.14$) [5]–[8]. The produced H_2 gas can be recovered and offers an avenue for energy production.

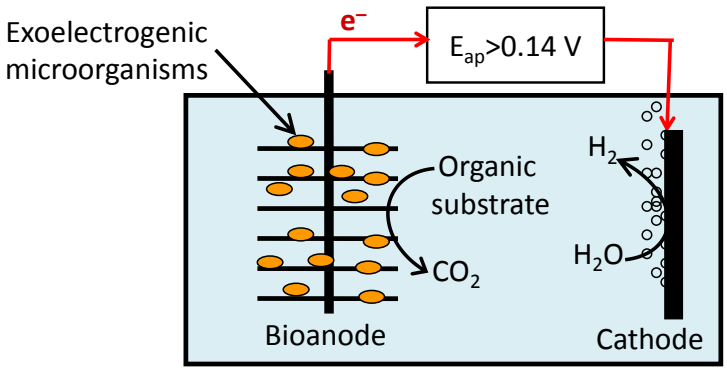

Figure 1.1: Conventional microbial electrolysis cell design

The coupled electrode reactions create an electric field that induces ionic transport between the electrodes. Therefore, energy efficient nutrient reconcentration can be achieved as the oxidation of organic substrates at the anode partially contributes energy required for ionic separation through ion exchange membranes (IEMs). This design principle was originally adopted from microbial desalination cells (MDCs) for desalination of seawater and brackish water [9]. However, no previous studies have applied the principle of MDCs in reconcentrating nutrient ions from diluted human urine. One of the important differences of this application with diluted urine from MDCs is the urine composition. The high concentration of organic substrates and sulfate ions in urine induces substantial sulfate reducing bacteria activity. In addition, MDCs do not have specific target ions for separation, while in diluted urine the target ions for reconcentration are restricted to only NH_4^+ and HPO_4^{2-}. Thus, unlike previous MDC studies, competitive separation of nutrient ions vs. other common ions (e.g., Na^+, Cl^-, SO_4^{2-}) is an important aspect of this study.

One of the primary concerns with treating human urine using bioelectrochemical systems is the effect of high ammonium concentrations on the exoelectrogenic bacteria. The electricity generated from these systems, as well as the electric field in the reactor relies on exoelectrogenic bacteria that form a biofilm on the anode. The performance of bioelectrochemical systems as a wastewater treatment and energy recovery process centers on the activity of exoelectrogenic bacteria to transfer electrons to the anode; hence, the sensitivity of exoelectrogenic bacteria to high ammonia concentration needs to be investigated.

Methanogenesis is one of the greatest challenges in achieving practical applications of the MEC technology in wastewater treatment and H_2 production. Hydrogenotrophic methanogens consume H_2 gas from the cathode and produce methane. Methane production consequently reduces H_2 purities and severely decreases H_2 yield from MECs. For effective control of methanogenesis in a feasible and cost-efficient manner, an electrolytic O_2-production method is suggested in this research. In this method, pure electrolytic O_2 gas is produced intermittently. Even though the effectiveness of O_2 in methane control has been reported in previous studies [10]–[13], the frequency with which O_2 treatment needs to be provided has not been clearly confirmed. The frequency of O_2 treatment is important because hydrogenotrophic methanogens can grow rapidly, requiring only ~12 hours to initiate active methanogenesis [14]. In addition, there are no quantified criteria on how much O_2 should be provided for effective control

of methane. Thus, a clear guideline on the amount of O_2 supply is necessary because excessive O_2 can weaken the exoelectrogenic bacteria present on bioanodes.

1.2 Research objectives

The broad research goal of this study is to develop an energy efficient nutrient reconcentration method that enables the effective recovery of nutrients while simultaneously removing organic substrates present in wastewater. Since the activity of exoelectrogenic bacteria is critical to the performance of bioelectrochemical systems, various wastewater conditions such as threshold levels of ammonia inhibition and the effects of methanogenesis were investigated. Therefore the detailed research objectives are to:

1) Demonstrate energy efficient reconcentration of nutrients from 1:10 diluted hydrolyzed urine using an IEM stack in an MEC;
2) Determine the rate of nutrient reconcentration as a function of the IEM stack size and applied potential (E_{ap});
3) Investigate the competitive separation of the target nutrient ions (NH_4^+ and HPO_4^{2-}) with other common ions in human urine (Na^+, Cl^-, SO_4^{2-});
4) Examine the volume ratio between the diluate (urine solution losing ions through IEMs) and the concentrate (urine solution collecting ions from the diluate); and
5) Investigate the effects of sulfate reducing bacteria on nutrient reconcentration, organic removal and energy recovery.

To investigate the effects of ammonia inhibition in MFCs, this study also aims to:

1) Investigate the effect of initial substrate concentration on the threshold level of ammonia inhibition; and
2) Examine the frequency of substrate feed on the capability of exoelectrogenic bacteria to continue to create electric current under high ammonia conditions.

To establish O_2 treatment as a cost-effective and practically available method for high purity H_2 production in MECs, this study aims to:

1) Examine the electrolytic O_2 production method for methane control;
2) Suggest the optimal frequency of O_2 treatment;
3) Find the minimal amount of O_2 that can effectively limit methanogenesis; and
4) Quantify the adverse effect of O_2 treatment on the exoelectrogenic activity of bioanodes.

1.3 Approach

An extensive literature review was performed and is summarized in Chapter 2 to fully understand each of the research topics and verify assumptions made in this study. Chapter 3 is dedicated to demonstrating the energy efficient nutrient reconcentration from diluted urine through the use of microbial electrolysis cells and ion exchange membranes. Chapter 4 focuses on the ammonia inhibition to exoelectrogenic bacteria under various substrate feed

conditions. Since the reconcentration of nitrogen is in the form of ammonium it is important not to exceed the threshold level for ammonia inhibition. Chapter 5 addresses the methanogenesis problem in potential MEC applications in wastewater treatment; in addition, a new methane control method based on intermittent pure O_2 generation was investigated.

Chapter 2: Literature Review

Bioelectrochemical systems offer a potential method for sustainable wastewater treatment and simultaneous energy production. Different configurations of bioelectrochemical systems have been investigated in literature, contributing to the continual development of these systems. The energy efficient design of the microbial electrolysis cell (MEC) can be reconfigured to enable the removal of soluble organics and the effective recovery of nutrients (nitrogen and phosphorus) from diluted urine. Using the principles of microbial desalination cells (MDCs), the energy released from organic oxidation can be used for the separation of nutrient ions.

In this literature review, conventional nutrient removal processes are discussed primarily from an energy consumption perspective. The concept of source-separated urine is introduced, outlining both the benefits and challenges associated with keeping urine as a separate waste stream from municipal wastewater. Since a certain degree of dilution of urine is inevitably required to prevent clogging problems in collection systems, subsequent reconcentration (or volume reduction) is important to enable nutrient recovery. Different volume reduction technologies suitable for reconcentrating urine are discussed in this chapter. Lastly, bioelectrochemical systems are discussed and the main nutrient recovery mechanism (struvite precipitation) is examined.

One potential challenge of the application of bioelectrochemical systems for source-separated urine treatment is the inhibition effects from high ammonium

concentrations on the exoelectrogenic bacteria. The electric energy generated in bioelectrochemical systems, as well as the electric field in the reactor relies on the activity of exoelectrogenic bacteria that form a biofilm on the anode. Threshold ammonia levels that trigger inhibition effects in bioelectrochemical systems are examined in this literature review.

Lastly, methanogenesis is often considered as the major challenge in achieving practical applications of MECs in wastewater treatment. Methane production and consequent reduction in H_2 purities have been addressed as a potential limitation of MEC applications in a number of research studies. A literature review is provided for the different methods to control methanogenesis in MECs.

2.1 Energy efficient nutrient separation

2.1.1 Nutrient recovery in wastewater

Human urine is known to contribute 80% of the nitrogen (N) and 50% of the phosphorus (P) in domestic wastewater [3], [4]. Nitrogen compounds in domestic wastewater typically include organic nitrogen (8-25 mg-N·L^{-1}) and ammonia (NH_3-N) (12-45 mg-N·L^{-1}), while phosphorus is generally in the form of organic phosphorus (1-4 mg-P·L^{-1}) or phosphate (PO_4-P) (3-8 mg-P·L^{-1}) [15]. The need for nutrient removal arises from three main water quality concerns: (1) the toxicity effects of ammonia, (2) the control of eutrophication, and (3) the need for nitrogen control in water reclamation (i.e. groundwater recharge) [15]. The

strict requirements for nutrient levels in wastewater effluent have resulted in the implementation of several nutrient removal processes in wastewater treatment.

In municipal wastewater treatment, high nutrient levels require relatively expensive nutrient removal processes. In biological nitrification, long sludge retention times (SRT > 10 d) are necessary in activated sludge, where ammonia is oxidized in a two-step process by aerobic autotrophic bacteria and converted into nitrate. Such long SRT conditions result in the consumption of additional electric energy for return sludge and aeration. Similarly, biological denitrification (the conversion of nitrate to N_2 gas) and phosphorus removal (using phosphorus accumulating organisms) also necessitate large volume reactors to establish anoxic and anaerobic conditions and a large pumping capacity for internal recycle of wastewater. The removal of phosphorus can also be achieved by precipitation, although it is costly as it requires an extra cost for ferric or aluminum chemicals. Although these conventional nutrient removal processes can achieve sufficiently good effluent quality, there is little opportunity for effective resource recovery. Since the nutrients in wastewater are the components necessary for plant growth, nutrient recovery can be beneficial for agricultural applications (i.e. fertilizers).

2.1.2 Source-separated urine

The concept of separate collection and treatment of urine has received considerable attention in recent years and is seen as a viable option to increase the flexibility of centralized wastewater treatment facilities. The extra costs for nutrient removal can be greatly reduced or even eliminated in wastewater

treatment if human urine is separated at the source level [3]. The concept of source-separated urine entails the immediate separation of urine (yellow water) from fecal (brownwater) and other wastewater (greywater). Separation can be achieved through waterless urinals or urine separating (NoMix) flush toilets which were invented in Sweden in the 1990's [4]. These toilets are primarily used in pilot projects, although some Swedish municipalities have adopted them for broader applications [16]. The guiding momentum behind source separation of urine is resource efficiency. It is much more resource efficient to treat concentrated and unmixed solutions than substantially diluted and combined solutions [4]. The high nutrient concentration in source separated urine enables effective recovery of nutrients as valuable raw materials, e.g., struvite ($MgNH_4PO_4$) and gaseous ammonia (NH_3) in addition to the separation of micropollutants, which are relatively dilute in human urine [17]–[19].

Source separation favours on-site technologies for treatment from a practicality perspective. Centralized treatment is technically feasible, but the separation of waste streams requires a separate collection system, which is expensive to implement. Regardless of whether treatment occurs centrally or on-site, several key challenges exist for practical recoveries of nutrients from source-separated urine. One significant challenge is the dilution with large amounts of flushing water at urinals and toilets, substantially decreasing nutrient concentration. Even though specialized urinals or toilets have been suggested and developed to minimize the amount of flushing water, a certain degree of dilution

is still necessary to prevent precipitation and clogging problems in collection systems. Rapid hydrolysis of urea ($[NH_2]_2CO$) substantially increases pH. High pH conditions induce precipitation of insoluble struvite salts on the surface of collection pipes [18], [19]. Therefore, source separated urine should be diluted below the solubility limit of struvite (or other minerals) for sustainable maintenance of urine collection systems.

2.1.3 Volume reduction methods

For effective nutrient recovery, the diluted urine must be reconcentrated once it has been transported (i.e. to a centralized treatment facility, or an on-site collection system). Even if source-separated urine can be directly used as a liquid fertilizer, a reconcentration step will substantially reduce required liquid volume for land applications. Reconcentration or separation of nutrients from human urine can be achieved by various treatment processes, such as evaporation, freeze-thaw, reverse osmosis and electrodialysis previously demonstrated in literature [3], [20].

Evaporation is a straightforward method of removing water from urine [3]. There are a number of approaches reported in literature such as vapour compression distillation (VCD), thermoelectric integrated membrane evaporation systems (TIMES), air evaporation systems (AES), and lyophilization [21], [22]. Evaporation technologies have been used in space applications to recycle water to the best possible quality. VCD has been installed on the international space station as a unit for processing urine [3], [21]. Although evaporation methods can recover more than 96% of the water content, two of the major challenges faced are the

loss of ammonia and the energy consumption. Evaporation methods can have energy requirements between 400 and 2,600 $MJ \cdot m^{-3}$ depending on the efficiency of heat exchange systems [23].

Freeze-thaw was also demonstrated as a method for urine reconcentration [24]. By freezing urine at -14 °C approximately 80% of the nutrients can be concentrated with a volume reduction of 25% of the original volume. The energy requirement is relatively high for the freeze-thaw method; approximately 1,100 $MJ \cdot m^{-3}$ for a five-fold volume reduction [25].

The reconcentration of nutrient ions (NH_4^+ and HPO_4^{2-}) can also be achieved using reverse osmosis, although the membrane filtration performance strongly depends on pH. Studies have shown urine reconcentration by a factor of 5 at a pressure of 50 kPa [26]. It was found that reverse osmosis membranes also have a high retention for micropollutants [27]. The energy consumption can be high, but largely depends on the operational and technical parameters. Energy recovery systems, such as pressure exchangers, can be implemented to help reduce the energy consumption. The greatest limiting factor of reverse osmosis for urine reconcentration is the severe scaling problems that occur on the membrane surface due to the high salt content in urine [3]. Antiscalents can be applied; however, antiscalent applications limit struvite recovery in the following precipitation steps [3], [28]–[30].

Electrodialysis was also examined for nutrient reconcentration and micro-pollutant removal [20]. In continuously operated processes, nutrients can be

concentrated up to a factor of 3.2 [20]. Electrodialysis has also been proven very successful for separating micro-pollutants from human urine. However, similar to reverse osmosis, electrodialysis has intensive energy requirements for the separation of ionic compounds [31], requiring high energy demand for the reconcentration of diluted urine.

2.1.4 Microbial electrolysis cells for nutrient separation

The technologies currently available for reconcentration of diluted urine require relatively high energy consumption. Bioelectrochemical systems offer a potential method for energy efficient reconcentration of nutrients from diluted urine using energy released from the oxidation of organic substrates in MECs. The MEC is an emerging technology and can be used to treat wastewater and simultaneously recover energy as hydrogen gas (H_2) [6]–[8]. In an MEC, exoelectrogenic bacteria oxidize soluble organic matter and transfer electrons to the anode. At the cathode, hydrogen gas is produced through the reduction of water. To drive the redox reactions at MEC electrodes (i.e., oxidation of organics and reduction of water), a small amount of electric potential needs to be applied (>0.14 V) [5], [6], [8]. This energy requirement is substantially small compared to the minimum threshold voltage of 1.23 V for conventional water electrolysis. With the low energy requirement, the energy recovered as hydrogen gas in a well-controlled MEC is substantially high, up to 2-4 times the electric energy provided [10], [32], [33].

Nutrients in hydrolyzed urine are present as ions (NH_4^+ and HPO_4^{2-}). Therefore, ion exchange membranes (IEMs) can be used to reconcentrate these ions. Ion exchange membranes are mechanically reinforced sheets of ion exchange resin that have immobile charges. For instance, cation exchange membranes (CEMs) have a high concentration of fixed anionic groups (e.g., amines) and anion exchange membranes (AEMs) cationic groups (e.g., sulfonates) [34]. Under the influence of an applied electrical field, cations are free to pass through CEMs as highly concentrated fixed anions reject anions. Similarly, AEMs allow only anionic transport. By schematically placing IEMs between the electrodes in an MEC, nutrient ions (NH_4^+ and HPO_4^{2-}) can be reconcentrated from diluted urine. This design principle was originally adopted from MDCs for desalination of seawater and brackish water [9]. None of the previous studies in literature have applied the principle of MDCs in reconcentrating nutrient ions from diluted human urine. One of the important differences of this application with diluted urine from MDCs is the urine composition. High concentrations of organic substrates and sulfate ions can activate sulfate reducing bacteria. Also, organic substrate removal is simultaneously achieved with nutrient reconcentration with the same urine solution, requiring a different urine flow configuration from the previous stacked MDC designs [35], [36]. In addition, the target ions for reconcentration are restricted to only NH_4^+ and HPO_4^{2-} from diluted urine, while MDCs do not have specific target ions for separation. Thus, unlike

previous MDC studies, competitive separation of nutrient ions vs. other common ions (e.g., Na^+, Cl^-, SO_4^{2-}) is an important aspect to consider.

2.1.5 Struvite formation

A well-known precipitate in wastewater treatment is magnesium ammonium phosphate ($MgNH_4PO_4 \cdot 6H_2O$), commonly known as struvite. It is well known for causing issues on equipment surfaces, particularly within pipes, fouling pumps, aerators, screens and other equipment in anaerobic digestion and post-digestion processes. Dissolution of scaled struvite is difficult and often impractical, significantly increasing costs of labor, materials, and system downtime [37], [38]. Prediction of struvite precipitation potential has been critical for designers and operators to avoid and mitigate such scaling problems [38]. Therefore, many studies have been devoted to developing methods to predict precipitation potential [39]–[45].

Although struvite is often seen as a problem in wastewater treatment plants, it is possible to optimize the conditions and exploit this precipitation for nutrient recovery and use as a commercial product [46]–[49]. Consequently, this has caused a shift to investigating conditions where struvite precipitation is promoted and optimized. The recovery of struvite is attractive because it can be used as a high quality slow release fertilizer [46], [50]. Many researchers have examined struvite formation in waste streams [37], [42], [51]–[55]. Struvite forms according to the following reaction [56]:

$$Mg^{2+} + NH_4^+ + PO_4^{3-} + 6H_2O \rightleftharpoons Mg\,NH_4PO_4 \cdot 6H_2O \qquad (2.1)$$

The major governing factors in struvite precipitation are pH, degree of supersaturation, temperature and the presence of other ions (i.e. calcium) in solution [37], [57]. A great deal of effort has been made to determine the solubility product, K_{sp}. If the ionic strength and ion activity are taken into account the value is expressed as a conditional solubility product (K_{so}) and is solution specific [58]. A summary of K_{sp} values found in literature is provided in Table 2.1:

Table 2.1: Solubility products for struvite formation (adapted from [37], [56])

K_{sp}	*pK_{sp}*	*References*
3.98×10^{-10}	9.4	[59]
1.15×10^{-10}	9.94	[60]
4.36×10^{-13}	12.36	[61], [62]
4.36×10^{-13}	12.6	[40]
2.51×10^{-13}	12.6	[39]
2.51×10^{-13}	12.6	[44]
1.15×10^{-13}	12.94	[51]
1×10^{-13}	13.0	[45]
7.58×10^{-14}	13.12	[42]
7.08×10^{-14}	13.15	[41]
5.50×10^{-14}	13.26	[38]

The speciation of constituent ions is also highly dependent on pH levels. It is unlikely for the total individual concentrations of magnesium, ammonium and phosphate to be fully available for struvite formation. Therefore, the total concentration of individual ions may not give an accurate indication of the solubility of struvite in solution [38]. Different methods for calculating K_{so} have all shown a similar dependence on pH [38], [63], [64]. In general, the conditional solubility product of struvite decreases with increasing pH. The typical pH range that enhances struvite precipitation is between 7 and 11. However, at pH greater

than 9 the solubility of struvite begins to increase again, due to the decrease in ammonium ion concentration [65]. The pH values in different studies at which the solubility of struvite is at a minimum are reported in Table 2.2:

Table 2.2: pH values for minimum struvite solubility (adapted from [37])

pH values	*References*
8.0-10.6	[66]
9.0	[61], [62]
9-9.4	[65]
10.3	[38], [43]
10.7	[39], [40]

The influence of temperature on struvite precipitation has also been studied. Aage et al. (1997) determined the struvite solubility product at various temperatures [51]. Likewise, Burns and Finlayson (1982) investigated the influence of temperature on the solubility product [42]. Aage et al. (1997) found increased solubility over the temperature range of 10 to 65 °C. The maximum solubility was found at 50 °C. At temperatures above 64 °C the solubility began to decrease. Under such a high temperature, the structure of the struvite crystal changes, affecting the solubility [51].

The interaction of other ions in solution can also affect struvite formation. This is especially pertinent for wastewater treatment where various ionic compounds are present (i.e. potassium, chloride, calcium, carbonates, zinc). These compounds can perturb, be absorbed on crystal surfaces, and retard struvite formation [67]. Depending on the concentration levels of calcium and magnesium, struvite formation can be limited due to the formation of calcium phosphates [52], [66], [68]. The precipitation of calcium apatite occurs at pH 9.5, whereas effective

struvite precipitation begins at 8.0. Therefore, by controlling pH and Mg:Ca ratios preferential precipitation of struvite can be achieved [69]. However, calcium ions can also affect struvite nucleation and growth particularly at high calcium concentrations. A similar effect on struvite precipitation was reported for carbonate species. It has been shown that both calcium and carbonate can lengthen the induction time delaying initial crystal growth and thus negatively affecting the crystal growth rate. Interference with the crystallization of struvite formation itself is also likely, but this interference effect has not been assessed [67].

Le Corre et al. (2005) found that increasing magnesium concentration led to an increase in pH and a reduction in induction time. There was no difference in crystal purity, but the morphology of the crystals was influenced by the initial magnesium concentration. The typical orthorhombic shaped crystals were observed more frequently at elevated magnesium concentrations and the crystals were consistently larger. The addition of calcium ions in solution had a significant impact on the size, shape, and purity of the produced crystals. Le Corre et al. (2005) found that elevated calcium concentrations reduce the crystal size and limit the struvite crystal growth. The formation of an amorphous substance rather than crystalline struvite was observed with high calcium concentration [67].

The effect of citrate and phosphocitrate ions on struvite kinetics and crystal morphology has also been investigated [70]. Kofina et al. (2007) found that both citrate and phosphocitrate are effective inhibitors of struvite

precipitation in synthetic wastewater supersaturated solutions. In the presence of 1 μM citrate, the induction times preceding struvite precipitation increased. At the same concentration no effect on the induction time was observed for phosphocitrate. The rate of struvite precipitation decreased in the presence of both additives. The struvite precipitation rates continuously decreased between the concentration range of 1 and 10 μM for phosphocitrate. In the case of citrate, a plateau was observed for the struvite precipitation rate at a concentration of 5 μM, after which the rate remained constant for increasing citrate levels. There were no distinguishable differences in crystal morphologies between wastewater solutions with and without the additives. However, the crystals were smaller in size, typically shorter and wider with the presence of citrate [70].

2.2 Ammonia inhibition in bioelectrochemical systems

The performance of bioelectrochemical systems for wastewater treatment and energy recovery centers on the activity of exoelectrogenic bacteria that transfer electrons to the anode. Hence, the sensitivity of exoelectrogenic bacteria to various wastewater treatment conditions (e.g., ammonia, salinity, oxygen, etc.) needs to be investigated. This study focused mainly on the sensitivity of exoelectrogenic bacteria to high ammonia conditions.

2.2.1 Microbial fuel cells

Microbial fuel cells (MFCs) are a type of bioelectrochemical system that can remove organics from wastewater and simultaneously produce electrical energy. Recent developments in MFC design (e.g., air cathodes [71]; sandwiched

electrode assemblies [72]; inexpensive cathode catalysts [73]) along with pilot-scale demonstrations [74]–[77], make MFCs an attractive alternative for sustainable wastewater treatment and energy recovery [78]. Similar to MECs, electric energy generation in MFCs relies on electrochemically active bacteria that form a biofilm on the anode. The exoelectrogenic bacteria oxidize organic substrates present in wastewater and transfer electrons to the anode, creating electric current. At the cathode of MFCs, water is formed through the reduction of oxygen that can be provided directly from the atmosphere using air cathodes [79].

Recent studies have examined MFC performance with various sources of wastewater, including swine wastewater, anaerobic digester supernatant and human urine [17], [80], [81]. These high strength wastewaters contain excessive amounts of ammonia that can inhibit microbial metabolism and thus limit electric current generation from exoelectrogenic bacteria in MFCs.

2.2.2 Ammonia inhibition

Ammonia is well known for its cytotoxic effects on microorganisms [82], [83]. Specifically, ammonia inhibition mechanisms include enzymatic activity disruption, alteration in the intracellular pH and dehydration due to osmotic stress [84]–[86]. Previous experimental studies consistently demonstrated negative responses of MFC bioanodes to high total ammonia nitrogen (TAN) levels beyond 4,000 mg-N·L^{-1} [87]–[89]. However, the previous studies showed inconsistent results on threshold TAN levels that trigger the ammonia inhibition effects in bioelectrochemical systems. Nam et al. (2010) reported that TAN concentrations

exceeding 500 mg-N·L^{-1} at a neutral pH of 7 can result in severe inhibition of electricity generation in single-chamber MFCs, implying a relatively low ammonia concentration triggers limited performance of bioanodes [87]. In another study using a continuously operated MFC, electric current generation gradually increased with increasing TAN concentration up to 3,500 mg-N·L^{-1} [88]. Likewise, a study by Kuntke et al. (2011) found no cytotoxic effects of ammonia up to 4,000 mg-N·L^{-1} [89]. It should be noted that experiments in these previous studies were performed under neutral pH conditions using phosphate buffer, indicating that equilibrium between free ammonia (NH_3) and ammonium ions (NH_4^+) did not affect the degree of ammonia inhibition, as free ammonia is known to be more toxic to microorganisms than ammonium ions in biological wastewater treatment [14], [83].

2.3 Methanogen control in bioelectrochemical systems

Methanogenesis is considered as the major challenge in achieving practical applications of MECs in wastewater treatment. The growth conditions for exoelectrogenic bacteria are also ideal for methanogens and consequently methane production is commonly observed in MEC-based studies [11]. However, methanogens are highly sensitive to environmental conditions and thus, previous studies have investigated possible methods to suppress methanogenesis. These methods includes exposure to air, heat treatment, acid/base treatment, and chemical inhibitors [10]–[13], [90]–[92].

A recent pilot-scale experiment confirmed that methanogenesis is a limiting factor for practical H_2 production from wastewater using MECs [93]. While a lab-scale reactor achieved high hydrogen recovery (70% H_2 gas by composition) [94], the pilot-scale system rapidly produced methane after only 14 days of operation. Methanogenesis can be controlled in laboratory experiments by using 2-bromoethanesulfonate or chloroform [95]–[98]. However, these chemicals cannot be applied in practical wastewater treatment due to their toxic effects and high costs.

While methanogenic activities are known to decrease under low pH conditions in fermentation processes [97], mildly acidified solutions (pH ~5-6) in single chamber MECs were not effective in controlling methanogenesis in MECs [10], [11]. The methane concentration detected with a medium fixed at pH 5.8 was comparable to that at pH 7 after only three batch cycles [10].

In dark fermentation, methanogens are completely inactivated during initial heat treatment (e.g., 100 °C for 10 min) while H_2–producing and spore-forming fermenters survive such harsh conditions [92], [99]. Similar heat treatment (100 °C for 15 min) was employed in MEC operation for the control of methanogens; however, exoelectrogenic bacteria could not survive the high temperature as they are not spore-forming microorganisms [10]. In addition, such heat treatment cannot be a sustainable method for practical wastewater treatment due to substantial heat energy requirement. Operation of bioelectrochemical

systems at relatively low temperatures (e.g., 15 °C) was also proven to be ineffective for methane control [11].

All methanogens are strict anaerobes [100]; thus, the methanogenic activity can be controlled through regular O_2 treatment during MEC operation. When MEC cathodes were exposed to the air for 15 min, methane production was effectively controlled over 120 hours [10]. However, the air exposure method was not effective with bioanodes, as short-term exposure (30 min or less) could not inactivate methanogens on bioanodes [11]. Effective inactivation was only achieved for a substantially extended exposure of bioanodes in the air (24 hr) [13]. These results in the previous studies imply that the air exposure method does not have immediate influence in methane control. In another study, a relatively short-term exposure of bioanodes to air (30-50 min) was followed by a brief aeration step (3-5 min) [11], [12]. Methane production was substantially reduced, indicating that aeration is effective for methane control. However, in practical MEC applications, the construction and operation of aeration systems will require extra costs, making the MEC technology a less sustainable and less energy-efficient alternative for wastewater treatment.

Chapter 3: Energy efficient reconcentration of diluted human urine using ion exchange membranes in bioelectrochemical systems[1]

Abstract

Nutrients can be recovered from source separated human urine; however, nutrient reconcentration (i.e., volume reduction of collected urine) requires energy-intensive treatment processes, making it practically difficult to utilize human urine. In this study, energy efficient nutrient reconcentration was demonstrated using ion exchange membranes (IEMs) in a microbial electrolysis cell (MEC) where substrate oxidation at the MEC anode provides energy for the separation of nutrient ions (e.g., NH_4^+, HPO_4^{2-}). The rate of nutrient separation was magnified with increasing number of IEM pairs and electric voltage application (E_{ap}). Ammonia and phosphate were reconcentrated from diluted human urine by a factor of up to 4.5 and 3.0, respectively (E_{ap} = 1.2 V; 3-IEM pairs). The concentrating factor increased with increasing degrees of volume reduction, but it remained stationary when the volume ratio between the diluate (urine solution that is diluted in the IEM stack) and concentrate (urine solution that is reconcentrated) was 6 or greater. The energy requirement normalized by the mass of nutrient reconcentrated was 6.48 MJ·kg-N^{-1} (1.80 kWh·kg-N^{-1}) and 117.6 MJ·kg-P^{-1} (32.7 kWh·kg-P^{-1}). In addition to nutrient separation, the examined MEC reactor with three IEM pairs showed 54% removal of COD (chemical oxygen demand) in 47-

[1] Manuscript submitted to the journal *Water Research*

hr batch operation. The high sulfate concentration in human urine resulted in substantial growth of both acetate-oxidizing and H_2-oxidizing sulfate reducing bacteria, greatly diminishing the energy recovery and Coulombic efficiency. However, the high microbial activity of sulfate reducing bacteria hardly affected the rate of nutrient reconcentration. With the capability to reconcentrate nutrients at a minimal energy consumption and simultaneous COD removal, the examined bioelectrochemical treatment method with an IEM application has a potential for practical nutrient recovery and sustainable treatment of source-separated human urine.

Keywords
Volume reduction; nutrient separation and recovery; sulfate reducing bacteria; microbial electrolysis cell (MEC); sustainable wastewater treatment; source separated urine

3.1 Introduction

Human urine is known to contribute 80% of the nitrogen (N) and 50% of the phosphorus (P) in domestic wastewater [3], [4]. In municipal wastewater treatment, high nutrient levels require relatively expensive nutrient removal processes. Long sludge retention times (SRT > 10 d) are necessary for nitrification in activated sludge, consuming additional electric energy for return sludge and aeration. In addition, phosphorus removal by precipitation requires an extra cost for ferric or aluminum chemicals. Biological denitrification and phosphorus removal also necessitate large volume reactors to establish anoxic and

anaerobic conditions and a large pumping capacity for internal recycle of wastewater. Such extra costs for nutrient removal can be greatly reduced or even eliminated in wastewater treatment if human urine is separated at the source level [3]. Source separation of urine also enables effective recovery of nutrients as valuable raw materials, e.g., struvite ($MgNH_4PO_4$) and gaseous ammonia (NH_3) [17]–[19].

Even with the beneficial aspects, several key challenges exist for practical recoveries of nutrients from source-separated urine. One significant challenge is the dilution with large amounts of flushing water at urinals and toilets, substantially decreasing nutrient concentration. Even though specialized urinals or toilets have been suggested and developed to minimize the amount of flushing water, a certain degree of dilution is still necessary to prevent precipitation and clogging problems in collection systems. Rapid hydrolysis of urea substantially increases pH and high pH conditions induce precipitation of insoluble struvite salts on the surface of collection pipes [18], [19]. Therefore, source separated urine should be diluted below the solubility limit of struvite (or other minerals) for sustainable maintenance of urine collection systems. For efficient recovery of nutrients the collected urine needs to be reconcentrated above the solubility limit of struvite at a centralized treatment facility. In addition, if source-separated urine is directly used as a liquid fertilizer, a reconcentration step will substantially reduce required liquid volume for land applications. Reconcentration or separation of nutrients from human urine can be achieved by various treatment

processes, such as evaporation, freeze thaw, reverse osmosis and electrodialysis as previously demonstrated [3], [20].

Since the technologies currently available require relatively high energy consumption, this study aims to demonstrate energy efficient reconcentration of nutrients from diluted urine using energy released from oxidation of organic substrates in microbial electrolysis cells (MECs). In MECs, exoelectrogenic bacteria oxidize organic substrates and transfer electrons to the anode. Water is reduced to H_2 in water electrolysis at the cathode with a small external voltage application (E_{ap} > 0.14 V) [5], [7], [8], [101]. These coupled electrode reactions create an electric field that induces ionic transport between the electrodes. By schematically placing ion exchange membranes (IEMs) between the electrodes, nutrient ions (NH_4^+ and HPO_4^{2-}) can be reconcentrated from diluted urine (Fig. 3.1A). Thus, energy efficient nutrient reconcentration can be achieved as the oxidation of organic substrates at the anode partially contributes energy required for ionic separation through IEMs. This design principle was originally adopted from microbial desalination cells (MDCs) for desalination of seawater and brackish water [9]. To our knowledge, none of the previous studies have applied the principle of MDCs in reconcentrating nutrient ions from diluted human urine. One of the important differences of this application with diluted urine from MDCs is the urine composition. High concentrations of organic substrates and sulfate ions induce substantial sulfate reducing bacteria activity. Also, organic substrate removal is simultaneously achieved with nutrient reconcentration with the same

urine solution, requiring a different urine flow configuration from the previous stacked MDC designs [35], [36]. In addition, the target ions for reconcentration are restricted to only NH_4^+ and HPO_4^{2-} from diluted urine, while MDCs do not have specific target ions for separation. Thus, unlike previous MDC studies, competitive separation of nutrient ions vs. other common ions (e.g., Na^+, Cl^-, SO_4^{2-}) is an important aspect in this study.

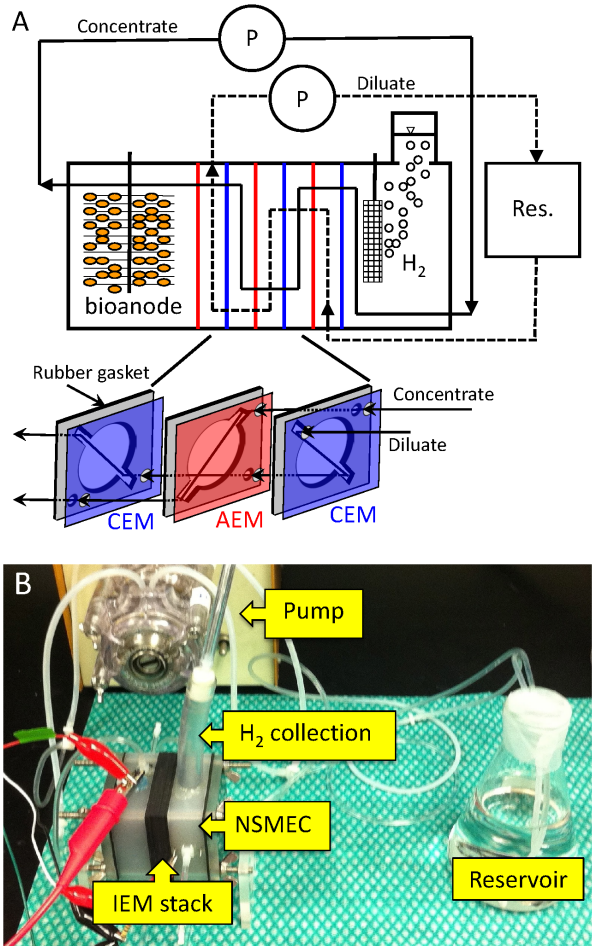

Figure 3.1: (A) NSMEC schematic design for urine reconcentration by integrating MEC and IEM stack. (P: pump; AEM: anion exchange membrane; CEM: cation exchange membrane; Res.: diluate reservoir) (B) Experimental set-up for continuous flow operation of NSMEC. The concentrate reservoir was always kept in an ice box.

Dilution of urine below the struvite solubility limit is inevitable to collect source-separated urine into a centralized treatment facility. Currently available methods for reconcentration (e.g., evaporation, thaw-freeze, reverse osmosis and electrodialysis) are relatively expensive with intensive energy demand. Thus, this study aims to demonstrate nutrient reconcentration from diluted urine and simultaneous organic removal by using the principle of MDCs where energy released from organic oxidation is partially used for the separation of nutrient ions. With reduced energy demand, a sustainable method for the utilization of source-separated urine is examined in this study. Detailed research objectives are to: (1) demonstrate energy efficient reconcentration of nutrients from 1:10 diluted hydrolyzed urine using an IEM stack in an MEC; (2) determine the rate of nutrient reconcentration as a function of the IEM stack size and applied potential (E_{ap}); (3) investigate the competitive separation of the target nutrient ions (NH_4^+ and HPO_4^{2-}) by comparing changes in their concentration and solution conductivity; (4) examine the volume ratio between the diluate (urine solution losing ions through IEMs) and the concentrate (urine solution collecting ions from the diluate); and (5) investigate the effects of sulfate reducing bacteria on nutrient reconcentration, organic removal and energy recovery.

3.2 Material and methods

3.2.1 Reactor construction

The nutrient separation microbial electrolysis cell (NSMEC) was constructed using polypropylene blocks with an interior cylindrical chamber (5

cm^2 in cross section). The assembled reactor consisted of the anode and cathode chambers (10 mL each) separated by a stack of IEMs (Fig. 3.1). A graphite fiber brush anode (2 cm diameter and 2.5 cm length; Mill-Rose, OH) was pretreated in a muffle furnace at 450 °C for 30 min [102] and inoculated with primary effluent from a municipal wastewater treatment facility. It should be noted that the anode was previously used in a methanogen dominated single-chamber MEC for approximately 10 months [103], indicating that methanogens were initially present in this constructed nutrient separation reactor. A piece of stainless steel mesh (5 cm^2 area; AISI 304, 100 mesh; McMaster-Carr, OH) was used as the cathode without any catalyst applications. A gas collection tube was glued to the top of the cathode chamber as previously described [33].

An IEM stack consisting of either one pair or 3 pairs of cation- and anion-exchange membranes (Selemion CMV; and Selemion AMV, respectively; AGC Engineering, Japan) was sandwiched between the anode and cathode chambers (Fig. 3.1A) as previously described [36]. The cross sectional area of IEMs for ionic transport was 5 cm^2. The inter-membrane distance was maintained ~1 mm by using a plastic gasket, creating relatively thin cells with reduced resistance for ionic separation. The average distance between the bioanode and cathode was 15 mm with 3 IEM pairs in the stack while the distance was 10 mm with the single IEM pair. In the IEM stack, the diluate (solution that loses ions) flowed serially through each diluate cell as the detailed flow scheme in the IEM stack cell is shown in Fig. 3.1A. The diluate was continuously circulated from an external

reservoir (200 mL unless otherwise noted) using a peristaltic pump (0.5 $mL \cdot min^{-1}$; AFP-101; New Brunswick Scientific, NJ) (Fig. 3.1B). To establish a strict anaerobic condition, the diluate reservoir was sealed using a laboratory paraffin film (Parafilm M; Pechiney Plastic Packaging Co., IL). For the stack with 3 IEM pairs, the concentrate (solution that gains nutrient ions) flowed from the cathode chamber serially through two concentrate cells in the IEM stack to the anode chamber (Fig. 3.1A). The concentrate solution in the anode chamber was continuously pumped to the cathode chamber (0.5 $mL \cdot min^{-1}$). Without an external reservoir, the volume of the concentrate solution was ~20 mL. For the stack with one IEM pair, the concentrate was continuously recirculated between the anode and cathode chambers (0.5 $mL \cdot min^{-1}$) to avoid a pH imbalance as previously described [104], [105]. Because of the relatively complicated urine flow in the IEM stack, the constructed reactor was examined for its airtightness by pressurizing water flow lines to avoid any water leaks and establish strict anaerobic conditions.

3.2.2 Diluted synthetic urine

A synthetic urine medium was prepared with 3.4 $g \cdot L^{-1}$ Na_2HPO_4, 5.7 $g \cdot L^{-1}$ NH_4Cl, 21.0 $g \cdot L^{-1}$ NH_4HCO_3, 14.5 $g \cdot L^{-1}$ NH_4CH_3COO, 6.2 $g \cdot L^{-1}$ $(NH_4)_2SO_4$ in accordance with previously reported urine compositions (Table 3.1). Note that acetate was used as the organic substrate since the primary objective of this study was to demonstrate nutrient reconcentration rather than investigating the organic removal capability of the bioanode. The prepared urine was diluted using

deionized water (1:10 dilution). This dilution ratio was determined based on the amount of urination of healthy adults (0.15 – 0.6 L) [106], [107] and the flushing volume in water-efficient urinals (1.9 L per flush or less) and toilets (4.8 L per flush or less) suggested by USEPA [108], [109]. The diluted synthetic urine was further prepared by adding trace amounts of vitamins and minerals [110] to ensure proper biological activities in NSMEC. Note that relevant minerals in human urine (Mg^{2+}, Ca^{2+} and K^{+}) in the trace vitamins and minerals are included in Table 3.1 with a notation.

Table 3.1: Synthetic urine composition (undiluted)

Species	Unit	Synthetic Urine Composition	Hydrolyzed urine [a]	Fresh urine [b]
Total nitrogen	[mg-N·L^{-1}]	8,714	4,841-9,200	4,000-9,136
Total phosphorus	[mg-P·L^{-1}]	742	292-636	350-2,000
Sodium	[mg·L^{-1}]	1,101	1,613-3,219	1,800-5,800
Potassium	[mg·L^{-1}]	0.1 [c]	1,333-3,484	1,300-3,100
Magnesium	[mg·L^{-1}]	75.7 [c]	0-15	29-121
Calcium	[mg·L^{-1}]	3.4 [c]	0-108	96-233
Chloride	[mg·L^{-1}]	3,777	2,357-7,576	2,300-7,700
Sulfate	[mg-SO_4·L^{-1}]	4,507	1,129-4,660	353-1,500
Bicarbonate	[mg-HCO_3·L^{-1}]	16,206	12,498-23,053	0

[a] Adapted from [3]
[b] [3], [18], [111]–[113]
[c] Added as trace metals and vitamins from [110]. Factored by 10 to be written as undiluted urine compositions while experiments were performed with 1:10 diluted urine.

3.2.3 Reactor operation

The prepared diluted urine was used both as the concentrate and diluate solution in the nutrient separation reactor. The reactor was operated under fed-batch mode for cycles lasting 47 hr. In each fed-batch cycle, the anode chamber

(10 mL), cathode chamber (10 mL) and diluate reservoir (200 mL or given otherwise) were refilled with the diluted urine. For instance, when the diluate reservoir volume is 200 mL and concentrate volume is 20 mL, the expected concentrating factor is 10 (200 mL / 20 mL). The diluate reservoir was completely sealed to avoid oxygen introduction and ammonia evaporation. The reservoir was kept in an ice box to minimize microbial activities in the reservoir.

The applied voltage (E_{ap}) from a power supply was 0.9 V unless otherwise noted (GPS-1850D; GW Instek, CA). The electric current was determined by measuring the voltage drop every 20 min across a 10 Ω resistor using a multimeter and data acquisition system (Model 2700; Keithley Instruments, OH). All experiments were performed in an air-conditioned laboratory and temperature was stationary at 22.8 ± 0.6 °C.

3.2.4 Experimental measurements

After each fed-batch cycle, the diluate and concentrate effluents were analyzed for conductivity and pH (SevenMulti; Mettler-Toledo International Inc., OH). The chemical oxygen demand (COD), ammonia nitrogen, phosphate and sulfate were determined according to standard methods [114]. Note that the other common ions in the synthetic urine (i.e., Na^+, Cl^- and HCO_3^-) were not measured in the experimental analysis since the objectives of this study are focused more on investigating nutrient reconcentration capacities of NSMEC and effects of sulfate reducing bacteria. Volatile suspended solids (VSS) were also measured to approximate the biosolids production from the nutrient separation reactor [114].

For each fed-batch cycle, gas was collected in a gas bag (250-mL capacity; Calibrated Instruments Inc., NY). Two packed columns were used for the analysis of the collected gas by gas chromatography (Varian Star 3400 CX; Agilent Technologies, CA). A Molecular Sieve 5a column was used for the analysis H_2, CH_4 and O_2 and a Porapak Q column for NH_3, CO_2 and air (Chromatographic Specialties Inc., Canada). Nitrogen and helium were used as the carrier gases for the Molecular Sieve 5a and Porapak Q columns, respectively. The total volume of gas was determined by the gas bag method as previously described [115].

When the reactor was disassembled after 2 months of operation, distinct crystal grains were observed on the surface of the cathode and CEM placed next to the cathode. The crystal grains were imaged and characterized using scanning electron microscopy (SEM) and energy dispersive X-ray spectroscopy (EDS) technology (JEOL JSM-6610LV, Japan).

3.2.5 Coulombic efficiency

The Coulombic efficiency (*CE*) is the ratio between the measured electron generation and theoretical amount of electron production by substrate oxidation as [78]:

$$CE = \frac{8 \int i dt}{F(V_D \Delta COD_D + V_C \Delta COD_C)} \qquad (3.1)$$

F is the Faraday's constant (96,485 C·mol^{-1}), *i* is the electric current, *ΔCOD* is the change in COD over a fed-batch cycle and *V* is the volume of diluate and concentrate solutions. The subscripts *D* and *C* denote the diluate and concentrate,

respectively. Note that the Coulombic efficiency is different from the current efficiency (ratio between total ion separated and electron transferred), which was not measured in this study as we mainly focused on nutrient reconcentration.

3.3 Results and discussion

3.3.1 Separation performance

The rate of ionic separation (including ammonium and phosphate ions) was magnified in the NSMEC with increasing number of IEM pairs and electric voltage application (E_{ap}) (Fig. 3.2). The larger NSMEC with 3-IEM pairs resulted in a higher degree of ammonium and phosphate ion separation compared to the single-pair IEM. In addition, the degree of nutrient separation with 3-IEM pairs increased almost linearly with E_{ap} up to 1.2 V while the single IEM pair demonstrated only a limited increase. Ammonia (initially 745 mg-N·L^{-1}) was concentrated by a factor of 4.5 to a maximum concentration of 3,340 mg-N·L^{-1} (E_{ap} = 1.2 V; 3-IEM pairs) (Fig. 3.2A). The rate of ammonia separation normalized by the reactor volume (25 mL) was 49,929 mg-N·hr^{-1}·m^{-3} (E_{ap} = 1.2 V; 3-IEM pairs). Similarly, phosphate was reconcentrated by a factor of up to 3.0 from an initial concentration of 73 up to 219 mg-P·L^{-1} (Fig. 3.2B). The resulting rate of phosphate reconcentration was 2,751 mg-P·hr^{-1}·m^{-3}. (E_{ap} = 1.2 V; 3-IEM pairs). The measured conductivity was also magnified by a factor of up to 3.9 (Fig. 3.2C). As a result of the reconcentration of ions (including nutrient ions) in the concentrate solution (20 mL), the diluate solution (200 mL) showed decreases in ionic contents by up to 61% for ammonia, 46% for phosphorus and 51% for

measured conductivity (E_{ap} = 1.2 V; 3-IEM pairs). This result shows that NSMEC can be used to recover nutrient ions from diluted human urine and the rate of nutrient recovery improves with increasing number of IEM pairs.

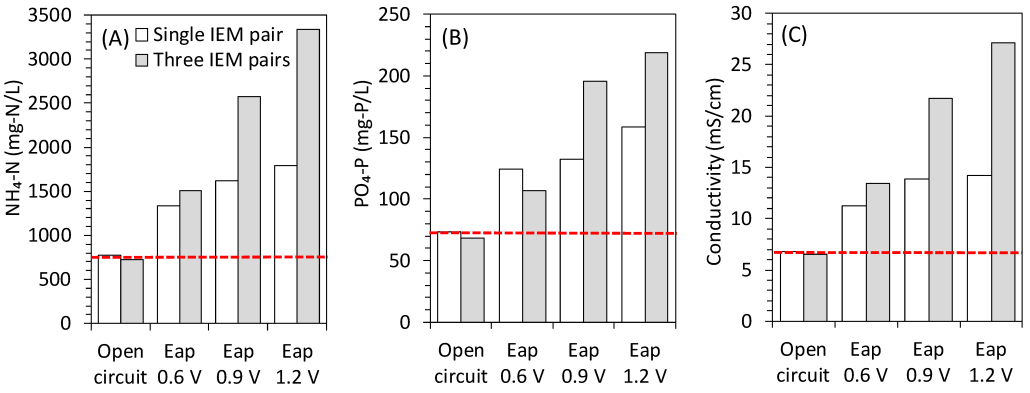

Figure 3.2: Effects of IEM stack size and voltage application on reconcentration of (A) ammonia, (B) phosphate and (C) conductivity. The red dotted line indicates the initial concentration and conductivity. (Diluate = 20 mL; concentrate = 200 mL; 47-hr operation)

The separation of ammonia was consistently faster than that of phosphate. For the given pH conditions (pH 7.9 - 8.5), ammonium (NH_4^+) is dominant over free ammonia (NH_3) and phosphate is present primarily as HPO_4^{2-}. The diffusivity of ammonium ions is greater than sodium ions (Table 3.2), resulting in more favourable separation of NH_4^+ than sodium. It should be noted that ammonium and sodium are the most common cations in hydrolyzed human urine [3].

Table 3.2: Equivalent ionic conductivity (Λ) and diffusivity (D) for typical ions present in hydrolyzed human urine [116].

Species	Λ (10^{-4} $m^2 \cdot S \cdot mol^{-1}$)	D (10^{-5} $cm^2 \cdot s^{-1}$)
Na^+	50.08	1.334
NH_4^+	73.5	1.957
HPO_4^{2-}	57	0.759
SO_4^{2-}	80.0	1.065
HCO_3^-	44.5	1.185
CH_3COO^-	40.9	1.089
Cl^-	76.31	2.032

The equivalent ionic conductivity (Λ_i) of an individual ionic species *i* is defined as a charge weighted diffusivity as:

$$\Lambda_i = \frac{|z_i|F^2}{RT} D_i. \quad (3.2)$$

D is the diffusivity, *z* is the ionic charge, *R* is the gas constant and *T* is the absolute temperature. Among common anions in hydrolyzed human urine, phosphate, acetate and bicarbonate have relatively small values of the ionic conductivity compared to sulfate and chloride (Table 3.2). This comparison of the ionic conductivity explains the relatively slow separation of phosphate compared to the ammonia separation results and conductivity changes (Fig. 3.2). Therefore, to enhance selective phosphate separation from other common anions we recommend that future studies should focus on possible utilization and development of specialized anion exchange membranes (AEMs) selective for phosphate.

While the large stack with 3 IEM pairs showed more rapid reconcentration of nutrients than the small stack with 1 IEM pair (Fig. 3.2), the small stack

showed a greater nutrient flux though an individual IEM (Fig. 3.3). This increasing nutrient flux with the decreasing number of IEMs can be explained by relatively small amounts of electric energy available for ionic separation as previously discussed [35], [36], [117]. As a result, the smallest voltage application (E_{ap} = 0.6 V) showed the greatest discrepancy in the ion flux through an individual IEM between the large and small IEM stacks (Fig. 3.3). This finding confirms that the IEM stack in NSMEC should carefully be designed to minimize resistive losses as previously discussed with IEM-stacked microbial desalination cells [35], [36], [117].

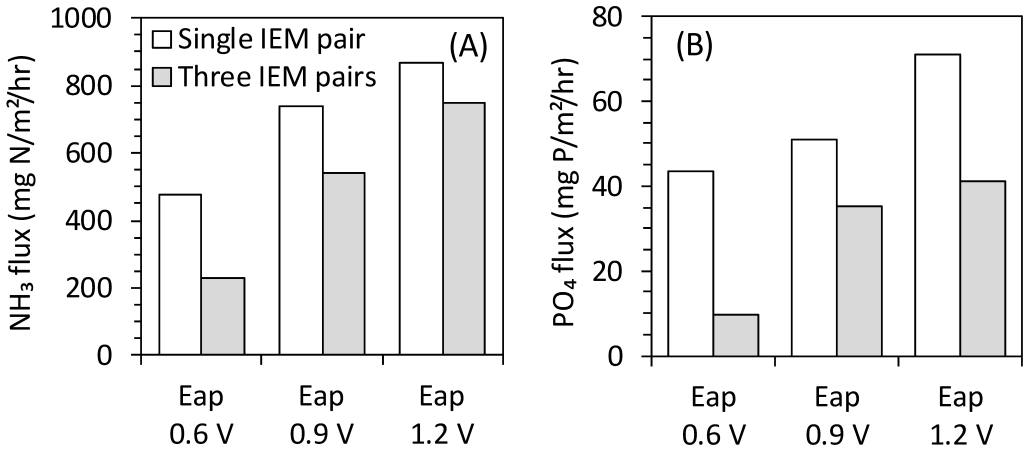

Figure 3.3: Nutrient flux through an individual IEM for (A) ammonia and (B) phosphate. The rate of nutrient reconcentration was normalized by the area of IEMs (15 cm^2 for 3 IEM pairs and 5 cm^2 for single IEM pair). (Diluate = 20 mL; concentrate = 200 mL; 47-hr operation).

3.3.2 Volume ratio between diluate and concentrate ($V_{D/C}$)

The degree of nutrient reconcentration increased linearly with the increasing diluate volume up to 120 mL for the fixed 20 mL of the concentrate ($V_{D/C}$ = 6) (Fig. 3.4). Further increases in the diluate volume to 160 and 200 mL

($V_{D/C}$ of 8 and 10) did not enhance the reconcentration of nutrients. This result implies that there exists an upper-limit concentration of nutrients for a given E_{ap} condition and fed-batch cycle length. For instance, the highest ammonia concentration was 2,580 mg-N·L^{-1} (Fig. 3.4A) and phosphate could hardly be reconcentrated beyond 272 mg-P·L^{-1} (E_{ap} = 0.9 V; 47-hr fed-batch length; 3-IEM pairs) (Fig. 3.4B).

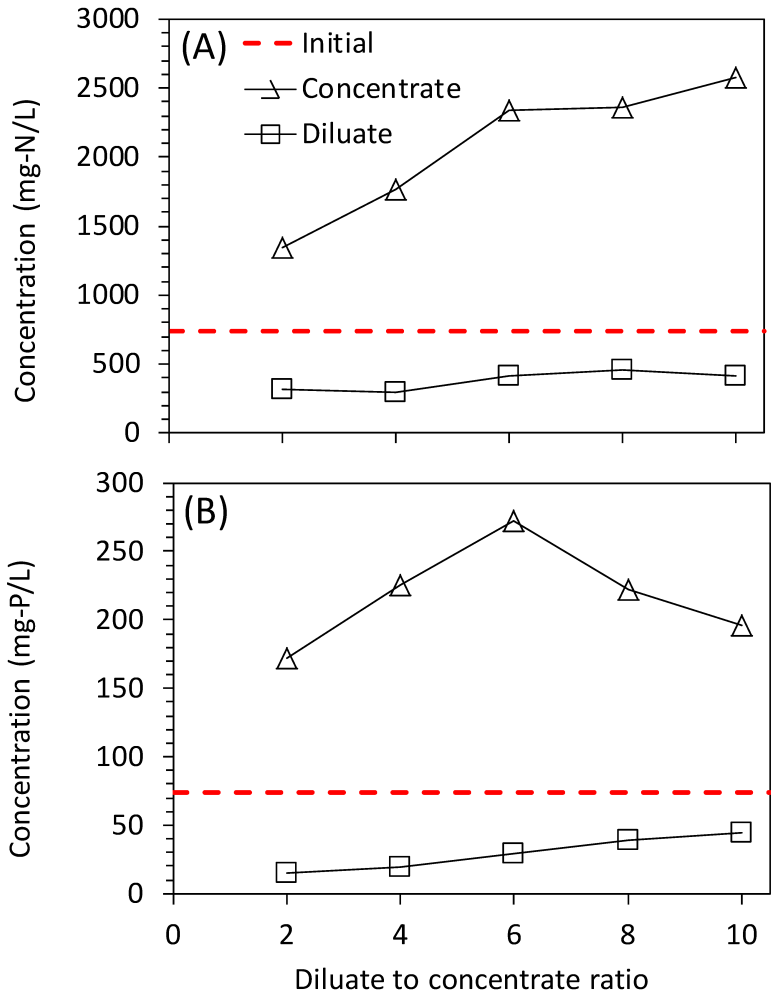

Figure 3.4: Effects of diluate-to-concentrate volume ratio on (A) ammonia separation and (B) phosphate separation. (Diluate = 20 – 200 mL; concentrate = 20 mL; 3-pair IEM stack; E_{ap} = 0.9 V; 47-hr operation)

The degree of nutrient removal in the diluate decreased with the increasing diluate volume. When the diluate volume was small at 40 mL ($V_{D/C}$ = 2), the nutrient removal from the diluate solution was relatively high: 63% ammonia removal and 80% phosphate removal (Fig. 3.4). However, the nutrient removal decreased down to 39% (ammonia) and 27% (phosphate) when the diluate volume was 200 mL ($V_{D/C}$ = 10). This decreasing nutrient removal with increasing the diluate volume can be explained by the limited nutrient reconcentration in the concentrate solution.

This limited reconcentration capability can be explained by the junction potential loss. As a result of nutrient reconcentration, the ionic concentration in the concentrate solution became approximately 5 to 10 times that in the diluate (Fig. 3.4). Thus, it needs a greater junction potential loss to overcome the concentration difference across an IEM when an ion is driven from the diluate to the concentrate. In a separate experiment in accordance with Strathmann [31], the sum of junction potential losses across three IEM pairs was 0.25 V (ionic concentration in the concentrate was assumed to be 8 times that of the diluate). This substantial junction potential loss explains the upper-limit nutrient reconcentration.

3.3.3 Electric current in NSMEC

The current generation increased with increasing E_{ap} for both the 3- and single-pair IEM stacks (Fig. 3.5), resulting in enhanced nutrient separation (Fig. 3.2). The magnitude of electric current was higher with the single-pair IEM than

that with the 3-pair IEM stack by up to ~50% when E_{ap} was relatively low at 0.6 and 0.9 V. This result can be explained by relatively greater Ohmic losses with thicker IEM stacks. The resistivity of one cell pair (one diluate cell, one concentrate cell, one CEM, and one AEM) was 34.4 $\Omega \cdot cm^2$ (initial urine conductivity = 6.81 $mS \cdot cm^{-1}$; inter-membrane distance = 1 mm; AEM resistivity = 2.5 $\Omega \cdot cm^2$; CEM resistivity = 2.5 $\Omega \cdot cm^2$) [31]. This cell pair resistivity gives an Ohmic loss of 13.7 mV per cell pair at 1 mA (i.e., 0.4 $mA \cdot cm^{-2}$). Even with the greater Ohmic loss and thus lower electric current, the 3-pair IEM stack still showed enhanced nutrient separation (Fig. 3.2) because the increased number of IEM pairs magnified the rate of ionic separation. Thus, larger stacks not only enhance the rate of nutrient reconcentration but they also reduce electric power consumption due to relatively low electric current. Note that electric power consumption is the product of electric current and applied voltage.

While the NSMEC can be operated at small energy consumption, the resulting electric current is relatively low as the maximum current was about 2.2 mA or 0.44 $mA \cdot cm^{-2}$ (E_{ap} = 1.2 V; 3 IEM pairs) (Fig. 3.5). While this current density value is comparable to those in microbial desalination cells (0.1 – 0.8 $mA \cdot cm^{-2}$, [117]), it is still small compared to that in conventional electrodialysis systems, which can be operated under current conditions greater than 10 $mA \cdot cm^{-2}$ depending on the feed water conductivity. Thus, we recommend that future studies on ion separation using bioelectrochemical systems should focus on magnifying electric current to enhance the rate of ion separation.

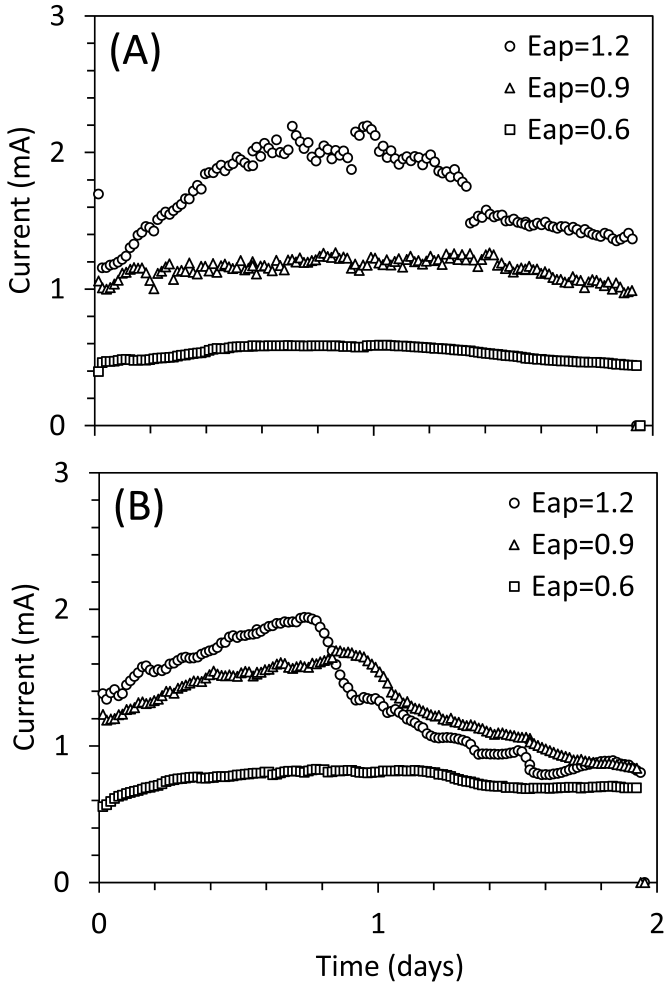

Figure 3.5: Electric current in NSMEC with (A) 3-pair IEM stack and (B) 1-pair IEM stack. (Diluate = 200 mL; concentrate = 20 mL; 47-hr operation)

3.3.4 Energy consumption

The NSMEC requires 1.6 MJ (0.44 kWh) per m^3 of the total solution treated (both diluate and concentrate) to achieve concentration factors of 4.5 for ammonia and 3.0 for phosphate (E_{ap} = 1.2 V; diluate = 200 mL; concentrate = 20 mL). The energy requirement normalized by the amount of nutrient reconcentrated was 6.48 MJ·kg-N^{-1} (1.80 kWh·kg-N^{-1}) and 117.6 MJ·kg-P^{-1} (32.7 kWh·kg-P^{-1}). Note that H_2 gas produced was not included in this energy

requirement calculation. If the rapid H_2 consumption problem is resolved, the energy requirement can be substantially reduced. Thus, it is recommended that future studies be directed toward resolving the low energy recovery problem.

3.3.5 COD removal and Coulombic efficiency

The COD removal was relatively low at 68.5% ± 20.7% (diluate = 200 mL; concentrate = 20 mL) because of the relatively short fed-batch cycle (47 hours). Even with the wide variation, the COD removal showed a decreasing trend with the larger IEM stack (83.3% removal with single-IEM pair; and 53.6% with 3-IEM pairs). With this incomplete COD removal, residual organic substrates kept the bioanode active throughout the fed-batch cycle with more stable electric current generation with 3-IEM pairs than that with the single-IEM pair (Fig. 3.5). Note that the bioanode can generate stable electric current as long as organic substrates are present above a certain threshold concentration (e.g., 87 $mg \cdot L^{-1}$ COD for acetate-fed bioelectrochemical systems; [101]). The Coulombic efficiency was consistently low with a wide variation (CE = 14.4% ± 8.1%).

The wide variations in CE and COD removal imply that there are multiple factors affecting the consumption of organic substrates in NSMEC. It is important to note that the majority of organic substrates (i.e., acetate) were initially present in 200 mL of the diluate solution while only a small fraction of acetate (10%) was in 20 mL in the concentrate solution. Thus, acetate ions (CH_3COO^-) must be transported through the AEM to the concentrate solution where exoelectrogenic bacteria on the anode utilize the acetate ions (Fig. 3.1A). This preceding substrate

transport step can explain the relatively low COD removals and Coulombic efficiencies in NSMEC.

The preceding step for the substrate utilization is likely to have resulted in the sudden drop in the current at ~0.8 d for the single-IEM pair NSMEC (E_{ap} = 1.2 V; Fig. 3.5B). However, the 3-IEM paired stack with three pieces of AEMs allowed relatively rapid acetate transfer enough to maintain the high current (~2 mA) under the high voltage application conditions (E_{ap} = 1.2 V; Fig. 3.5A). This result indicates that large IEM stacks are necessary under high current conditions to keep the rate of anionic substrate transport to the concentrate solution greater than the rate of substrate utilization at the bioanode in NSMEC.

3.3.6 Sulfate reducing bacteria

Another reason for the low CE and COD removal can be explained by the presence of sulfate reducing bacteria. High sulfate concentration in human urine (Table 3.1) provides favourable growth conditions, and as a result the COD removal and Coulombic efficiency were greatly diminished by the activity of sulfate reducing bacteria. A substantial amount of sulfate (up to 59% or 283 mg-$SO_4 \cdot L^{-1}$) was lost over the relatively short 47-hr fed-batch cycle (Fig. 3.6). Active sulfate- and sulfide-related reactions have been reported in a number of previously studies in BESs [118]–[120].

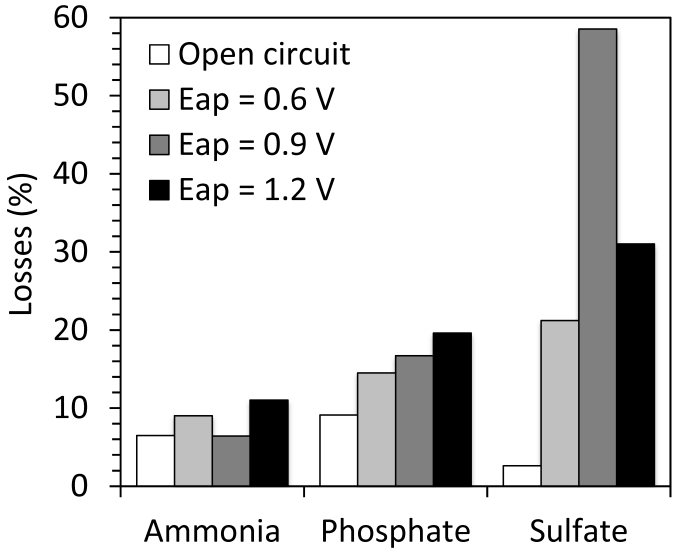

Figure 3.6: Effects of voltage application (E_{ap}) on the loss of ammonia, phosphate and sulfate in NSMEC. (3-pair IEM stack; diluate = 200 mL; concentrate = 20 mL; 47-hr operation).

Sulfate reducing bacteria are categorized into acetate oxidizers and non-acetate oxidizers [100]. The treatment of hydrolyzed human urine in an NSMEC provides favourable conditions for both types of sulfate reducing bacteria. The acetate oxidizers use sulfate as the electron acceptor while they use acetate (or other fatty acids) as the terminal electron donor and carbon source. Since anaerobic conditions can quickly produce large amounts of acetate and short-chain fatty acids through fermentation and anaerobic oxidation [14], acetate oxidizers can grow rapidly in any anaerobic processes treating source-separated human urine. Therefore, the low CE (CE = 14.4% ± 8.1%) in NSMEC can be explained by the microbial activity of acetate oxidizers.

Operation of the NSMEC with synthetic urine also showed substantial activities of the non-acetate oxidizers. The non-acetate oxidizers use sulfate as the

electron acceptor while they oxidize H_2 and use carbonate species as the carbon source. In the NSMEC, the synthetic urine contained a substantial amount of bicarbonate (1,631 $mg \cdot L^{-1}$) and sulfate (451 $mg \cdot L^{-1}$) (Table 3.1). Thus, the NSMEC with a sufficient amount of H_2 gas, HCO_3^- and SO_4^{2-} provided an ideal anaerobic condition for non-acetate oxidizers. Consequently, substantial consumption of H_2 gas was observed in the NSMEC operation. In the GC analysis of collected gas, the average amount of H_2 gas was 1.4 ± 2.3 mL (47-hr reaction time), indicating rapid consumption of H_2 in the NSMEC. The largest H_2 gas production was 8.0 mL at the highest voltage application (E_{ap} = 1.2 V) while the H_2 gas volume was constantly negligible below 3 mL at E_{ap} of 0.9 and 0.6 V. This rapid consumption of H_2 is driven mainly by non-acetate oxidizing sulfate reducers, not by hydrogenotrophic methanogens because CH_4 was not detected in GC analysis. This result indicates that hydrogenotrophic methanogens cannot compete with non-acetate oxidizing sulfate reducing bacteria under their ideal growth conditions with sufficient carbon sources (CO_2), electron donors (H_2) and electron acceptors (CO_2 for hydrogenotrophic methanogens and SO_4^{2-} for sulfate reducers).

Even with the intensive activity of sulfate reducing bacteria, the rate of nutrient reconcentration was hardly affected by sulfate reducing bacteria. The sulfate loss was highest at E_{ap} = 0.9 V (Fig. 3.6), indicating the greatest activity of sulfate reducing bacteria. However, the degree of nutrient reconcentration showed consistent increasing trends with increasing E_{ap} and increasing number of IEM

pairs without any notable differences at E_{ap} of 0.9 V (Fig. 3.2). This insensitivity of nutrient reconcentration to sulfate reducing bacteria can be explained by relatively high organic substrate concentration in hydrolyzed human urine. For instance, COD of undiluted urine is ~10,000 mg·L^{-1} [3]; thus, 1:10 dilution still gives 1,000 mg L^{-1} COD. Even with substrate consumption by acetate oxidizing sulfate reducers, there are still sufficient amounts of organic substrates for exoelectrogenic bacteria that provide the driving force for nutrient ion separation.

The experimental results indicate that sulfate reducing bacteria played multiple roles in diminishing the Coulombic efficiency and energy recovery in the NSMEC. Acetate oxidizing sulfate reducers decreased the Coulombic efficiency by consuming organic substrates. The non-acetate reducers rapidly consumed H_2 gas, decreasing energy recovery in the NSMEC. It should be noted that sulfate reducing bacteria are ubiquitous in anaerobic environments. Therefore, if energy recovery is targeted from source-separated urine using strictly anaerobic bioelectrochemical systems (e.g., MECs), we recommend that sulfate reducing bacteria be completely controlled because they outgrow most anaerobic microorganisms [14], [121]. H_2 gas was consumed by sulfate reducing bacteria not by hydrogenotrophic methanogens. It should be emphasized that hydrogenotrophic methanogens are one of the rapidly growing microorganisms in anaerobic digestion, requiring only 1 day for active methanogenesis from H_2 [14].

3.3.7 Crystal formation near the cathode

In the NSMEC operation, the stainless steel mesh cathode created favourable conditions for precipitation of nutrient crystals (e.g., struvite) as previously described [1]. When the NSMEC was disassembled after 56 days of operation, crystal grains were found on the cathode (Fig. 3.7A and 3.7B) and on the cathode-side CEM surface (Fig. 3.7C and 3.7D). In an energy dispersive X-ray spectra (EDS) analysis, the crystal grains on the cathode (Fig. 3.8A) and on the CEM (Fig. 3.8B) showed similar results to hydrated pure struvite (Fig. 3.8C), implying that the observed crystals are struvite or at least they have comparable elemental compositions to struvite.

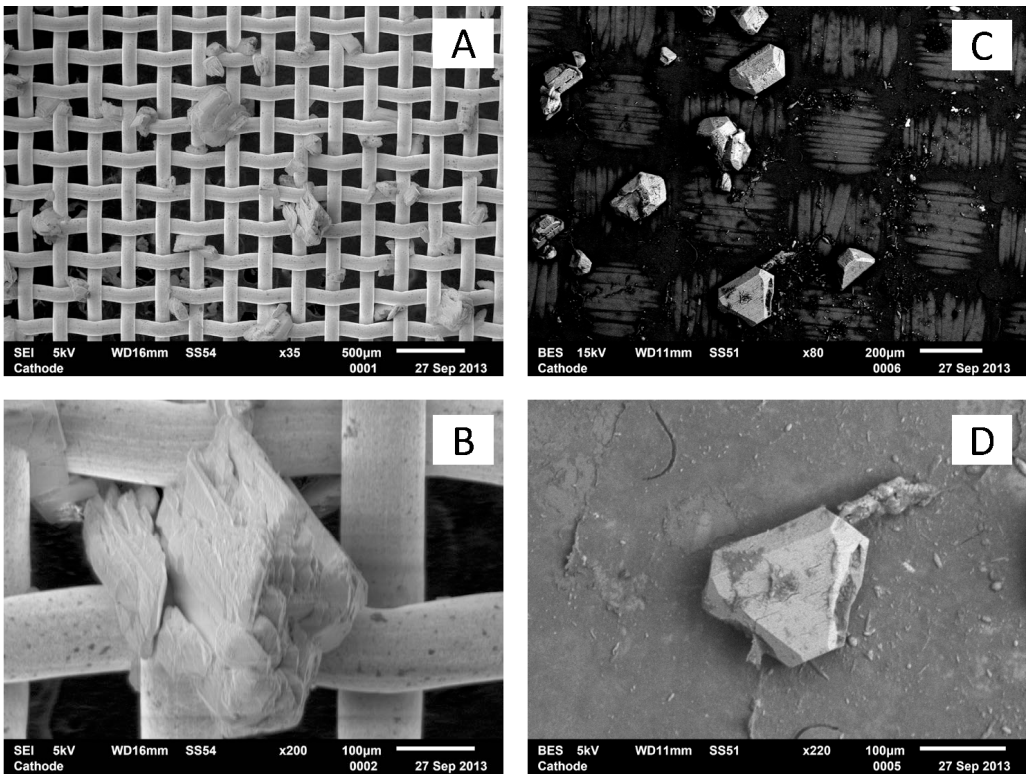

Figure 3.7: SEM images of crystal grains on the cathode with (A) 500-µm scale bar and (B) 100-µm scale bar; and on the CEM with (C) 200-µm scale bar and (D) 100-µm scale bar.

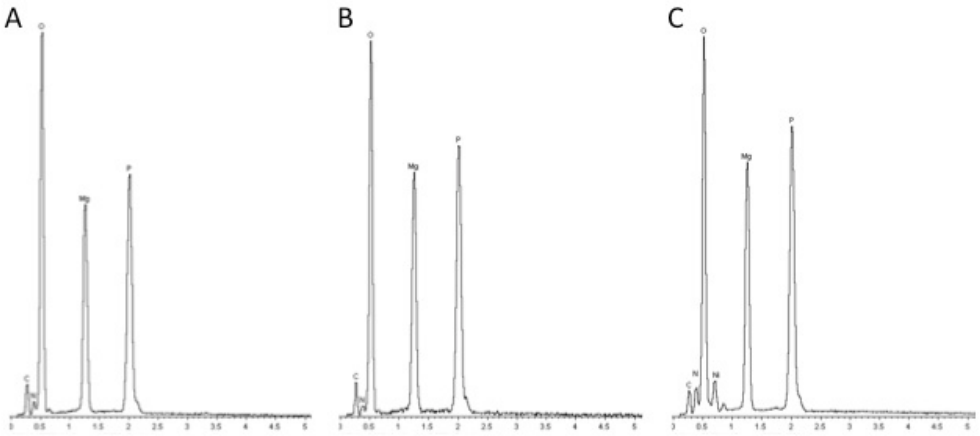

Figure 3.8: Energy dispersive X-ray spectroscopy (EDS) results for elemental composition of the crystal grains (A) on the cathode and (B) on cation exchange membrane. (C) EDS results with hydrated pure struvite crystals (99.99x purity).

The crystal morphology from the NSMEC is distinctly different from the prismatic needle shaped struvite crystals reported in a recent MEC study [1]. This distinction in the crystal morphology can be explained by the significantly different magnesium concentrations: 3.11×10^{-4} mol·L^{-1} in the NSMEC and 1.75×10^{-2} mol·L^{-1} in Cusick and Logan (2012) [1]. Previous studies demonstrated that struvite morphology can be different and highly dependent on precipitation conditions such as pH, ionic strength and rate of crystal formation [122]–[124]. The accumulation of struvite crystals was not expected because of the very low magnesium concentration (3.11×10^{-4} mol·L^{-1} or 7.57 mg·L^{-1}), which was provided primarily as a trace mineral for microbial growth [110]. This unexpected struvite precipitation confirms the strong capability of MEC cathodes to recover nutrients from wastewater as previously demonstrated [1], [125].

3.3.8 Nutrient losses

Nutrient losses were observed during the fed-batch operation. Up to 10% of ammonia was lost and phosphorus losses were up to ~20% (Fig. 3.6). The phosphorus loss increased gradually with the increasing voltage application (E_{ap}) while ammonia showed a less discernable correlation between its loss and E_{ap}. Even though the percent loss was greater for phosphate compared to ammonia, the ammonia loss was always 2-3 times the phosphate loss on a molar basis, indicating there were reactions that consumed ammonia more rapidly than phosphate.

The accumulation of struvite ($MgNH_4PO_4$) on the cathode and CEM explains a portion of the nutrient loss. The increasing nutrient loss with the increasing E_{ap} indicates that the crystal accumulation contributed to the nutrient loss. Note that precipitation of struvite is accelerated by high nutrient concentration in the concentrate solution and high local pH near the cathode. Higher nutrient concentration was achieved at greater E_{ap} applications (Fig. 3.2); and higher local pH conditions are established at greater E_{ap} applications. Thus, the increasing trend of the nutrient loss with increasing E_{ap} (Fig. 3.6) can partially be explained by the struvite accumulation on the cathode and CEM surfaces.

Microbial cell growth is also responsible to some extent for the nutrient loss. Rapid sulfate reducing activities imply that the growth of sulfate reducing bacteria consumed nutrients during NSMEC operation. In addition, fully developed bioanodes are known to produce a small amount of biosolids [126]

consuming a certain amount of nutrients for cell synthesis. A substantial amount of volatile suspended solids (VSS) was produced in the concentrate solution (73.5 ± 40.2 mg $VSS \cdot L^{-1}$), indicating active microbial cell synthesis and thus consumption of ammonia and phosphate.

Gaseous ammonia was not detected in the GC analysis of the collected gas. This result is not consistent with a recent study where aqueous ammonia was successfully volatilized from human urine through cathode aeration in microbial fuel cells (MFCs) [17]. This inconsistency can be explained by the different cathode system, implying that aeration is necessary for gaseous ammonia recovery. Note that the initial ammonia concentration in the NSMEC was relatively low at 745 mg-$N \cdot L^{-1}$; however, ammonia was reconcentrated up to 3,300 mg-$N \cdot L^{-1}$, which is comparable to 4,000 mg-$N \cdot L^{-1}$ in Kuntke et al. (2012) [17]. Thus, the absence of gaseous ammonia in this study indicates that the operation conditions of NSMEC cannot sufficiently drive ammonia volatilization.

3.4 Conclusions

The NSMEC (a bioelectrochemical system coupled with an IEM stack) demonstrated energy efficient nutrient reconcentration and simultaneous COD removal from diluted human urine. The rate of nutrient reconcentration was magnified in the NSMEC with an increasing number of IEM pairs and electric voltage application. The target nutrient ions (ammonium and phosphate) were concentrated by a factor of 4.5 and 3.0, respectively (E_{ap} = 1.2 V; 3-IEM pairs). It was found that the separation of ammonia was consistently faster than that of

phosphate because the diffusivity of ammonium ions is greater than sodium ions (both are common cations in hydrolyzed human urine), resulting in more favourable separation of ammonium ions through CEMs. Phosphate has a relatively small equivalent ionic conductivity (i.e., charged weighted diffusivity) compared to sulfate and chloride ions, which are also more abundant than phosphate in human urine. This competitive separation with sulfate and chloride reduces the effective phosphate separation.

The degree of nutrient reconcentration increased linearly with increasing diluate volume up to 120 mL at a fixed concentrate volume (20 mL). However, further increases in the diluate volume did not enhance the reconcentration of nutrients. The limited nutrient reconcentration is mainly due to the relatively low voltage application (E_{ap} = 0.9 V). Thus, for complete nutrient recovery and COD removal, it is recommended that NSMEC be operated in multiple stages as previously demonstrated with microbial desalination cells [36].

Dilution of source-separated urine below the solubility limit of struvite is essential to avoid clogging problems in urine collection system to a centralized treatment facility. Therefore, reconcentration of collected urine is critical above the solubility limit for nutrient recovery. The requirement for nutrient separation was substantially small at 1.6 $MJ \cdot m^{-3}$ (0.44 $kWh \cdot m^{-3}$) when the NSMEC with 3-IEM pairs was operated at the relatively high voltage application (E_{ap} = 1.2 V). This energy requirement is smaller than other conventional treatment processes for urine volume reduction (e.g., electrodialysis reversal, nanofiltration, freeze-

thaw, evaporation methods) by up to three orders of magnitude. The NSMEC configuration offers an energy efficient solution to enable the reconcentration of source separated urine and subsequent or simultaneous recovery of target nutrients as valuable raw materials in the form of struvite.

The high sulfate concentration in human urine provided favourable conditions for the growth of sulfate reducing bacteria. However, the intensive activity of sulfate reducing bacteria did not affect the rate of nutrient reconcentration in the NSMEC. On the other hand, the microbial activity greatly diminished the energy recovery as H_2 gas (by H_2-oxidizing sulfate reducers) and Coulombic efficiency (by acetate-oxidizing sulfate reducers). In addition, the H_2-oxidizing sulfate reducing bacteria were found to outcompete hydrogenotrophic methanogens as only a small amount of methane was observed in the gas analysis. If energy recovery is targeted from source separated urine using strictly anaerobic bioelectrochemical systems (e.g., MECs), sulfate reducing bacteria must be properly controlled.

NSMEC can be constructed using relatively low cost materials. The bioanode can be prepared using carbon materials (e.g., activated carbon granules or graphite fibers). Stainless steel mesh can be used as the cathode without precious metal catalysts. High costs for IEMs can be a limiting factor for NSMEC applications in nutrient reconcentration from human urine. Thus, we suggest that future research be directed toward long-term operation and fouling control in IEM

applications [127] for the treatment of source-separated urine as well as for the nutrient recovery.

Acknowledgements

This study was supported by New Faculty Start-up Fund (Faculty of Engineering, McMaster University) and Discovery Grants (Natural Science and Engineering Research Council of Canada). The authors thank Ms. Anna Robertson and Mr. Peter Koudys for their help on equipment operation and reactor construction.

Chapter 4: Influence of substrate concentration and feed frequency on ammonia inhibition in microbial fuel cells[2]

Abstract

Excessive amounts of ammonia are known to inhibit exoelectrogenic activities in microbial fuel cells (MFCs). However, the threshold ammonia concentration that triggers toxic effects is not consistent among literature papers, indicating that ammonia inhibition can be affected by other operational factors. Here, we examined the effect of substrate concentration and feed frequency on the capacity of exoelectrogenic bacteria to resist against ammonia inhibition. The high substrate condition (2 $g \cdot L^{-1}$ sodium acetate, 2-day feed) maintained high electricity generation (1.1 and 1.9 $W \cdot m^{-2}$) for total ammonia concentration up to 4,000 mg-$N \cdot L^{-1}$. The less frequent feed condition (2 $g \cdot L^{-1}$ sodium acetate, 6-day feed) and the low substrate condition (0.67 $g \cdot L^{-1}$ sodium acetate, 2-day feed) resulted in substantial decreases in electricity generation at total ammonia concentrations of 2,500 and 3,000 mg-$N \cdot L^{-1}$, respectively. It was determined that the power density curve serves as a better indicator than continuously monitored electric current for predicting ammonia inhibition in MFCs. The chemical oxygen demand (COD) removal gradually decreased at high ammonia concentration even without ammonia inhibition in electricity generation. The experimental results demonstrated that high substrate concentration and frequent feed substantially

[2] Manuscript submitted to the *Journal of Power Sources*

enhance the capacity of exoelectrogenic bacteria to resist against ammonia inhibition.

Keywords

Total ammonia nitrogen (TAN); ammonia cytotoxicity; source-separated human urine; power density; animal manure wastewater; ammonia inhibition indicator; bioelectrochemical system (BES)

4.1 Introduction

Bioelectrochemical systems can be used to effectively treat wastewater and produce renewable energy. Microbial fuel cells (MFCs) are a type of bioelectrochemical system that can remove organics in wastewater and simultaneously produce electrical energy. Recent developments in MFC design (e.g., air cathodes [71]; sandwiched electrode assemblies [72]; inexpensive cathode catalysts [73]) along with pilot-scale demonstrations [74]–[77], make MFCs an attractive alternative for sustainable wastewater treatment and energy recovery [78]. Electric energy generation in MFCs relies on electrochemically active bacteria that form a biofilm on the anode. These exoelectrogenic bacteria oxidize organic substrates present in wastewater and transfer electrons to the anode, creating electric current. At the cathode of MFCs, water is formed through the reduction of oxygen that can be provided directly from the atmosphere using air cathodes [79]. The performance of MFCs as a wastewater treatment and energy recovery process centers on the activity of exoelectrogenic bacteria to transfer electrons to the anode; hence, the sensitivity of exoelectrogenic bacteria

to various wastewater treatment conditions (e.g., ammonia, salinity, oxygen, etc.) needs to be investigated.

Recent studies have examined MFC performance with various sources of wastewater, including swine wastewater, anaerobic digester supernatant and human urine [17], [80], [81]. These high strength wastewaters contain excessive amounts of ammonia that can inhibit microbial metabolism and thus prevent exoelectrogenic bacteria from generating electric current in MFCs. In this study, we primarily focused on the effect of TAN (total ammonia nitrogen) on MFC performance under various substrate feed conditions.

Ammonia is well known for its cytotoxic effects on microorganisms [82], [83]. Specifically, ammonia inhibition mechanisms include enzymatic activity disruption, alteration in the intracellular pH, and dehydration due to osmotic stress [84]–[86]. Previous experimental studies consistently demonstrated negative responses of MFC bioanodes to significantly high TAN levels beyond 4,000 mg-$N \cdot L^{-1}$ [87]–[89]. However, the previous studies showed inconsistent results on the threshold TAN level that triggers ammonia inhibition effects in bioelectrochemical systems. For instance, Nam et al. (2010) reported that TAN concentrations exceeding 500 mg-$N \cdot L^{-1}$ at neutral pH of 7 can result in severe inhibition of electricity generation in MFCs, implying a relatively low ammonia concentration triggers limited performance of bioanodes [87]. In another study using a continuously operated MFC, electric current generation gradually increased with increasing TAN concentrations up to 3,500 mg-$N \cdot L^{-1}$ [88].

Similarly, Kuntke et al. (2011) found no cytotoxic effects of ammonia up to 4,000 mg-N·L^{-1} [89]. It should be noted that experiments in these previous studies were performed under neutral pH conditions using phosphate buffer, indicating that equilibrium between free ammonia (NH_3) and ammonium ion (NH_4^+) did not affect the degree of ammonia inhibition as free ammonia is known to be more toxic to microorganisms than ammonium ions in biological wastewater treatment [14], [83]. Thus, here we aim to explain the reported inconsistent TAN concentrations that trigger the ammonia inhibition effects in MFCs.

To further investigate the effects of ammonia inhibition in MFCs, we hypothesized that the concentration and frequency of substrate feed can affect the capability of exoelectrogenic bacteria to create electric current under high ammonia conditions. To our knowledge, none of the previous studies have investigated potential effects of the level and frequency of substrate feed on ammonia inhibition effects in MFCs. MFC performance is often described with continually monitored current results as well as power density curves developed using various external resistors. Between the two performance indicators, we also investigated which can better predict ammonia inhibition before MFC bioanodes are completely damaged by high ammonia conditions.

4.2 Material and methods

4.2.1 MFC configuration and operation

Five single-chamber MFCs were constructed using polypropylene blocks with an inner cylindrical chamber (23 mL; 7 cm^2 in cross section). Graphite fiber

brushes (2 cm diameter and 2.5 cm in length; Mill-Rose, OH) were pretreated in a muffle furnace at 450 °C for 30 min [102] and used as the bioanode. The bioanodes were inoculated with primary effluent and digested sludge collected from a domestic wastewater treatment plant. All MFCs underwent an enrichment period of about 5 months. The air cathodes (7 cm^2 in cross section) were constructed from wet proofed carbon cloth (Fuel Cell Earth, MA) with a Pt/C catalyst (0.5 $mg \cdot cm^{-2}$), as previously described [71]. Constructed MFCs were operated under fed-batch mode with an external resistance (100 Ω).

To study the inhibitory effect of ammonia at different substrate levels and feed frequencies, 2 MFCs were fed with 2 $g \cdot L^{-1}$ sodium acetate every two days (high acetate and short cycle, HASC-1 and -2); one with 0.67 $g \cdot L^{-1}$ sodium acetate every two days (low acetate and short cycle, LASC); and two with 2 $g \cdot L^{-1}$ sodium acetate every 6 days (high acetate and long cycle, HALC-1 and -2) (Table 4.1). The feed medium was prepared with sodium acetate (according to Table 4.1) in 50 mM phosphate buffer solution (4.7 $g \cdot L^{-1}$ Na_2HPO_4; 0.6 $g \cdot L^{-1}$ $NH_4H_2PO_4$; 1.6 $g \cdot L^{-1}$ KH_2PO_4; 0.4 $g \cdot L^{-1}$ $NaHCO_3$), and trace amounts of vitamins and minerals [110]. The total amount of ammonia was adjusted by adding NH_4Cl in the feed medium and was gradually increased from 100 to 4,000 mg-$N \cdot L^{-1}$. For each ammonia condition, MFCs were operated for 6 days (i.e., 3 short fed-batch cycles or one long fed-batch cycle) except for the very high ammonia concentrations (3,500 and 4,000 mg-$N \cdot L^{-1}$).

Table 4.1: MFC operation conditions

MFC	Substrate Level ($g \cdot L^{-1}$)	Batch Cycle Length (days)
HASC (high acetate, short cycle)	2.0	2
LASC (low acetate, short cycle)	0.67	2
HALC (high acetate, long cycle)	2.0	6

4.2.2 Experimental measurements

Electric current in the reactors was determined by measuring the voltage drop every 20 min across an external resistor of 100 Ω using a multimeter and data acquisition system (Model 2700; Keithley Instruments, OH). After each fed-batch cycle, effluent was analyzed for conductivity and pH (SevenMulti; Mettler-Toledo International Inc., OH). The chemical oxygen demand (COD) was determined according to standard methods (Hach Co., CO) [114]. All experiments were performed in an air-conditioned laboratory and temperature was stationary over the course of MFC operation at 23.2 ± 0.8 °C.

To prepare power density curves, the MFC electrodes were disconnected (open circuit) for 60 min and then serially connected to an external resistor of 10, 100, 200, 400 and 1000 Ω every 10 min. The power density (P) was calculated from $P = VI$, where V is the measured voltage drop across the external resistor, I is the current density normalized by the projected surface area of the cathode (7 cm^2). This power density test was performed on the last day of an applied ammonia condition.

4.2.3 Coulombic efficiency

The Coulombic efficiency (*CE*) is the ratio between the measured electron generation and theoretical amount of electron production by substrate oxidation as [78]:

$$CE = \frac{8 \int idt}{F(V \Delta COD)} \qquad (4.1)$$

F is the Faraday's constant (96,485 C·mol^{-1}), *i* is the electric current, *ΔCOD* is the change in COD over a fed-batch cycle and *V* is the volume of the MFC reactor.

4.3 Results and discussion

4.3.1 Inhibition of current generation

The exoelectrogenic microorganisms were capable of generating current at a maximum capacity (~3.8 mA) for all MFC reactors in TAN solutions up to 2,500 mg-N·L^{-1} (Fig. 4.1). The current results for TAN solutions from 100 to 2,000 (not shown) exhibited increases from 2.5 to 3.8 mA due to the incremental conductivity increase in the solution. The effect of conductivity on reactor performance has been demonstrated previously [87], [88]. HASC-1 and -2 maintained high current generation for the high TAN concentrations up to 4,000 mg-N·L^{-1} (~3.5 mA) (Fig. 4.1A). Some variability existed between HASC-1 and -2, particularly at the start of the high ammonia conditions (i.e., 3,500 and 4,000 mg-N·L^{-1}). HASC-2 showed consistently high current generation while HASC-1 experienced a substantial decrease in current generation for the first few fed-batch cycles under 3,500 and 4,000 mg-N·L^{-1}. However, the current generation in HASC-1 was rapidly restored in ~5 days to comparable levels of that in HASC-2.

This recovery back to maximum current generation was unique to the HASC reactors, indicating the importance of both substrate level and feed cycle length. Both LASC and HALC reactors showed no ability to recover once a decrease in current generation was experienced.

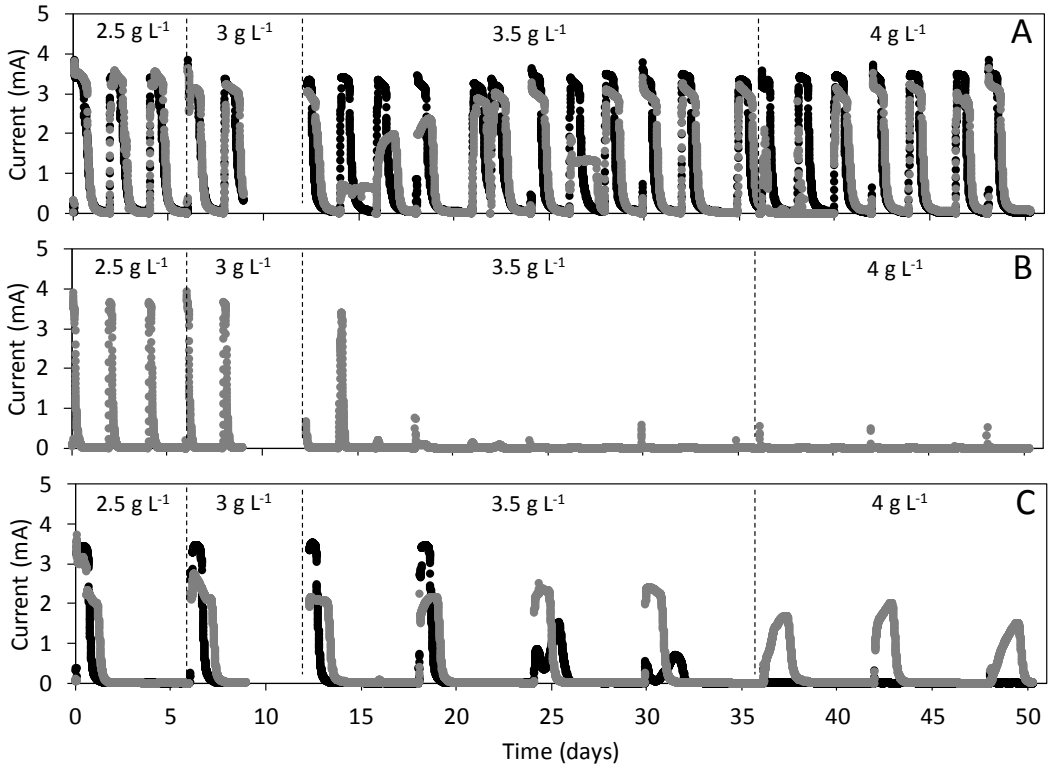

Figure 4.1: Effects of ammonia concentration on current generation in single chamber MFCs. (A) HASC-1 (•), HASC-2 (•) (2d - 2 g·L^{-1} NaAc); (B) LASC-1 (•) (2d - 0.67 g·L^{-1} NaAc), (C) HALC-1 (•), HALC-2 (•) (6d - 2 g·L^{-1} NaAc). Note: Data was lost between days 9 and 12 due to a malfunction with the data collection system.

The low substrate condition (0.67 g·L^{-1} sodium acetate) resulted in immediate impairment of current generation at 3,500 mg-N·L^{-1} for LASC-1 (Fig. 4.1B). In comparison with the current generation from HASC (2 g·L^{-1} sodium acetate) (Fig. 4.1A), it is concluded that a certain level of substrate concentration

should be provided to keep exoelectrogenic bacteria active under high ammonia conditions.

The frequency of substrate feed was also an important factor that determines the capability of exoelectrogenic bacteria to resist against high ammonia concentration. The HALC MFCs (fed with 2 $g \cdot L^{-1}$ sodium acetate, but less frequently every 6 days) showed gradual decreases in current generation at 3,500 mg-$N \cdot L^{-1}$ (Fig. 4.1C). HALC-1 exhibited a reduction in current by ~20% at 3,000 mg-$N \cdot L^{-1}$ and a further decrease at 3,500 mg-$N \cdot L^{-1}$, but remained consistent across the four batch cycles at this level. HALC-2 exhibited no decreases in current until the third batch cycle at 3,500 mg-$N \cdot L^{-1}$, but showed a rapid drop in current generation thereafter. While HALC-1 and -2 responded differently to the high ammonia conditions, current generation in both MFCs was substantially inhibited by the high ammonia concentration. This result compared to the consistently high current generation in HASC-1 and -2 (fed every 2-days) clearly demonstrates that the capacity of exoelectrogenic bacteria to resist against high ammonia concentration is substantially enhanced by feeding MFCs frequently.

4.3.2 Ammonia inhibition on power generation

HASC-1 and -2 (2 $g \cdot L^{-1}$ sodium acetate and 2-day feed) maintained high maximum power densities between 1.1 and 1.9 $W \cdot m^{-2}$ (35 and 59 $W \cdot m^{-3}$) for all TAN concentrations up to 4,000 mg-$N \cdot L^{-1}$ (Fig. 4.2). The maximum power density was also high between 1.4 and 2.0 $W \cdot m^{-2}$ (45 and 62 $W \cdot m^{-3}$) for LASC-1 only at TAN concentrations of 3,000 mg-$N \cdot L^{-1}$ or less (Fig. 4.2A, B, C and D),

indicating the low substrate concentration (0.67 $g \cdot L^{-1}$ sodium acetate) did not limit the electric power generation. However, at 3,500 mg-$N \cdot L^{-1}$ or higher, the maximum power density decreased to 7.1×10^{-8} and 1.7×10^{-6} $W \cdot m^{-2}$ (2.2×10^{-6} and 5.4×10^{-5} $W \cdot m^{-3}$) respectively (Fig. 4.2E and F). The maximum power density for HALC-1 and -2 showed a gradual decrease from 2.3 to 0.6 $W \cdot m^{-2}$ (72 to 17 $W \cdot m^{-3}$) (HALC-1) and from 1.1 to 0.9 $W \cdot m^{-2}$ (35 to 28 $W \cdot m^{-3}$) (HALC-2) as the TAN concentration increased from 1,000 to 3,000 mg-$N \cdot L^{-1}$. It should be noted that the maximum power density of HALC-1 was the highest (2.3 $W \cdot m^{-2}$) among the 5 MFCs at TAN of 1,000 mg-$N \cdot L^{-1}$, indicating that the less frequent fed-batch operation (every 6 days) did not limit the power generation at the relatively low TAN concentration (1,000 mg-$N \cdot L^{-1}$). The high TAN concentration (4,000 mg-$N \cdot L^{-1}$) resulted in substantial reduction in the maximum power density to 4.7×10^{-4} and 5.0×10^{-5} $W \cdot m^{-2}$ (1.4×10^{-2} and 1.5×10^{-3} $W \cdot m^{-3}$) for HALC-1 and -2 respectively. The power density results confirmed that a higher initial substrate concentration coupled with frequent feed keeps exoelectrogenic bacteria in MFCs robust against high ammonia concentrations at 3,000 mg-$N \cdot L^{-1}$ or higher.

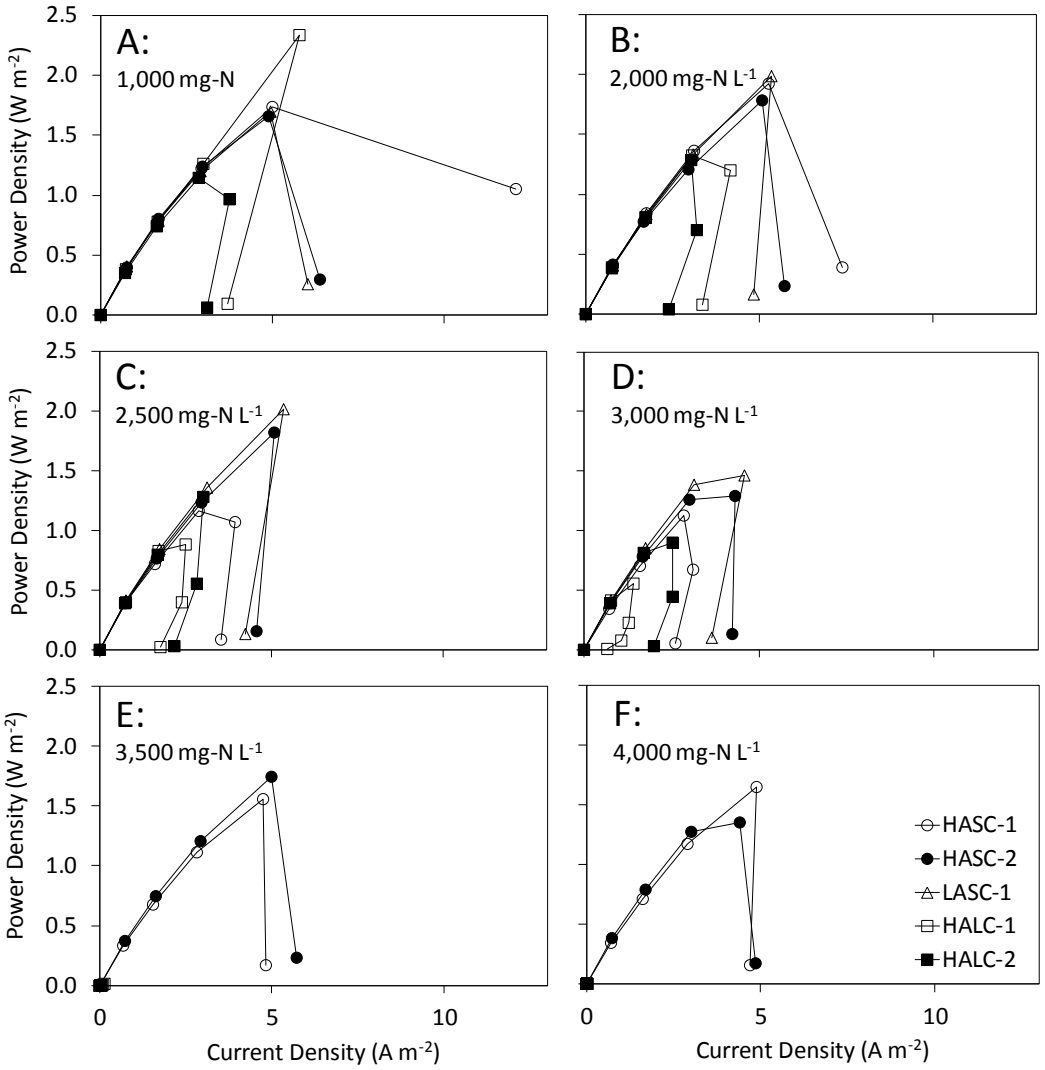

Figure 4.2: Power density curves. (A) 1,000 mg-N·L^{-1}, (B) 2,000 mg-N·L^{-1}, (C) 2,500 mg-N·L^{-1}, (D) 3,000 mg-N·L^{-1}, (E) 3,500 mg-N·L^{-1}, (F) 4,000 mg-N·L^{-1}.

The current generation and power density results consistently showed that the HASC reactors outperformed the LASC and HALC reactors under relatively high ammonia concentration conditions (>3,000 mg-N·L^{-1}). The higher organic substrate level (2 g·L^{-1} sodium acetate) and frequent fed-batch cycle (every 2 days) negate the inhibitory effects of ammonia that influenced the other reactors. Even though HASC-1 showed a sudden drop in current generation when the ammonia

concentration was increased to 3,500 and 4,000 mg-N·L^{-1}, the current was rapidly restored in 2 or 3 fed-batch cycles (Fig. 4.1A). Neither the LASC nor HALC reactors were able to recover from the decreased current, indicating permanent damage on the bioanode from the high ammonia concentration. As a result, the power production was practically zero when the LASC and HALC reactors were examined in the polarization experiments.

It was determined that the power density curve serves as a better indicator for ammonia inhibition in bioelectrochemical systems than continuously monitored electric current. As the ammonia concentration gradually increased up to 3,000 mg·L^{-1}, the electric current was consistently high (>3 mA) for all of the five MFCs (Fig. 4.1) without showing any inhibition effects. However, the MFCs with either the low initial substrate or long fed-batch cycle condition (HALC-1, HALC-2 and LASC-1) showed clear decreases in the maximum power generation at the ammonia concentration of 3,000 mg-N·L^{-1} (Fig. 4.2D). In addition, HALC-1 maintained a non-zero electric current (1-2 mA in Fig. 4.1C) under the high ammonia concentration of 3,500 and 4,000 mg-N·L^{-1}; however, the power generation in HALC-1 was practically zero (Fig. 4.2E and F), indicating evident inhibition by the high ammonia concentration. Based on these experimental observations, we suggest that the ammonia inhibition in bioelectrochemical systems be determined using power density curves rather than monitoring electric current.

4.3.3 Effect of ammonia on COD removal in MFCs

The increasing ammonia level decreased the COD removal in MFCs (Fig. 4.3) as previously demonstrated [87]. The COD removal was almost complete (>90%) and consistent up to 1,000 mg-N·L^{-1}. However, the removal started to gradually decrease for all MFCs with the increasing ammonia concentration beyond 1,000 mg-N·L^{-1}. The MFCs with the high initial substrate concentration (2 g·L^{-1} sodium acetate in HASC and HALC) showed a similar COD removal trend with the increasing ammonia concentration up to 4,000 mg-N·L^{-1}, decreasing from 98% COD removal to 72%. The MFC with the low initial substrate concentration (LASC) exhibited a more drastic decrease in COD removal from 97 to 49% with the increasing ammonia concentration.

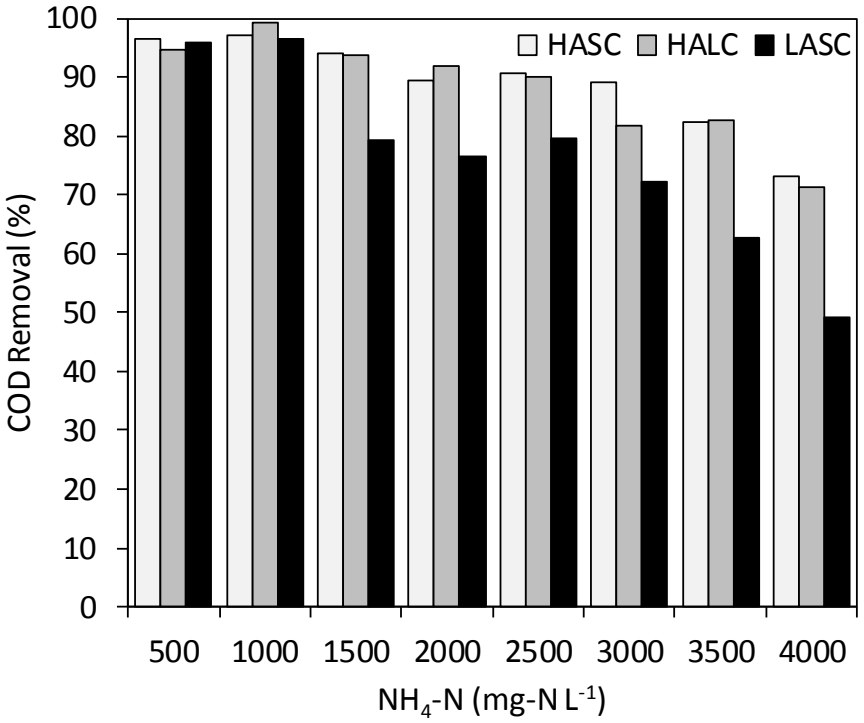

Figure 4.3: COD removal at different ammonia concentrations.

4.3.4 Coulombic efficiency

The Coulombic efficiency (CE) without ammonia inhibition at low TAN concentrations was approximately 70% (Fig. 4.4). The Coulombic efficiency for HASC was consistently high (>50%) throughout the experiment because the effect of ammonia inhibition was minimized by the high initial substrate (2 $g \cdot L^{-1}$ sodium acetate) and frequent fed-batch operation (every 2 days). HALC (2 $g \cdot L^{-1}$ sodium acetate and 6 day fed-batch operation) showed high CE ~70% for ammonia concentrations up to 3,000 mg-$N \cdot L^{-1}$. Higher ammonia concentrations (3,500 and 4,000 mg-$N \cdot L^{-1}$) significantly decreased the Coulombic efficiency down to 27% (Fig. 4.4). This decrease in CE is consistent with the drop-off in current generation in the HALC reactor (Fig. 4.1C). The Coulombic efficiency for LASC decreased to 52% at 2,500 mg-$N \cdot L^{-1}$ and then further dropped down to 2.6% at 3,500 mg-$N \cdot L^{-1}$. This substantial drop in CE can be explained by the negligible current generation at the ammonia concentration of 3,500 and 4,000 mg-$N \cdot L^{-1}$ (Fig. 4.1B).

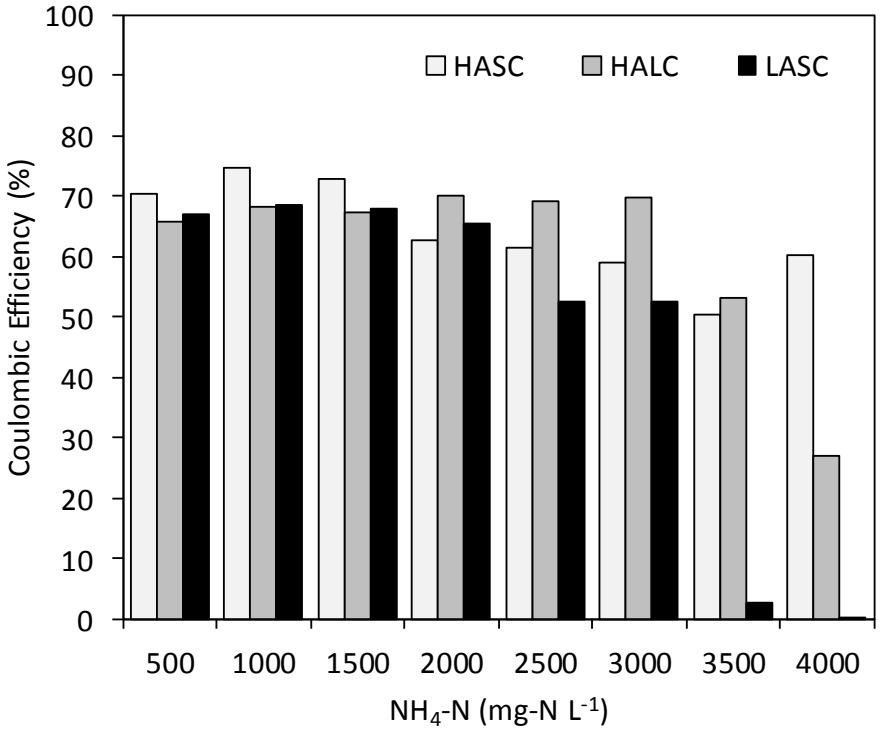

Figure 4.4: Coulombic efficiency at different ammonia concentrations.

Even with the Coulombic efficiency below 3% at the high TAN concentrations (3,500 and 4,000 mg-N·L^{-1}) (Fig. 4.4), LASC showed approximately 50-60% COD removal from the initial sodium acetate concentration of 0.67 g·L^{-1} (Fig. 4.3). This percent COD removal indicates that approximately 0.3-0.4 g·L^{-1} sodium acetate was consumed for 2 days by non-exoelectrogenic metabolisms (e.g., aerobic microorganisms in biofilms on the air cathode). For the HASC results at 3,500 and 4,000 mg-N·L^{-1}, the CE was 50-60% (Fig. 4.4) while the COD removal was ~80% from the initial sodium acetate concentration of 2 g·L^{-1} (Fig. 4.3). Thus, approximately 0.7 g·L^{-1} of sodium acetate was consumed for 2 days by non-exoelectrogenic metabolisms, indicating

that substrate consumption by non-exoelectrogenic microorganisms is ubiquitous regardless of the ammonia inhibition effect on exoelectrogenic bacteria.

4.4 Conclusions

The link between the level of substrate concentration and ammonia inhibition in single-chamber MFCs was investigated. The low substrate condition (0.67 $g \cdot L^{-1}$ sodium acetate) resulted in substantial impairment of current generation at 3,500 mg-$N \cdot L^{-1}$. However, under the high substrate condition (2 $g \cdot L^{-1}$ sodium acetate, every 2-day feed), high current generation was maintained for all TAN concentrations tested (up to 4,000 mg-$N \cdot L^{-1}$). The result clearly indicates that a certain level of substrate concentration should be provided to keep exoelectrogenic bacteria active under high ammonia conditions.

The frequency of substrate feed (i.e., length of fed-batch cycle) was also found to be an important factor as the short fed-batch cycle (2 days) substantially enhanced the capability of exoelectrogenic bacteria to resist against ammonia cytotoxicity. The MFCs fed less frequently (every 6 days) started showing limited current generation at 3,500 mg-$N \cdot L^{-1}$ and low power generation at 2,500 mg-$N \cdot L^{-1}$.

It was determined that the power density curve serves as a better indicator than continuously monitored electric current for characterizing ammonia inhibition in bioelectrochemical systems. Although the power density curves and current generation results showed consistent responses to the increasing ammonia concentration, the ammonia inhibition effect was reflected earlier in the power

density curves compared to the current generation results. It is suggested that ammonia inhibition in bioelectrochemical systems be determined using power density curves rather than continuously monitored electric current.

The COD removal decreased with increasing ammonia concentrations. MFCs with the high substrate concentration (HASC and HALC) showed a similar COD removal trend with increasing ammonia concentrations while the low substrate concentration (LASC) exhibited a more drastic decrease in COD removal. The Coulombic efficiency was consistently high for the high substrate and frequent feed MFCs (HASC). The reactors with the high substrate and less frequent feeding (HALC) experienced lower Coulombic efficiencies for ammonia concentrations of 3,500 and 4,000 mg-N·L^{-1}. These CE results are consistent with the continuously monitored current generation. The CE for the low substrate experiment (LASC) started decreasing at an ammonia concentration of 2,500 mg-N·L^{-1} and substantially dropped down to less than 5% at 3,500 mg-N·L^{-1}.

The high current and power generation for the high substrate concentration (2 g·L^{-1} sodium acetate) and frequent substrate feed (2 day fed-batch cycles) clearly demonstrated that the capacity of exoelectrogenic bacteria to resist against high ammonia concentration is substantially enhanced by keeping the substrate concentration high in MFCs. This conclusion along with findings in the previous studies [87]–[89] will allow reliable MFC applications for energy recovery and treatment of agricultural wastewater and source-separated human urine that contain high ammonia concentrations.

Acknowledgements

This study was supported by New Faculty Start-up Fund (Faculty of Engineering, McMaster University) and Discovery Grants (Natural Science and Engineering Research Council of Canada). The authors thank Ms. Anna Robertson and Mr. Peter Koudys for their help on equipment operation and reactor construction.

Chapter 5: Methanogenesis control by electrolytic oxygen production in microbial electrolysis cells[3]

Abstract

High purity H_2 production using microbial electrolysis cells (MECs) is often limited by methanogenesis. Here methanogenesis was effectively controlled by electrolytic oxygen production. Oxygen production was induced intermittently using two stainless steel electrodes, which were used as the MEC cathode during Normal operation. It was found that oxygen should be produced every 12 hours or more frequently because of rapid hydrogenotrophic methanogen growth with available pure H_2. This method was also effective in an initially methanogen-dominated MEC. However, the growth of aerobic biofilms in MECs weakened methanogen control. Residual oxygen after fed-batch cycles was found to be the key indicator for effective methane control. Methane content was consistently smaller than 10% at the threshold residual oxygen volume (3 mL) or greater. MEC operation at such threshold conditions will allow high purity H_2 production, low energy consumption for O_2 production and minimal O_2 exposure on bioanodes, enabling sustainable wastewater treatment and energy recovery using MECs.

[3] Manuscript published in the *International Journal of Hydrogen Energy*

Keywords

Hydrogenotrophic methanogens; oxygen evolution by electrolysis; oxygen threshold for methane control; bioelectrochemical system (BES); high purity hydrogen gas (H_2) production; sustainable wastewater treatment

5.1 Introduction

The microbial electrolysis cell (MEC) is an emerging technology and can be used to treat wastewater and simultaneously recover energy as hydrogen gas (H_2) [6]–[8]. In an MEC, exoelectrogenic bacteria oxidize soluble organic matter and transfer electrons to the anode. At the cathode, hydrogen gas is produced through the reduction of water. To drive the redox reactions at MEC electrodes (i.e., oxidation of organics and reduction of water), a small amount of electric potential needs to be applied (>0.2 V) [5], [6], [8]. This energy requirement is substantially small compared to the minimum threshold voltage of 1.23 V for conventional water electrolysis. With the low energy requirement, the energy recovered as hydrogen gas in a well-controlled MEC is substantially high, up to 2-4 times the electric energy provided [10], [32], [33]. This high energy recovery enables MECs to be a promising method for sustainable wastewater treatment [5]. This promising potential has helped drive substantial improvements in MEC design and operation through intensive research. With recent reports on pilot-scale experiments, MECs can be practically applicable in wastewater treatment and energy recovery in the near future [93], [128]–[130].

Methanogenesis is often considered as the greatest challenge in achieving practical applications of MECs. This study aims to suggest an effective and practical method for methane control in MECs. Methane production and consequent reduction in H_2 purities have been addressed as a potential limitation of MEC applications in a number of research studies [10]–[13], [90]–[92]. In addition, a recent pilot-scale experiment confirmed that methanogenesis is a limiting factor for practical H_2 production from wastewater using MECs [1]. Methanogenesis can be controlled in laboratory experiments by using 2-bromoethanesulfonate or chloroform [95]–[98]. However, these chemicals cannot be applied in practical wastewater treatment due to their toxic effects and high operational costs. While methanogenic activities are known to decrease under low pH conditions [97], mildly acidified solutions (pH ~5-6) were not effective in controlling methanogenesis in MECs [10], [11]. Operation of bioelectrochemical systems at relatively low temperatures (e.g., 15 °C) was also proven to be ineffective for methane control [11]. In dark fermentation, methanogens are completely inactivated during initial heat treatment (e.g., 100 °C for 10 min) while H_2–producing and spore-forming fermenters survive such harsh conditions [92], [99]. Similar heat treatment (100 °C for 15 min) was employed in MEC operation for the control of methanogens; however, exoelectrogenic bacteria could not survive the high temperature as they are not spore-forming microorganisms [10]. In addition, such heat treatment cannot be a sustainable

method for practical wastewater treatment due to substantial heat energy requirement.

All methanogens are strict anaerobes [100]; thus, the methanogenic activity can be controlled through regular O_2 treatment during MEC operation. When MEC cathodes were exposed to the air for 15 min, methane production was effectively controlled over 120 hours [10]. However, the air exposure method was not effective with bioanodes, as short-term exposure (30 min or less) could not inactivate methanogens on bioanodes [11]. Effective inactivation was only achieved for a substantially extended exposure of bioanodes in the air (24 hr) [13]. These results in the previous studies imply that the air exposure method does not have immediate influence in methane control. In another study, a relatively short-term exposure of bioanodes to air (30-50 min) was followed by a brief aeration step (3-5 min) [11], [12]. Methane production was substantially reduced, indicating that aeration is effective for methane control. However, in practical MEC applications, the construction and operation of aeration systems will require extra costs, making MEC technology a less sustainable and less energy-efficient alternative for wastewater treatment.

For effective control of methanogenesis in a feasible and cost-efficient manner, here an electrolytic O_2-production method was suggested for MEC reactors. In this method, two pieces of stainless steel mesh (H_2-producing cathodes during normal MEC operation) were used for the electrolytic pure O_2 production during a brief oxygen operation step. Thus, this method does not

require additional materials in MEC construction, such as aeration systems in practical applications. Even though the effectiveness of O_2 in methane control has been reported in a number of previous studies [10]–[13], the frequency of which O_2 treatment needs to be provided has not been clearly confirmed. The frequency of O_2 treatment is very important because hydrogenotrophic methanogens can grow rapidly, requiring only ~12 hours for active methanogenesis [14]. In addition, there are no quantified criteria on how much O_2 should be provided for effective control of methane. A clear guideline on the amount of O_2 supply is necessary because excessive O_2 can weaken exoelectrogenic bacteria on bioanodes. To establish O_2 treatment as a cost-effective and practically available method for high purity H_2 production in MECs, this study aims to: (1) examine the electrolytic O_2 production method for methane control; (2) suggest the optimal frequency of O_2 treatment; (3) find the minimal amount of O_2 that can effectively limit methanogenesis; and (4) quantify the adverse effect of O_2 treatment on the exoelectrogenic activity of bioanodes.

5.2 Material and methods

5.2.1 Reactor construction

Four single-chamber MECs were constructed using polypropylene blocks with an inner cylindrical chamber (37 mL; 7 cm^2 in cross section). A graphite fiber brush (2 cm diameter and 2.5 cm in length; Mill-Rose, OH) was pretreated in a muffle furnace at 450 °C for 30 min [102] and used as the bioanode (E1) (Fig. 5.1). The bioanode was originally inoculated with primary effluent from a

domestic wastewater treatment plant and enriched in a single chamber MFC. Two pieces of stainless steel mesh (6.5 cm^2 each; AISI 304, 100 mesh; McMaster-Carr, OH) were used as water electrolysis electrodes (E2 and E3) to produce hydrogen and oxygen gas (Fig. 5.1). A cation exchange membrane (6.5 cm^2 area; CMV; AGC Engineering, Japan) was sandwiched between E2 and E3 as a separator to avoid direct oxygen or hydrogen transport between the electrodes. Small incisions were made on the top and bottom of the sandwiched assembly of E2, E3 and the cation exchange membrane to allow unhindered solution distribution throughout the chamber. A Nylon barbed tube fitting (McMaster-Carr, OH) was glued on top of the polypropylene block for the collection of produced gas.

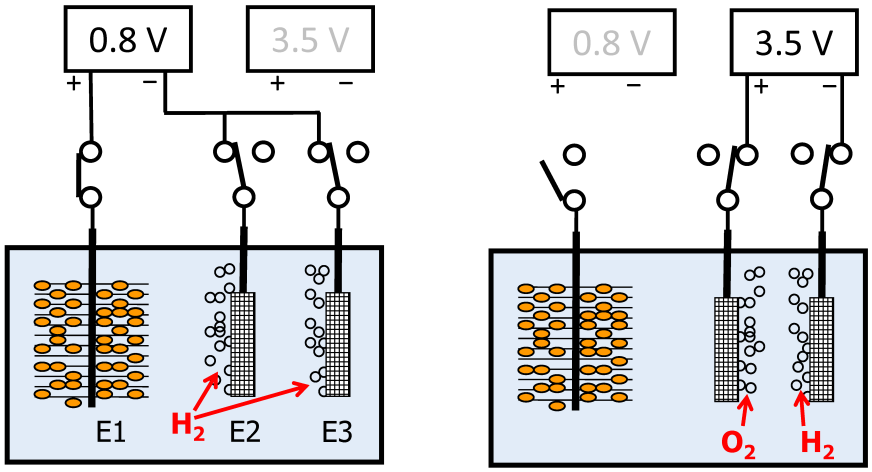

Figure 5.1: Schematic diagram of MEC design and electronic circuit arrangement: (A) Normal operation for H_2 generation and (B) O_2 operation. (E1: bioanode; E2 and E3: water electrolysis electrodes).

5.2.2 MEC operation

The MEC was operated under fed-batch mode (3-4 days per fed-batch cycle) and the MEC operation was divided into two separate stages: Normal and O_2 operations (Fig. 5.1). During the Normal operation, the oxidation of organic

substrates occurs at the bioanode (E1) as shown in Eq. 5.1 while the hydrogen evolution reaction (Eq. 5.2) is induced at E2 and E3 (Fig. 5.1A). The Normal operation lasted for either 6 or 12 hours at a fixed applied potential (E_{ap}) of 0.8 V using a power supply (GPS-1850D; GW Instek, CA).

$$CH_3COO^- + 4H_2O \rightarrow 2HCO_3^- + 9H^+ + 8e^- \quad (5.1)$$

$$2H^+ + 2e^- \rightarrow H_2 \quad (5.2)$$

During the O_2 operation, the bioanode (E1) is disconnected from the circuit while E2 becomes anodic for oxygen production (Eq. 5.3) and E3 works as the cathode for hydrogen evolution (Eq. 5.2) (Fig. 5.1B). To drive the abiotic water electrolysis reactions, the applied potential was relatively high at 3.5 V using another power supplier.

$$2H_2O \rightarrow O_2 + 4H^+ + 4e^- \quad (5.3)$$

The frequency and duration of the O_2 operation were different among the four MECs. MEC1 was the control operated under Normal operation without the O_2 operation; MEC2 was assigned with 12-hr Normal and 5-min O_2 operations; MEC3 with 12-hr Normal and 15-min O_2 operations; and MEC4 with 6-hr Normal and 15-min O_2 operations (Table 5.1) unless otherwise noted.

Table 5.1: MEC operation plan with the Normal and O_2 operations

	Normal operation	**O_2 operation**
MEC1 (Control)	Continuous[a]	None[a]
MEC2	12 hr	5 min
MEC3	12 hr	15 min
MEC4	6 hr	15 min

[a] MEC1 was operated as a control reactor unless otherwise noted.

A 5-min open-circuit condition prior to an O_2 operation and another 15-min open-circuit condition after the O_2 operation were assigned so that residual hydrogen or oxygen is not used as a reactant in following operations. During the open-circuit condition, all of the three electrodes were disconnected from the circuit. Due to the complicated operation layout, an example is provided to show electric current in MEC3 over 60 min. As shown in Fig. 5.2, the Normal operation was terminated at 10 min; MEC3 was disconnected between 10 and 15 min; the O_2 operation at ~30 mA continued for 15 min between 15 and 30 min; another open circuit condition was induced with zero current for 15 min; and the Normal operation resumed at 45 min.

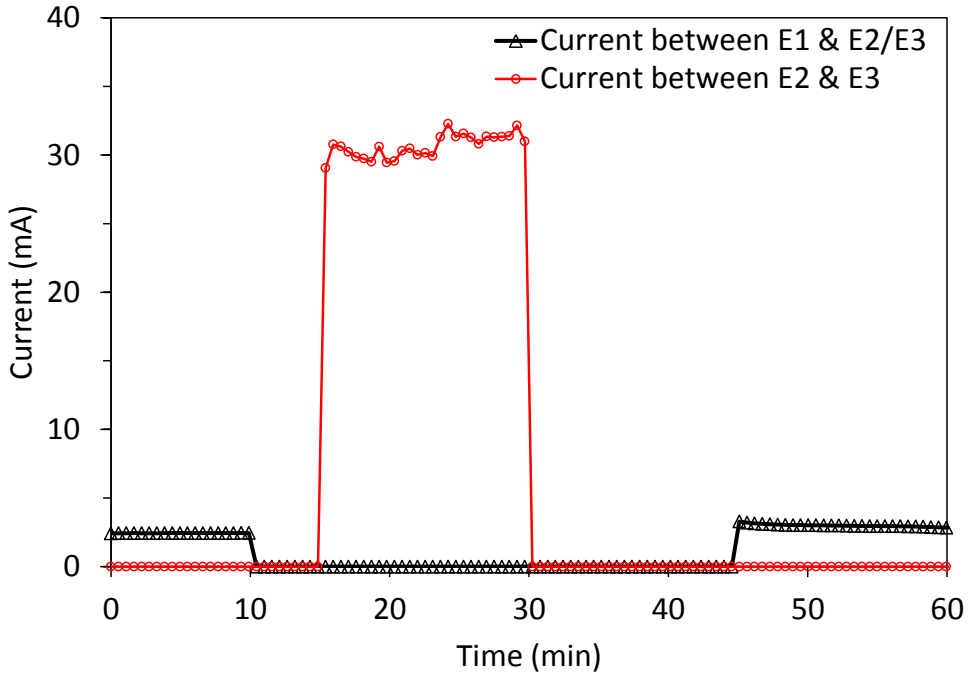

Figure 5.2: An example demonstration of MEC3 operation with the electric current results when a 15-min O_2 operation occurs. The current between E1 and E2/E3 is high during only Normal operation (until 10 min and after 45min). The current between E2 and E3 is high during only O_2 operation (between 15 and 30 min).

An external electronic circuit was built on a standard breadboard using two types of relay switches (DPDP and SPDT; 5VDC-1A; ABRA Electronics, Canada). The relay switches were regulated for the designed connection between the electrodes and power suppliers (Fig. 5.1) using a programmable microcontroller (Mega2560; Arduino, Italy).

5.2.3 Solution preparation

The feed medium for the MECs was prepared with 1 $g \cdot L^{-1}$ sodium acetate in 50 mM phosphate buffer solution (4.7 $g \cdot L^{-1}$ Na_2HPO_4; 0.6 $g \cdot L^{-1}$ $NH_4H_2PO_4$; 1.6 $g \cdot L^{-1}$ KH_2PO_4; 0.4 $g \cdot L^{-1}$ $NaHCO_3$), and trace amounts of vitamins and minerals [110]. In the prepared fresh medium (36 mL), 1 mL effluent from MEC1 (control reactor) was added as a methanogen inoculum. Bicarbonate was purposely added to the phosphate buffer solution to provide a favorable condition for hydrogenotrophic methanogenesis because carbonate species is used as the sole carbon source. It should be noted that chloride was excluded from the medium preparation to prevent the generation of chlorine gas during the O_2 operation.

5.2.4 Experimental measurements

For each cycle, gas was collected in a gas bag (250-mL capacity; Calibrated Instruments Inc., NY). The collected gas was analyzed for CH_4, O_2, N_2 and H_2 by gas chromatography (Varian Star 3400 CX; Agilent Technologies, CA) with a Molecular Sieve 5a column (Chromatographic Specialties Inc., Canada). For the gas chromatography analysis, helium was used as a carrier gas to

maximize the sensitivity of the thermal conductivity detector to CH_4. This selection of the carrier gas significantly decreased the detector sensitivity to H_2; thus analysis results for H_2 were not included in this study. The total volume of gas was determined by the gas bag method as previously described [115].

Electric current in the reactors was determined by measuring the voltage drop every 33 s across an external resistor of 10 Ω using a multimeter and data acquisition system (Model 2700; Keithley Instruments, OH). To quantify the sensitivity of exoelectrogens to oxygen, electric current values during Normal operation were averaged for the first 26 hr of each fed-batch cycle when the bioanode is active with sufficient amounts of organic substrates. All experiments were performed in an air-conditioned laboratory and temperature was stationary over the course of MEC operation at 22.4 ± 0.6 °C.

5.2.5 Oxygen recovery

The oxygen recovery (r_{O2}) was calculated in this study to correlate the effectiveness of methane control with the amount of residual O_2. The oxygen recovery is defined as the ratio between the molar amount of O_2 recovered in the gas bag (n_{O2}) and that produced by water electrolysis during O_2 operation (n_t).

$$r_{O2} = \frac{n_{O2}}{n_t} \qquad (5.4)$$

$$n_t = \frac{\int Idt}{4F} \qquad (5.5)$$

I is the electric current between E2 and E3 during O_2 operation, and F is the Faraday constant (96,485 $C \cdot mol^{-1}$).

5.3 Results and discussion

5.3.1 Methane control in MECs

Methanogenesis was effectively suppressed with periodic production of pure oxygen by water electrolysis. MEC1 (control; no O_2 operation) was quickly dominated by methanogens with methane production greater than 2 mL at the second fed-batch cycle; however, the amount of methane produced in MEC4 (15-min O_2 every 6 hr) was always smaller than 2 mL over 8 fed-batch cycles (30 days) (Fig. 5.3A). With the reduced frequency of O_2 operation in MEC3 (15-min O_2 every 12 hr), methane control was effective below 2 mL over 5 fed-batch cycles (19 days). In addition, the volume of methane produced in MEC4 was always lower by ~1 mL than that in MEC3 when methanogenesis was effectively controlled in both MECs (i.e., Cycles 2 through 5). This comparison indicates that the frequency of O_2 exposure is critical for effective control of methanogenesis in MECs and O_2 operation needs to be performed every 12 hours or more frequently.

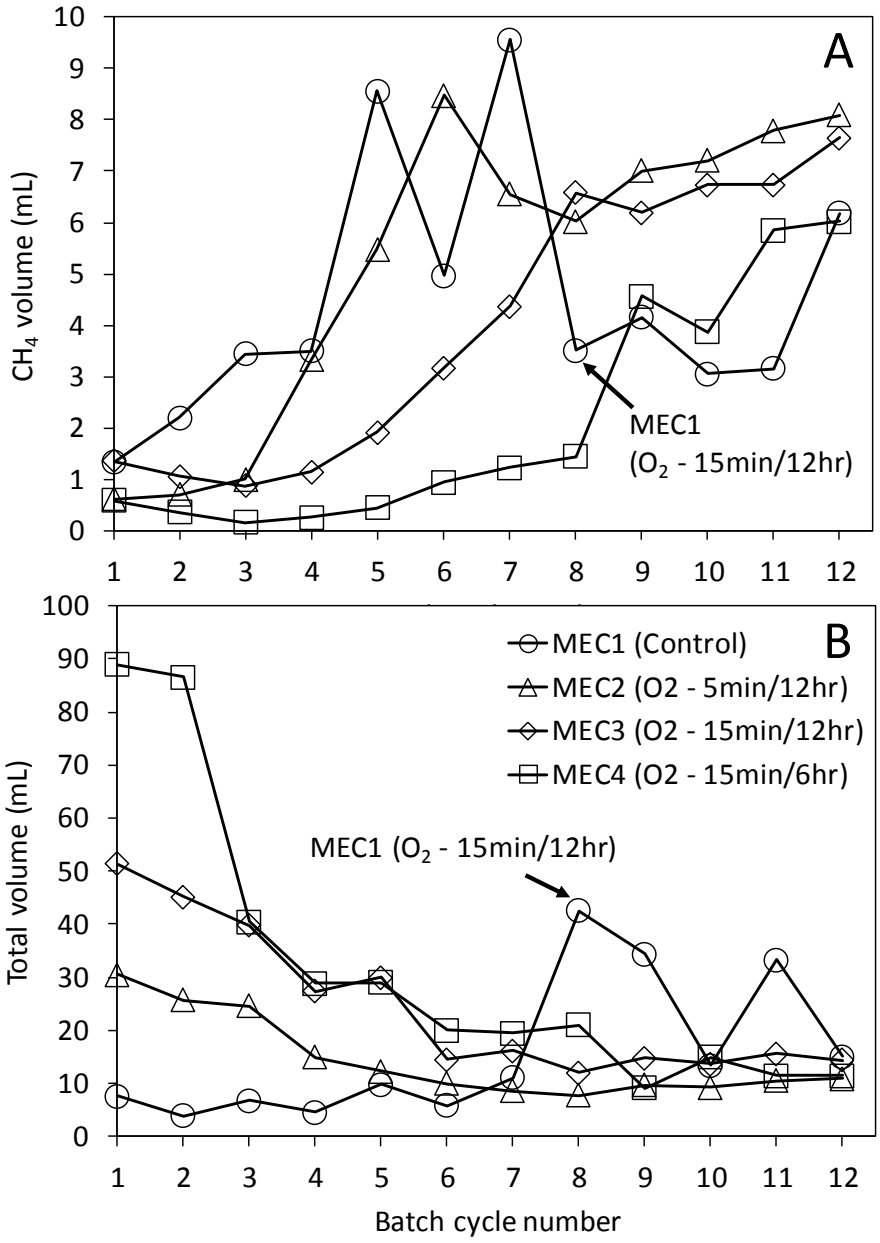

Figure 5.3: (A) Methane production and (B) total gas production from MECs with different schemes for O_2 operation.

Frequent O_2 operation (i.e., every 12 hours or more frequently) is important because hydrogenotrophic methanogens grow very rapidly in MECs. It should be emphasized that MECs are an optimal place for hydrogenotrophic

methanogens with the continuous supply of pure H_2 from the cathode. For instance, hydrogenotrophic methanogens multiply their population (X) by an order of magnitude in 12 hours and by ~7 orders of magnitude in 4 days (Fig. 5.4), indicating frequent O_2 operation is essential for proper methane control. The simulation results (Fig. 5.4) were calculated using the kinetic equation for the growth of methanogens in Anaerobic Digestion Model No. 1 (International Water Association) without the ammonia and pH inhibition terms [131], [132]:

$$\frac{dX}{dt} = \frac{\mu_{max} S X}{K_s + S} - bX \qquad (5.6)$$

X is the methanogen population, t is the time, μ_{max} is the maximum specific growth rate, S is the substrate concentration written in chemical oxygen demand (COD), K_s is the half-saturation constant, and b is the specific microorganism decay rate. Detailed simulation conditions are provided in Table 5.2.

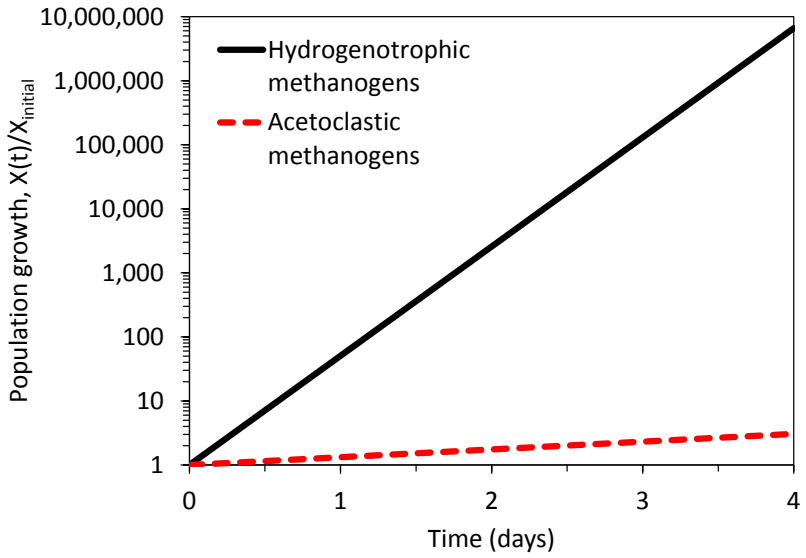

Figure 5.4: Methanogen growth simulated using Anaerobic Digestion Model No. 1. Simulation conditions are given in Table 5.2.

Table 5.2: Mathematical simulation conditions for the estimation of methanogen growth in MECs

	Hydrogenotrophic methanogens	Acetoclastic methanogens
μ_{max} (d^{-1})	4.02[a]	0.357[b]
K_s (mg COD·L^{-1})	0.018[a]	165[b]
b (d^{-1})	0.088[a]	0.015[b]
S (mg COD·L^{-1})	12.48[c]	780[d]

[a] Pavlostathis et al. [133], [134]
[b] Lawrence and McCarty [133], [135]
[c] calculated value using Henry's law constant (1,280 L atm·mol^{-1}) and 1 atm H_2 [34]
[d] calculated value from the initial acetate concentration (12.2 mM CH_3COO^-)

In addition to the frequency, the duration of O_2 operation also governed the effectiveness of methane control in the MECs. Methane production was low (<2 mL) over 5 fed-batch cycles in MEC3 (15-min O_2 every 12 hr) while MEC2 (5-min O_2 every 12 hr) started producing methane greater than 2 mL after Cycle 3 (Fig. 5.3A). This result explains the importance of providing a sufficient amount of O_2 during each O_2 operation event for the inactivation of methanogens in MECs.

This electrolytic O_2 production can also control methanogens in a malfunctioning MEC dominated by methanogenesis. MEC1 became dominated by methanogens after it was operated as the control reactor over 7 fed-batch cycles without O_2 operation. As a result, 86% of the total gas production was methane at Cycle 7 (Fig. 5.3). When the O_2 operation (15-min O_2 every 12 hr) was initiated at Cycle 8, methane production dropped from 9.5 to 3.5 mL (Fig. 5.3A) while the total gas volume increased from 11 to 43 mL (Fig. 5.3B). Also, the suppressed methane production (~3 mL) was maintained for 4 fed-batch

cycles (16 days). This result confirms the effectiveness of pure oxygen to inactivate methanogens in MECs.

5.3.2 Oxygen consumption

Although this method effectively controlled methanogenesis up to approximately one month, all MECs were eventually dominated by methanogens by Cycle 12 (Fig. 5.3A). The reduced effectiveness can be explained by rapid consumption of produced O_2 by biofilms that developed over the MEC operation. The polypropylene reactor body provided a good surface for thick biofilms (Fig. 5.5). Also, the biofilms were firmly attached on reactor surfaces so that they could not be removed with the effluent over fed-batch cycles. The biofilm matrix played two key roles in diminishing the effectiveness of this method: (1) protection of methanogens as previously confirmed [13]; and (2) rapid consumption of produced O_2. During the experiments, visible biofilms were only developed in MECs with O_2 operation, while there was no noticeable biofilm growth in the control reactor (Cycles 1 through 7 in MEC1), implying that the biofilms consist of aerobic microorganisms.

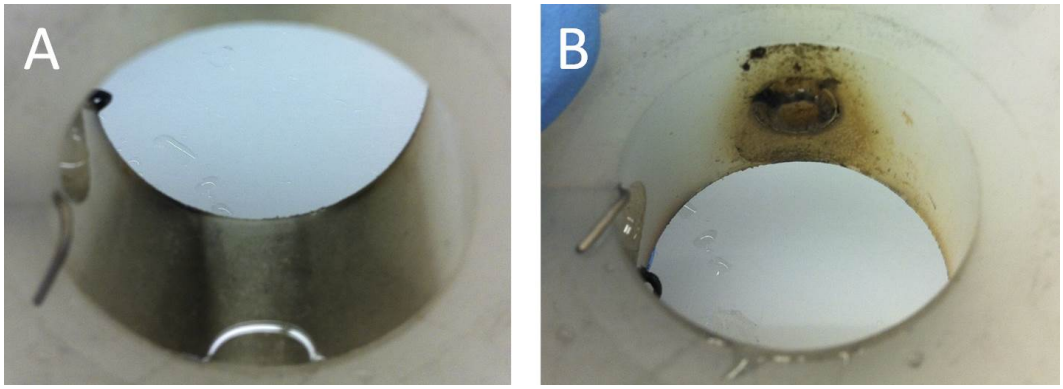

Figure 5.5: Biofilm growth in MEC4 (15-min O_2 every 6 hr): (A) on the bottom of the reactor and (B) on the top surface near the gas collection port.

The oxygen recovery (r_{O2}), the ratio of the amount of O_2 existing in the collected gas to the amount created during O_2 operations (Eq. 5.4), decreased over the first 6 fed-batch cycles for all oxygen-producing MECs (Fig. 5.6A). When all of these MECs were dominated by methanogens (i.e., Cycles 9 through 12), the oxygen recovery plateaued at approximately 25% (MEC2), 20% (MEC3) and 10% (MEC4). This result indicates that O_2 consumption is faster when a greater amount of O_2 was produced. Thus, the rate of O_2 consumption was dominant over the rate of O_2 production, eventually decreasing the effectiveness of this methane controlling method.

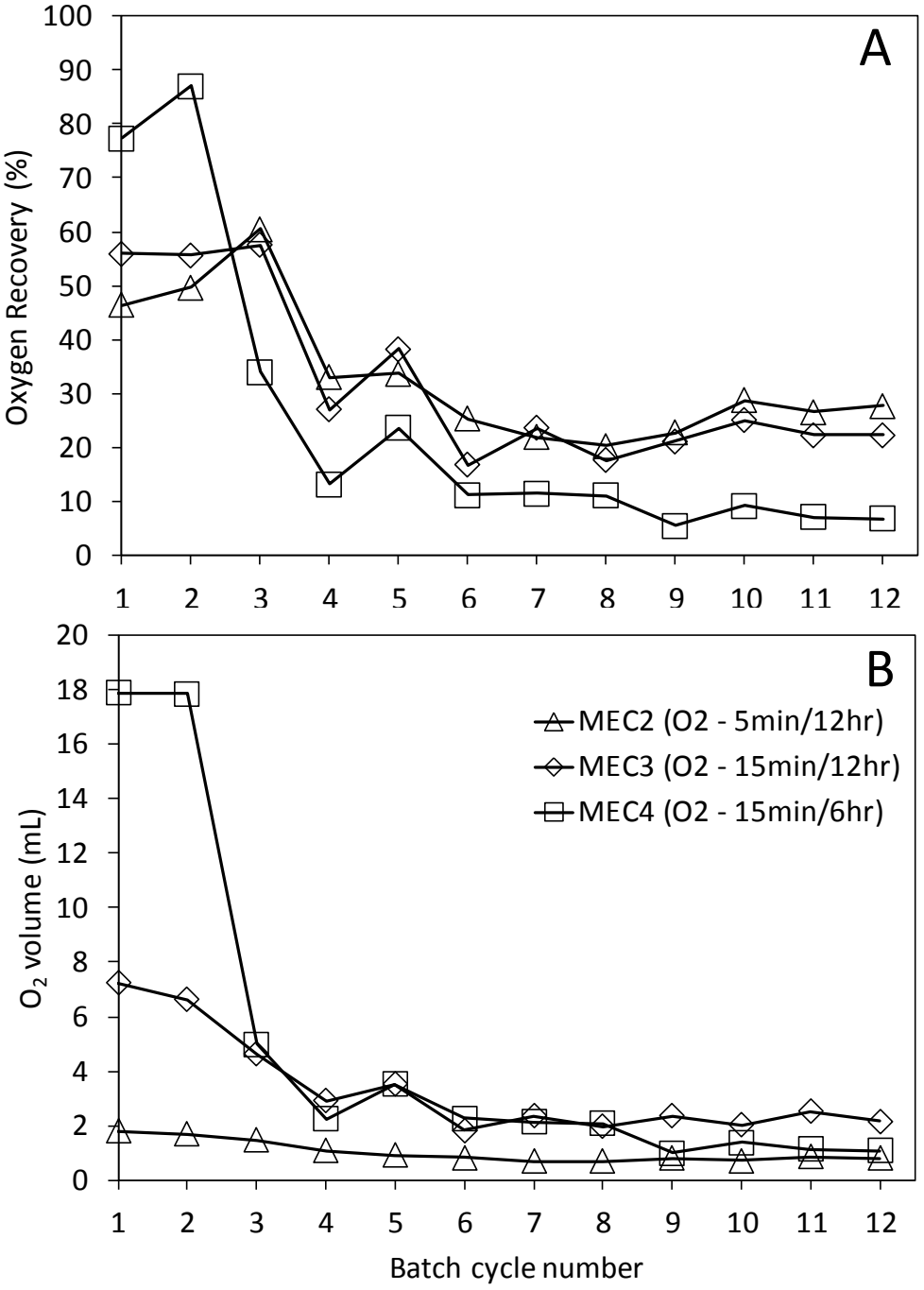

Figure 5.6: (A) Oxygen recovery (r_{O2}) and (B) Oxygen volume measured in the collected gas.

This substantial oxygen consumption was mainly attributed to the growth of the biofilm matrix. When the reactor body was cleaned (note that the anode

brush was kept in the feed solution while the reactor was cleaned), the O_2 recovery was restored and CH_4 production was successfully controlled (not shown). Therefore, biofilms on the reactor surface (Fig. 5.5) were mainly responsible for the rapid O_2 consumption and poor CH_4 control. To avoid or minimize the growth of biofilms, proper surface treatment (e.g., antibiotic coating or regular surface cleaning) is recommended to improve the control of methanogenesis in future studies or practical applications.

5.3.3 Threshold oxygen volume for effective methane control

The effectiveness of methane control was strongly dependent on the volume of O_2 collected in the gas bag. Gas analysis results for all oxygen-producing MECs over the 12 fed-batch cycles were rearranged for the percent CH_4 content as a function of measured O_2 volume collected in the gas bag (Fig. 5.7). When the measured O_2 volume was 3 mL or greater, the methane content was always smaller than 10% of the total volume. This finding implies that there exists a threshold oxygen volume that effectively controls methanogenic activities. O_2 operation at such threshold conditions not only reduces the consumption of electric energy during O_2 operation, but it also minimizes the O_2 exposure to anaerobic exoelectrogens on the bioanode.

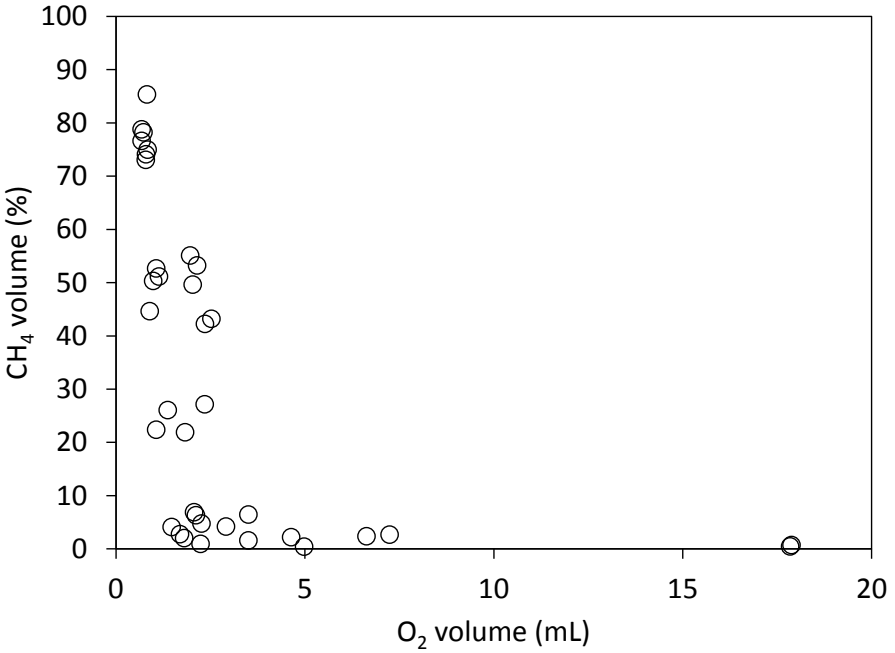

Figure 5.7: Correlation between CH_4 content and O_2 volume. Each data point represents the gas analysis result for an O_2-production MEC (MEC-2, -3 or -4). The gas analysis result was collected over all fed-batch cycles from all O_2 producing MECs and shown here without categorizing by the MEC number or Cycle number.

5.3.4 Hydrogenotrophic vs. acetoclastic methanogenesis

Hydrogenotrophic methanogens are thought to be more responsible for methanogenesis in MECs than acetoclastic methanogens as previously stated in literature [10], [99], [136]. As methane production increased with fed-batch cycles, the total gas production in the reactors decreased. The decrease in the total gas production was more pronounced than the increased methane volume. For instance, the methane volume increased by ~7 mL in MEC3 and the corresponding decrease in the total gas production was ~40 mL (Fig. 5.3). Since the volume of O_2 was always small compared to the total gas volume (Fig. 5.6B), this difference can be explained by hydrogenotrophic methanogenesis where four

H_2 molecules are consumed for the production of one molecule of CH_4 (Eq. 5.7) [100]. Due to the stoichiometry of hydrogenotrophic methanogenesis, the hydrogen yield and purity substantially decrease even with minor methanogenic activities [90].

$$4H_2 + CO_2 \rightarrow CH_4 + 2H_2O \quad (5.7)$$

While hydrogenotrophic methanogenesis is evident based on the gas analysis results, acetoclastic methanogenesis is not expected in this study because the fed-batch cycle was relatively short at 3-4 days. Acetoclastic methanogens require at least 5 days to reach meaningful microbial population for active methanogenesis [14]. Also, the simulation results indicate the microbial population of acetoclastic methanogens was only tripled for 4 days while hydrogenotrophic methanogens multiplied their population by ~7 million times (Fig. 5.4). This quantitative comparison makes it clear that future studies on methane control in MECs should be directed toward inactivating hydrogenotrophic methanogens.

5.3.5 Sensitivity of exoelectrogens to oxygen

The exoelectrogenic activity of the bioanode was adversely affected by O_2 operation. For the O_2-producing MECs (MEC-2, -3 and -4), the average current during Normal operation was 50-70% of the current in MEC1 (Cycles 1 through 7 in Fig. 5.8). In addition, the onset of O_2 operation in MEC1 at Cycle 8 resulted in a drop in the average current from about 3 to 2 mA. This adverse effect on the bioanode performance is consistent with findings in a previous study [12].

However, when O_2 operation was suspended for longer than 12 hours, electric current in the bioanode returned back to the level of the control (not shown). Therefore, the O_2 sensitivity of fully developed bioanodes can be considered as a temporary influence even though the preceding O_2 exposure was repeated continuously for an extended period of time (i.e., longer than a month). In addition, the adverse effect by O_2 exposure can be minimized by placing anti-fouling separator materials (e.g., polyvinyl alcohol separators [137]) between the bioanode and O_2-producing electrode. The anti-fouling property can also mitigate the formation of aerobic biofilms on separator surfaces.

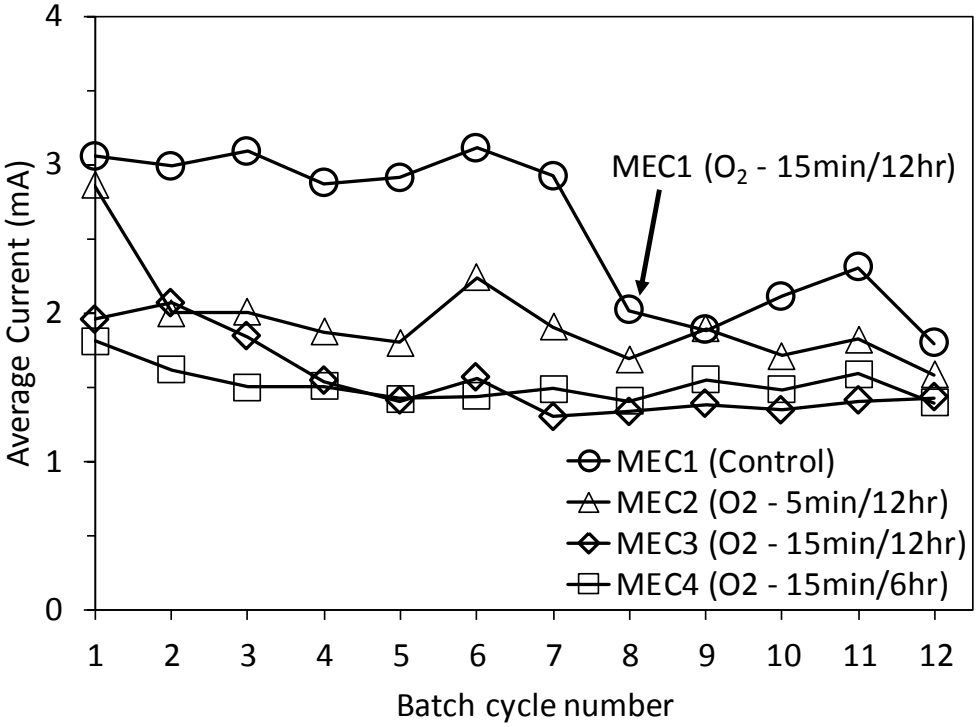

Figure 5.8: Effect of O_2 operation on the current generation from the bioanode during Normal operation.

5.4 Conclusions

The electrolytic O_2 production method developed here can be used to effectively control methanogenesis in MECs. When O_2 operation was set for 15-min every 6 hours, methane production was limited to less than 2 mL for 8 fed-batch cycles (30 days). Comparatively, the control was quickly dominated with methanogens, exceeding 2 mL of methane production after one fed-batch cycle. The optimal frequency of O_2 operation was investigated by increasing the interval of the O_2 operation to every 12 hours. The reduced frequency decreased the timeframe of effective methane control to 5 fed-batch cycles (19 days). This decreased effectiveness was explained by the rapid growth of hydrogenotrophic methanogens with available pure H_2. Therefore, frequent O_2 operation (i.e., every 12 hours or more frequent) is essential for proper methanogen control.

The gradual growth of a biofilm matrix resulted in decreased control of methanogenesis in the oxygen-producing reactors. The biofilm matrix was found to diminish the effectiveness of this method by consuming the produced O_2 rapidly. As a result, the diminished effectiveness coincided with the substantial decrease in oxygen recoveries (r_{O2}) and the formation of thick biofilms in all oxygen-producing reactors. To avoid such biofilm growth, anti-microbial surface treatment or regular cleaning is recommended.

The effectiveness of this method was strongly dependent on the amount of oxygen collected at the end of each fed-batch cycle. When the collected oxygen volume was 3 mL or greater, the methane content was consistently smaller than

10% of the total gas produced. This finding clearly indicates that there exists a threshold amount of residual oxygen that starts controlling methanogenic growth. O_2 operation at this threshold condition can both minimize the consumption of electric energy for pure O_2 generation and reduce the adverse effect of oxygen to exoelectrogenic microorganisms on the bioanode.

The adverse effect of O_2 operation on the exoelectrogen activity was quantified by averaging electric current in the bioanode during Normal operation. The average current in the O_2-producing reactors was approximately 50-70% of the current in the control. To avoid such adverse effects of O_2 on the bioanode performance, it is recommended that anti-fouling materials be used as a separator so that O_2 transfer to the bioanode can be minimized.

The electrolytic oxygen production method offers a practical solution for the methanogenesis problem in MEC applications. This method does not require expensive aeration systems, chemicals or other reactor materials to supply oxygen because the O_2-producing electrode is prepared simply by splitting the H_2-producing MEC cathode into multiple pieces. When aerobic biofilms are effectively controlled, this method can play a key role in establishing the MEC technology for sustainable wastewater treatment and high purity H_2 production.

Acknowledgements

This study was supported by New Faculty Start-up Fund (Faculty of Engineering, McMaster University) and Discovery Grants (Natural Science and Engineering Research Council of Canada). The authors thank Ms. Anna Robertson and Mr. Peter Koudys for their help on equipment operation and reactor construction.

Chapter 6: Conclusions

6.1 Energy efficient nutrient separation

One of the primary objectives of the research reported herein was to demonstrate energy efficient nutrient separation using bioelectrochemical systems. Source-separated human urine is a rich source of nutrients. However, dilution of source-separated urine below the solubility limit of struvite is essential to avoid clogging problems in urine collection system to a centralized treatment facility. Therefore, reconcentration of collected urine is critical above the solubility limit for nutrient recovery. The requirement for nutrient separation was substantially small at 1.6 $MJ \cdot m^{-3}$ (0.44 $kWh \cdot m^{-3}$) when the NSMEC (nutrient separation microbial electrolysis cell) with 3-IEM pairs was operated at the relatively high voltage application (E_{ap} = 1.2 V). This energy requirement is smaller than other conventional treatment processes for urine volume reduction (e.g., electrodialysis reversal, nanofiltration, freeze-thaw and evaporation methods) by up to three orders of magnitude [3]. The NSMEC configuration (a bioelectrochemical system coupled with an IEM stack) offers an energy efficient solution to enable the reconcentration of source separated urine and subsequent or simultaneous recovery of target nutrients as valuable raw materials in the form of struvite.

The NSMEC demonstrated energy efficient nutrient reconcentration and simultaneous COD removal from diluted human urine. The rate of nutrient reconcentration was magnified in the NSMEC with increasing both the number of

IEM pairs and electric voltage application. The target nutrient ions (ammonium and phosphate) were concentrated by a factor of 4.5 and 3.0, respectively (E_{ap} = 1.2 V; 3-IEM pairs). The rate of ammonium separation was consistently faster than the rate of conductivity increase in the concentrate (urine solution that collects ions in the IEM stack), indicating that ammonium ions are favorably separated through cation exchange membranes compared to the other common cations (i.e., sodium). In contrast, separation of phosphate was slow compared to the other major anions in urine (chloride and sulfate). The equivalent ionic conductivity of individual ionic species was found to have a significant impact on the rate of separation of nutrient ions, explaining the rapid separation of ammonium ions and slow concentration of phosphate.

Increasing the diluate volume up to 120 mL at a fixed concentrate volume (20 mL) linearly increased the degree of nutrient reconcentration. However, further increases in the diluate volume did not enhance the reconcentration of nutrients. The limited nutrient reconcentration is mainly due to the relatively low voltage application (E_{ap} = 0.9 V). For complete nutrient recovery and COD removal, it is recommended that NSMEC be operated in multiple stages as previously demonstrated with microbial desalination cells [36].

The high sulfate concentration in human urine provided ideal conditions for the growth of sulfate reducing bacteria. The rate of nutrient reconcentration was not affected by the intensive activity of sulfate reducing bacteria. However, the sulfate reducing microbial activity greatly diminished the energy recovery as

H_2 gas (by H_2-oxidizing sulfate reducers) and Coulombic efficiency (by acetate-oxidizing sulfate reducers). In addition, the H_2-oxidizig sulfate reducing bacteria were found to outcompete hydrogenotrophic methanogens as only a small amount of methane was observed in the gas analysis. If energy recovery is targeted from source-separated urine using strictly anaerobic bioelectrochemical systems (e.g., MECs), sulfate reducing bacteria must be properly controlled in future studies.

6.2 Ammonia inhibition in bioelectrochemical systems

The link between the level of substrate concentration and the threshold level for ammonia inhibition in single-chamber MFCs was investigated. The low substrate condition (0.67 $g \cdot L^{-1}$ sodium acetate) resulted in substantial impairment of current generation at an ammonia concentration of 3,500 mg-$N \cdot L^{-1}$. However, under the high substrate condition (2 $g \cdot L^{-1}$ sodium acetate, every 2-day feed), high current generation was maintained for all TAN concentration tested (up to 4,000 mg-$N \cdot L^{-1}$). Therefore a certain level of substrate concentration should be provided to keep exoelectrogenic bacteria active under high ammonia conditions.

The frequency of substrate feed (i.e., length of fed-batch cycle) was also found to be an important factor as the short fed-batch cycle (2 days) substantially enhanced the capability of exoelectrogenic bacteria to resist against ammonia cytotoxicity. The MFCs fed less frequently (every 6 days) started showing limited current generation at 3,500 mg-$N \cdot L^{-1}$ and low power generation at 2,500 mg-$N \cdot L^{-1}$.

It was determined that the power density curve serves as a better indicator for characterizing ammonia inhibition in bioelectrochemical systems than continuously monitored electric. Although the power density curves and current generation results showed consistent responses to the increasing ammonia concentration during the MFC operation, the ammonia inhibition effect was reflected in power density curves in an early stage of the inhibition while current generation results showed ammonia inhibition after the bioanode was damaged. It is suggested that ammonia inhibition in bioelectrochemical systems be determined using power density curves rather than continuously monitored electric current.

The high current and power generation for the high substrate concentration (2 $g \cdot L^{-1}$ sodium acetate) and frequent substrate feed (2 day fed-batch cycles) clearly demonstrated that the capacity of exoelectrogenic bacteria to resist against high ammonia concentration is substantially enhanced by keeping the substrate concentration high in MFCs. This conclusion along with findings in the previous studies [87]–[89] will allow reliable MFC applications for energy recovery and treatment of agricultural wastewater and source-separated human urine that contain high ammonia concentration

6.3 Methanogenesis in bioelectrochemical systems

The electrolytic O_2 production method developed here can be used to effectively control methanogenesis in MECs. When O_2 operation was set for 15-min every 6 hours, methane production was limited to less than 2 mL for 8 fed-batch cycles (30 days). Comparatively, the control was quickly dominated with

methanogens, exceeding 2 mL of methane production after one fed-batch cycle. The optimal frequency of O_2 operation was investigated by applying the O_2 operation every 6 and 12 hours. The reduced frequency (every 12 hours) decreased the timeframe of effective methane control to 5 fed-batch cycles (19 days). This decreased effectiveness was explained by the rapid growth of hydrogenotrophic methanogens with available pure H_2. Therefore, frequent O_2 operation (i.e., every 12 hours or more frequent) is essential for proper methanogen control.

The gradual growth of a biofilm matrix resulted in decreased control of methanogenesis in the oxygen-producing reactors. The biofilm matrix was found to diminish the effectiveness of this method by consuming the produced O_2 rapidly. As a result, the diminished effectiveness coincided with the substantial decrease in oxygen recoveries (r_{O2}) and the formation of thick biofilms in all oxygen-producing reactors. To avoid such biofilm growth, anti-microbial surface treatment or regular cleaning is recommended.

The effectiveness of this method was strongly dependent on the amount of oxygen collected at the end of each fed-batch cycle. When the collected oxygen volume was 3 mL or greater, the methane content was consistently smaller than 10% of the total gas produced. This finding clearly indicates that there exists a threshold amount of residual oxygen that starts controlling methanogenic growth. O_2 operation at this threshold condition can both minimize the consumption of

electric energy for pure O_2 generation and reduce the adverse effect of oxygen to exoelectrogenic microorganisms on the bioanode.

The adverse effect of O_2 operation on the exoelectrogen activity was quantified by averaging electric current in the bioanode during Normal operation. The average current in the O_2-producing reactors was approximately 50-70% of the current in the control. To avoid such adverse effects of O_2 on the bioanode performance, it is recommended that anti-fouling materials be used as a separator so that O_2 transfer to the bioanode can be minimized.

The electrolytic oxygen production method offers a practical solution for the methanogenesis problem in MEC applications. This method does not require expensive aeration systems, chemicals or other reactor materials to supply oxygen because the O_2-producing electrode is prepared simply by splitting the H_2-producing MEC cathode into multiple pieces. When aerobic biofilms are effectively controlled, this method can play a key role in establishing the MEC technology for sustainable wastewater treatment and high purity H_2 production.

6.4 Significance

The three main objectives of this research were to:

1) Develop an energy efficient method to reconcentrate nutrients in diluted urine;
2) Investigate the link between substrate concentration and the threshold level for ammonia inhibition in bioelectrochemical systems; and

3) Develop an electrolytic oxygen production method as a practical solution for controlling methanogenesis in MEC applications.

As sustainability gains a greater importance in the wastewater treatment industry, more energy efficient processes are being developed. In this research, the development of the NSMEC is a promising step towards recovering nutrients from wastewater, allowing sustainable wastewater treatment. For practical applications of bioelectrochemical systems in wastewater treatment for simultaneous energy recovery, the findings in this study on ammonia inhibition and methanogenesis control will help enhance the robustness and applicability of this bioelectrochemical technology for sustainable wastewater treatment.

6.5 Future work

The reconcentration of nutrients in the NSMEC was one of the primary objectives in this research (Chapter 3). Although struvite precipitation was observed in experiments, the reactor configuration and operation conditions were not optimized for effective struvite production. The system needs to be reexamined with optimized conditions (i.e., ideal magnesium concentration) for struvite precipitation. The extraction of struvite from the NSMEC will require careful consideration as mineral scales on the cathode and IEM surfaces can result in reduced energy efficiency for nutrient recovery with increased electric resistance.

In Chapter 3, the relatively slow separation of phosphate compared to the increase in conductivity was discussed. To improve the performance of the

NSMEC and enhance selective phosphate separation from other common anions (Cl^- and SO_4^{2-}), future studies should focus on possible utilization and development of specialized anion exchange membranes (AEMs) selective for phosphate.

The NSMEC can be constructed using relatively low cost materials. The bioanode can be prepared using carbon materials (e.g., activated carbon granules or graphite fibers). Stainless steel mesh can be used as the cathode without precious metal catalysts. However, relatively high costs for IEMs can be a limiting factor for NSMEC applications in nutrient reconcentration from human urine. Thus, it is suggested that future research be directed toward long-term operation and fouling control in IEM applications [127] so that IEMs can be used in NSMEC reactors for a long time without replacement.

The NSMEC can also be applied for the separation and recovery of heavy metals from wastewater. Preliminary experiments were conducted using the NSMEC; however, initial results were inconclusive and thus they are not incorporated into this research thesis. Additional work on the reactor design and analytical methods needs to be further explored for energy efficient heavy metal removal in wastewater.

List of References

[1] R. D. Cusick and B. E. Logan, "Phosphate recovery as struvite within a single chamber microbial electrolysis cell," *Bioresour. Technol.*, vol. 107, pp. 110–115, 2012.

[2] D. Cordell, J.-O. Drangert, and S. White, "The story of phosphorus: Global food security and food for thought," *Glob. Environ. Chang.*, vol. 19, no. 2, pp. 292–305, May 2009.

[3] M. Maurer, W. Pronk, and T. a Larsen, "Treatment processes for source-separated urine.," *Water Res.*, vol. 40, no. 17, pp. 3151–66, Oct. 2006.

[4] T. Larsen, A. Alder, R. Eggen, M. Maurer, and J. Lienert, "Source Separation: Will We See a Paradigm Shift in Wastewater Handling?," *Environ. Sci. Technol.*, vol. 43, no. 16, pp. 6121–6125, 2009.

[5] B. Logan, D. Call, S. Cheng, H. Hamelers, T. Sleutels, A. Jeremiasse, and R. Rozendal, "Microbial Electrolysis Cells for High Yield Hydrogen Gas Production from Organic Matter," ... *Sci. Technol.*, vol. 42, no. 23, pp. 8630–8640, 2008.

[6] H. Liu, S. Grot, and B. E. Logan, "Electrochemically assisted microbial production of hydrogen from acetate.," *Environ. Sci. Technol.*, vol. 39, no. 11, pp. 4317–4320, Jun. 2005.

[7] R. Rozendal and C. Buisman, "Process for producing hydrogen," WO2005005981, 2005.

[8] R. Rozendal, H. Hamelers, G. Euverink, S. Metz, and C. Buisman, "Principle and perspectives of hydrogen production through biocatalyzed electrolysis," *Int. J. Hydrogen Energy*, vol. 31, no. 12, pp. 1632–1640, Sep. 2006.

[9] X. Cao, X. Huang, P. Liang, K. Xiao, Y. Zhou, X. Zhang, and B. E. Logan, "A new method for water desalination using microbial desalination cells.," *Environ. Sci. Technol.*, vol. 43, no. 18, pp. 7148–7152, Sep. 2009.

[10] H. Hu, Y. Fan, and H. Liu, "Hydrogen production using single-chamber membrane-free microbial electrolysis cells.," *Water Res.*, vol. 42, no. 15, pp. 4172–4178, Sep. 2008.

[11] K.-J. Chae, M.-J. Choi, K.-Y. Kim, F. F. Ajayi, W. Park, C.-W. Kim, and I. S. Kim, "Methanogenesis control by employing various environmental stress conditions in two-chambered microbial fuel cells.," *Bioresour. Technol.*, vol. 101, no. 14, pp. 5350–5357, Jul. 2010.

[12] K.-J. Chae, M.-J. Choi, K.-Y. Kim, F. F. Ajayi, I.-S. Chang, and I. S. Kim, "Selective inhibition of methanogens for the improvement of biohydrogen production in microbial electrolysis cells," *Int. J. Hydrogen Energy*, vol. 35, no. 24, pp. 13379–13386, Dec. 2010.

[13] F. F. Ajayi, K.-Y. Kim, K.-J. Chae, M.-J. Choi, and I. S. Kim, "Effect of hydrodymamic force and prolonged oxygen exposure on the performance of anodic biofilm in microbial electrolysis cells," *Int. J. Hydrogen Energy*, vol. 35, no. 8, pp. 3206–3213, Apr. 2010.

[14] C. Grady Jr., G. Daigger, N. Love, and C. Filipe, *Biological wastewater treatment*, 3rd ed. Florida: Taylor and Francis Group, 2011.

[15] Metcalf and Eddy, *Wastewater Engineering: Treatment and Reuse*, 4th ed. New York: McGraw-Hill Higher Education, 2004.

[16] E. Kvarnstrom, K. Emilsson, A. Stintzing, M. Johansson, H. Jonsson, E. Petersens, C. Schonning, J. Christensen, D. Hellstrom, L. Qvarnstrom, P. Ridderstolpe, and J. Drangert, *Urine Diversion: One Step Towards Sustainable Sanitation*. Stockholm Environment Institute, 2006.

[17] P. Kuntke, K. Śmiech, and H. Bruning, "Ammonium recovery and energy production from urine by a microbial fuel cell," *water Res.*, vol. 46, no. 8, pp. 2627–2636, May 2012.

[18] K. M. Udert, T. a Larsen, M. Biebow, and W. Gujer, "Urea hydrolysis and precipitation dynamics in a urine-collecting system.," *Water Res.*, vol. 37, no. 11, pp. 2571–2582, Jun. 2003.

[19] K. Udert, T. Larsen, and W. Gujer, "Biologically induced precipitation in urine-collecting systems," *Water Sci. Technol. Water Supply*, vol. 3, pp. 71–78, 2003.

[20] W. Pronk, M. Biebow, and M. Boller, "Electrodialysis for recovering salts from a urine solution containing micropollutants," *Environ. Sci. ...*, vol. 40, no. 7, pp. 2414–2420, 2006.

[21] P. Wieland, "Designing for human presence in space - an introduction to environmental control and life support systems," 1994.

[22] P. Holland, D. Bird, and C. Miller, "Extraction of potable water from urine for space applications," *Am. Soc. Civ. Eng.*, vol. 2, pp. 1680–1689, 1992.

[23] F. Wood, "The changing face of desalination - a consulting engineer's viewpoint," *Desalination*, vol. 42, pp. 17–25, 1982.

[24] B. Lind, Z. Ban, and S. Byde, "Volume reduction and concentration of nutrients in human urine," *Ecol. Eng.*, vol. 16, pp. 561–566, 2001.

[25] H. Gulyas, P. Bruhn, M. Furmanska, K. Hartrampf, K. Kot, B. Lüttenberg, Z. Mahmood, K. Stelmaszewska, and R. Otterpohl, "Freeze concentration for enrichment of nutrients in yellow water from no-mix toilets.," *Water Sci. Technol.*, vol. 50, no. 6, pp. 61–68, Jan. 2004.

[26] L. Thorneby, K. Persson, and G. Tragardh, "Treatment of liquid effluents from dairy cattle and pigs using reverse osmosis," *J. Agric. Eng. Res.*, vol. 73, no. 2, pp. 159–170, 1999.

[27] J. Hofman, E. Beerendonk, H. Folmer, and J. Kruithof, "Removal of pesticides and other micropollutants with cellulose-acetate, polyamide and ultra-low pressure reverse osmosis membranes," *Desalination*, vol. 113, pp. 209–214, 1997.

[28] A. Al-Rammah, "The application of acid free antiscalent to mitigate scaling in reverse osmosis membranes," *Desalination*, vol. 132, pp. 83–87, 2000.

[29] L. F. Greenlee, D. F. Lawler, B. D. Freeman, B. Marrot, and P. Moulin, "Reverse osmosis desalination: water sources, technology, and today's challenges.," *Water Res.*, vol. 43, no. 9, pp. 2317–2348, May 2009.

[30] A. E. Jaffer, "The application of a novel chemical treatment program to mitigate scaling and fouling in reverse osmosis units," *Desalination*, vol. 96, no. 1–3, pp. 71–79, Jun. 1994.

[31] H. Strathmann, *Ion-exchange membrane separation processes*. Amsterdam: Elsevier B.V., 2004.

[32] S. Cheng and B. Logan, "Sustainable and efficient biohydrogen production via electrohydrogenesis," *Proc. Natl. Acad. Sci.*, vol. 104, no. 47, pp. 18871–18873, 2007.

[33] D. Call and B. E. Logan, "Hydrogen production in a single chamber microbial electrolysis cell lacking a membrane.," *Environ. Sci. Technol.*, vol. 42, no. 9, pp. 3401–3406, May 2008.

[34] M. Benjamin and D. Lawler, *Water quality engineering: physical / chemical treatment processes*. Hoboken, NJ: John Wiley & Sons, 2013.

[35] X. Chen, X. Xia, P. Liang, X. Cao, H. Sun, and X. Huang, "Stacked microbial desalination cells to enhance water desalination efficiency.," *Environ. Sci. Technol.*, vol. 45, no. 6, pp. 2465–2470, Mar. 2011.

[36] Y. Kim and B. E. Logan, "Series assembly of microbial desalination cells containing stacked electrodialysis cells for partial or complete seawater desalination.," *Environ. Sci. Technol.*, vol. 45, no. 13, pp. 5840–5845, Jul. 2011.

[37] J. D. Doyle and S. a Parsons, "Struvite formation, control and recovery.," *Water Res.*, vol. 36, no. 16, pp. 3925–40, Sep. 2002.

[38] K. N. Ohlinger, T. M. Young, and E. D. Schroeder, "Predicting struvite formation in digestion," *Water Res.*, vol. 32, no. 12, pp. 3607–3614, Dec. 1998.

[39] V. L. Snoeyink and D. Jenkins, *Water Chemistry*. John Wiley, 1980.

[40] W. Stumm and J. Morgan, *Aquatic Chemistry*. New York: Wiley-Interscience, 1970.

[41] A. Taylor, A. Frazier, and E. Gurney, "Solubility Products of Magnesium Ammonium and Magnesium Potassium Phosphates," *Trans. Faraday ...*, pp. 1580–1584, 1963.

[42] J. R. Burns and B. Finlayson, "Solubility product of magnesium ammonium phosphate hexahydrate at various temperatures," *J. Urol.*, vol. 128, no. 2, pp. 426–428, 1982.

[43] C. V Booram, S. R. J, and H. T. E, "Crystalline phosphate precipitation from anaerobic animal waste treatment lagoon liquors," *Trans. ASAE*, vol. 18, 1975.

[44] R. Loewenthal, "Modelling struvite precipitation in anaerobic treatment systems," *Water Sci. ...*, 1994.

[45] D. Mamais, P. Pitt, and Y. Cheng, "Determination of ferric chloride dose to control struvite precipitation in anaerobic sludge digesters," *Water Environ. ...*, 1994.

[46] G. Bridger, "Micronutrient sources, Metal Ammonium Phosphates as Fertilizers," *J. Agric. ...*, vol. 10, no. 3, pp. 181–188, 1962.

[47] a. E. Durrant, M. D. Scrimshaw, I. Stratful, and J. N. Lester, "Review of the Feasibility of Recovering Phosphate from Wastewater for Use as a Raw Material by the Phosphate Industry," *Environ. Technol.*, vol. 20, no. 7, pp. 749–758, Jul. 1999.

[48] N. O. Nelson, R. L. Mikkelsen, and D. L. Hesterberg, "Struvite precipitation in anaerobic swine lagoon liquid: effect of pH and Mg:P ratio and determination of rate constant," *Bioresour. Technol.*, vol. 89, no. 3, pp. 229–236, Sep. 2003.

[49] W. Schipper and A. Klapwijk, "Phosphate recycling in the phosphorus industry," *Environ. ...*, vol. 22, pp. 1337–1345, 2001.

[50] a. E. Johnston and I. R. Richards, "Effectiveness of the water-insoluble component of triple superphosphate for yield and phosphorus uptake by plants," *J. Agric. Sci.*, vol. 140, no. 3, pp. 267–274, May 2003.

[51] H. K. Aage, B. L. Andersen, A. Biota, and I. Jensen, "The solubility of struvite," vol. 223, pp. 213–215, 1997.

[52] P. Battistoni, G. Fava, P. Pavan, A. Musacco, and F. Cecchi, "Phosphate removal in anaerobic liquors by struvite crystallization without addition of chemicals: preliminary results," *Water Res.*, vol. 31, no. 11, pp. 2925–2929, 1997.

[53] Y. Jaffer, T. a Clark, P. Pearce, and S. a Parsons, "Potential phosphorus recovery by struvite formation.," *Water Res.*, vol. 36, no. 7, pp. 1834–42, Apr. 2002.

[54] A. Adnan, M. Dastur, D. S. Mavinic, and F. A. Koch, "Preliminary investigation into factors affecting controlled struvite crystallization at the bench scale," vol. 202, pp. 195–202, 2004.

[55] Q. Wu, P. L. Bishop, and T. C. Keener, "A strategy for controlling deposition of struvite in municipal wastewater treatment plants.," *Water Environ. Res.*, vol. 77, no. 2, pp. 199–207.

[56] M. Hanhoun, L. Montastruc, C. Azzaro-Pantel, B. Biscans, M. Frèche, and L. Pibouleau, "Temperature impact assessment on struvite solubility product: A thermodynamic modeling approach," *Chem. Eng. J.*, vol. 167, no. 1, pp. 50–58, Feb. 2011.

[57] N. C. Bouropoulos and P. G. Koutsoukos, "Spontaneous precipitation of struvite from aqueous solutions," vol. 213, pp. 381–388, 2000.

[58] J. W. Mullin, *Crystallization*. Butterworth-Heinemann, 2001.

[59] J. Borgerding, "Phosphate deposits in digestion systems," *J. Water Pollut. Control Fed.*, vol. 44, no. 5, pp. 813–819, 1972.

[60] F. Abbona, H. E. Lundager Madsen, and R. Boistelle, "Crystallization of two magnesium phosphates, struvite and newberyite: effect of pH and concentration," *J. Cryst. Growth*, vol. 57, pp. 6–14, 1982.

[61] J. R. Buchanan, C. R. Mote, and R. B. Robinson, "Struvite control by chemical treatment," *Trans. ASAE*, vol. 37, 1994.

[62] J. R. Buchanan, C. R. Mote, and R. B. Robinson, "Thermodynamics of struvite formation," *Trans. ASAE*, vol. 37, 1994.

[63] E. V Musvoto, M. C. M. Wentzel, R. E. Loewenthal, and G. A. M. Ekama, "Integrated chemical-physical process modelling-I. Development of a kinetic-based model for mixed weak acid/base systems," *Water Res.*, vol. 34, no. 6, 2000.

[64] E. V Musvoto, M. C. M. Wentzel, and G. A. M. Ekama, "Integrated chemical-physical processes modeilling-II. Simulating aeration treatment of anaerobic digester supernatants," *Water Res.*, vol. 34, no. 6, pp. 1868–1880, 2000.

[65] N. a. Booker, a. J. Priestley, and I. H. Fraser, "Struvite Formation in Wastewater Treatment Plants: Opportunities for Nutrient Recovery," *Environ. Technol.*, vol. 20, no. 7, pp. 777–782, Jul. 1999.

[66] G. A. Momberg and R. A. Oellermann, "The removal of phosphate by hydroxyapatite and struvite crystallisation in South Africa," *Water Sci. Technol.*, vol. 26, no. 5–6, pp. 987–996, 1992.

[67] K. S. Le Corre, E. Valsami-Jones, P. Hobbs, and S. a. Parsons, "Impact of calcium on struvite crystal size, shape and purity," *J. Cryst. Growth*, vol. 283, no. 3–4, pp. 514–522, Oct. 2005.

[68] D. Wild, A. Kisliakova, and H. Siegrist, "P-Fixation by Mg, Ca and zeolite a during stabilization of excess sludge from enhanced biological p-removal," *Water Sci. Technol.*, vol. 34, no. 1–2, pp. 391–398, 1996.

[69] P. Battistoni, P. Pavan, M. Prisciandaro, and F. Cecchi, "Struvite crystallization: a feasible and reliable way to fix phosphorus in anaerobic supernatants," *Water Res.*, vol. 34, no. 11, 2000.

[70] A. N. Kofina, K. D. Demadis, and P. G. Koutsoukos, "The Effect of Citrate and Phosphocitrate On Struvite Spontaneous Precipitation," *Cryst. Growth Des.*, vol. 7, no. 12, pp. 2705–2712, Dec. 2007.

[71] S. Cheng, H. Liu, and B. E. Logan, "Increased performance of single-chamber microbial fuel cells using an improved cathode structure," *Electrochem. commun.*, vol. 8, no. 3, pp. 489–494, Mar. 2006.

[72] L. Gil-Carrera, P. Mehta, A. Escapa, A. Morán, V. García, S. R. Guiot, and B. Tartakovsky, "Optimizing the electrode size and arrangement in a microbial electrolysis cell.," *Bioresour. Technol.*, vol. 102, no. 20, pp. 9593–9598, Oct. 2011.

[73] H. Hu, Y. Fan, and H. Liu, "Hydrogen production in single-chamber tubular microbial electrolysis cells using non-precious-metal catalysts," *Int. J. Hydrogen Energy*, vol. 34, no. 20, pp. 8535–8542, Oct. 2009.

[74] A. Ter Heijne, F. Liu, L. S. van Rijnsoever, M. Saakes, H. V. M. Hamelers, and C. J. N. Buisman, "Performance of a scaled-up Microbial Fuel Cell with iron reduction as the cathode reaction," *J. Power Sources*, vol. 196, no. 18, pp. 7572–7577, Sep. 2011.

[75] D. Jiang, M. Curtis, E. Troop, K. Scheible, J. McGrath, B. Hu, S. Suib, D. Raymond, and B. Li, "A pilot-scale study on utilizing multi-anode/cathode microbial fuel cells (MAC MFCs) to enhance the power production in wastewater treatment," *Int. J. Hydrogen Energy*, vol. 36, no. 1, pp. 876–884, Jan. 2011.

[76] A. Dewan, H. Beyenal, and Z. Lewandowski, "Scaling up microbial fuel cells.," *Environ. Sci. Technol.*, vol. 42, no. 20, pp. 7643–7648, Oct. 2008.

[77] A. Dekker, A. Ter Heijne, M. Saakes, H. V. M. Hamelers, and C. J. N. Buisman, "Analysis and improvement of a scaled-up and stacked microbial fuel cell.," *Environ. Sci. Technol.*, vol. 43, no. 23, pp. 9038–9042, Dec. 2009.

[78] B. Logan, B. Hamelers, R. Rozendal, U. Schroder, J. Keller, S. Freguia, P. Aelterman, W. Verstraete, and K. Rabaey, "Microbial Fuel Cells: Methodology and Technology," *Environ. Sci. Technol.*, vol. 40, no. 17, pp. 5181–5192, 2006.

[79] H. Liu and B. E. Logan, "Electricity generation using an air-cathode single chamber microbial fuel cell in the presence and absence of a proton exchange membrane," *Environ. Sci. Technol.*, vol. 38, no. 14, pp. 4040–4046, Jul. 2004.

[80] J. Jiang, Q. Zhao, J. Zhang, G. Zhang, and D.-J. Lee, "Electricity generation from bio-treatment of sewage sludge with microbial fuel cell.," *Bioresour. Technol.*, vol. 100, no. 23, pp. 5808–5812, Dec. 2009.

[81] J. R. Kim, J. Dec, M. A. Bruns, and B. E. Logan, "Removal of odors from Swine wastewater by using microbial fuel cells," *Appl. Environ. Microbiol.*, vol. 74, no. 8, pp. 2540–2543, Apr. 2008.

[82] T. Müller, B. Walter, A. Wirtz, and A. Burkovski, "Ammonium toxicity in bacteria," *Curr. Microbiol.*, vol. 52, no. 5, pp. 400–406, May 2006.

[83] B. E. Rittmann and P. McCarty, *Environmental Biotechnology: Principles and Applications*. McGraw-Hill Higher Education, 2001.

[84] G. D. Sprott, K. M. Shaw, and K. F. Jarrell, "Ammonia/potassium exchange in methanogenic bacteria," *J. Biol. Chem.*, vol. 259, no. 20, pp. 12602–12608, Oct. 1984.

[85] P. C. Kadam and D. R. Boone, "Influence of pH on Ammonia Accumulation and Toxicity in Halophilic, Methylotrophic Methanogens," *Appl. Environ. Microbiol.*, vol. 62, no. 12, pp. 4486–4492, 1996.

[86] L. De Baere, M. Devocht, P. Van Assche, and W. Verstraete, "Influence of high NaCl and NH4Cl salt levels on methanogenic associations," *Water Res.*, vol. 18, no. 5, pp. 543–548, 1984.

[87] J. Y. Nam, H. W. Kim, and H. S. Shin, "Ammonia inhibition of electricity generation in single-chambered microbial fuel cells," *J. Power Sources*, vol. 195, no. 19, pp. 6428–6433, Oct. 2010.

[88] H. W. Kim, J. Y. Nam, and H. S. Shin, "Ammonia inhibition and microbial adaptation in continuous single-chamber microbial fuel cells," *J. Power Sources*, vol. 196, no. 15, pp. 6210–6213, Aug. 2011.

[89] P. Kuntke, M. Geleji, H. Bruning, G. Zeeman, H. V. M. Hamelers, and C. J. N. Buisman, "Effects of ammonium concentration and charge exchange on ammonium recovery from high strength wastewater using a microbial fuel cell," *Bioresour. Technol.*, vol. 102, no. 6, pp. 4376–4382, Mar. 2011.

[90] P. Clauwaert and W. Verstraete, "Methanogenesis in membraneless microbial electrolysis cells.," *Appl. Microbiol. Biotechnol.*, vol. 82, no. 5, pp. 829–836, Apr. 2009.

[91] A. Wang, W. Liu, S. Cheng, D. Xing, J. Zhou, and B. E. Logan, "Source of methane and methods to control its formation in single chamber microbial electrolysis cells," *Int. J. Hydrogen Energy*, vol. 34, no. 9, pp. 3653–3658, May 2009.

[92] H. Zhu, W. Parker, D. Conidi, R. Basnar, and P. Seto, "Eliminating methanogenic activity in hydrogen reactor to improve biogas production in a two-stage anaerobic digestion process co-digesting municipal food waste and sewage sludge.," *Bioresour. Technol.*, vol. 102, no. 14, pp. 7086–7092, Jul. 2011.

[93] R. D. Cusick, B. Bryan, D. S. Parker, M. D. Merrill, M. Mehanna, P. D. Kiely, G. Liu, and B. E. Logan, "Performance of a pilot-scale continuous flow microbial electrolysis cell fed winery wastewater.," *Appl. Microbiol. Biotechnol.*, vol. 89, no. 6, pp. 2053–2063, Mar. 2011.

[94] R. D. Cusick, P. D. Kiely, and B. E. Logan, "A monetary comparison of energy recovered from microbial fuel cells and microbial electrolysis cells fed winery or domestic wastewaters," *Int. J. Hydrogen Energy*, vol. 35, no. 17, pp. 8855–8861, Sep. 2010.

[95] H. Liu, J. Wang, A. Wang, and J. Chen, "Chemical inhibitors of methanogenesis and putative applications.," *Appl. Microbiol. Biotechnol.*, vol. 89, no. 5, pp. 1333–1340, Mar. 2011.

[96] K. Xu, H. Liu, X. Li, J. Chen, and A. Wang, "Typical methanogenic inhibitors can considerably alter bacterial populations and affect the interaction between fatty acid degraders and homoacetogens.," *Appl. Microbiol. Biotechnol.*, vol. 87, no. 6, pp. 2267–2279, Aug. 2010.

[97] Y. Chen, J. J. Cheng, and K. S. Creamer, "Inhibition of anaerobic digestion process: a review.," *Bioresour. Technol.*, vol. 99, no. 10, pp. 4044–4064, Jul. 2008.

[98] R. Dumitru, H. Palencia, S. Schroeder, B. DeMontigny, J. Takacs, M. Rasche, J. Miner, and W. Ragsdale, "Targeting Methanopterin Biosynthesis To Inhibit Methanogenesis," *Appl. Environ. Microbiol.*, vol. 69, no. 12, pp. 7236–7241, 2003.

[99] H.-S. Lee, W. F. J. Vermaas, and B. E. Rittmann, "Biological hydrogen production: prospects and challenges.," *Trends Biotechnol.*, vol. 28, no. 5, pp. 262–271, May 2010.

[100] M. Madigan and J. Martinko, *Brock biology of microorganisms*, 11th ed. New Jersey: Pearson Education Inc., 2006.

[101] H. Liu, S. Cheng, and B. E. Logan, "Production of electricity from acetate or butyrate using a single-chamber microbial fuel cell.," *Environ. Sci. Technol.*, vol. 39, no. 2, pp. 658–662, Jan. 2005.

[102] X. Wang, S. Cheng, Y. Feng, M. D. Merrill, T. Saito, and B. E. Logan, "Use of carbon mesh anodes and the effect of different pretreatment methods on power production in microbial fuel cells.," *Environ. Sci. Technol.*, vol. 43, no. 17, pp. 6870–4, Sep. 2009.

[103] R. C. Tice and Y. Kim, "Methanogenesis control by electrolytic oxygen production in microbial electrolysis cells," *Int. J. Hydrogen Energy*, vol. 39, no. 7, pp. 3079–3086, Feb. 2014.

[104] R. Davis, Y. Kim, and B. Logan, "Increasing Desalination by Mitigating Anolyte pH Imbalance Using Catholyte Effluent Addition in a Multi-Anode Bench Scale Microbial Desalination Cell," *ACS Sustain. Chem. …*, pp. 1200–1206, 2013.

[105] Y. Qu, Y. Feng, X. Wang, J. Liu, J. Lv, W. He, and B. E. Logan, "Simultaneous water desalination and electricity generation in a microbial desalination cell with electrolyte recirculation for pH control.," *Bioresour. Technol.*, vol. 106, pp. 89–94, Feb. 2012.

[106] J. Hole, *Human Anatomy and Physiology*, 2nd ed. McGraw-Hill Higher Education, 1981.

[107] A. Chang, H. Hawley, L. Katz, N. Piotrowski, and C. Rizzo, Eds., *Magill's Medical Guide Volume III*. Englewood Cliffs, NJ: Salem Press, 1998.

[108] USEPA, "WaterSense specification for flushing urinals; Version 1.0." 2009.

[109] USEPA, "WaterSense specification for tank-type toilets; Version 1.1." 2011.

[110] S. Cheng, D. Xing, D. F. Call, and B. E. Logan, "Direct biological conversion of electrical current into methane by electromethanogenesis.," *Environ. Sci. Technol.*, vol. 43, no. 10, pp. 3953–3958, May 2009.

[111] H. Jönsson, T. Stenström, J. Svensson, and A. Sundin, "Source separated urine-nutrient and heavy metal content, water saving and fecal contamination," *Water Sci. Technol.*, vol. 35, no. 9, pp. 145–152, 1997.

[112] K. M. Udert, T. a Larsen, and W. Gujer, "Estimating the precipitation potential in urine-collecting systems.," *Water Res.*, vol. 37, no. 11, pp. 2667–2677, Jun. 2003.

[113] W. Pronk, H. Palmquist, M. Biebow, and M. Boller, "Nanofiltration for the separation of pharmaceuticals from nutrients in source-separated urine.," *Water Res.*, vol. 40, no. 7, pp. 1405–1412, Apr. 2006.

[114] American Water Works Association and Water Environment Federation, *APHA (American Public Health Association). Standard Methods for examination of Water and Wastewater*, 21st ed. Washington DC, 2005.

[115] J. R. Ambler and B. E. Logan, "Evaluation of stainless steel cathodes and a bicarbonate buffer for hydrogen production in microbial electrolysis cells using a new method for measuring gas production," *Int. J. Hydrogen Energy*, vol. 36, no. 1, pp. 160–166, Jan. 2011.

[116] D. Lide, Ed., *CRC Handbook of Chemistry and Physics*, 89th ed. Cleveland: CRC Press, 2008.

[117] Y. Kim and B. E. Logan, "Microbial desalination cells for energy production and desalination," *Desalination*, vol. 308, pp. 122–130, Jan. 2013.

[118] M. Coma, S. Puig, N. Pous, M. D. Balaguer, and J. Colprim, "Biocatalysed sulphate removal in a BES cathode.," *Bioresour. Technol.*, vol. 130, pp. 218–23, Feb. 2013.

[119] K. Rabaey, P. Clauwaert, P. Aelterman, and W. Verstraete, "Tubular microbial fuel cells for efficient electricity generation.," *Environ. Sci. Technol.*, vol. 39, no. 20, pp. 8077–8082, Oct. 2005.

[120] K. Rabaey, K. Van De Sompel, L. Maignien, N. Boon, P. Aelterman, P. Clauwaert, L. De Schamphelaire, H. Pham, P. Lens, and W. Verstraete, "Microbial Fuel Cells for Sulfide Removal," *Environ. Sci. Technol.*, vol. 40, no. 17, pp. 5218–5224, 2006.

[121] S. Elferink, A. Visser, L. Pol, and J. Stams, "Sulfate reduction in methanogenic bioreactors," *FEMS Microbiol. ...*, vol. 15, pp. 119–136, 1994.

[122] M. Ronteltap, M. Maurer, R. Hausherr, and W. Gujer, "Struvite precipitation from urine - Influencing factors on particle size.," *Water Res.*, vol. 44, no. 6, pp. 2038–2046, Mar. 2010.

[123] A. Triger, J.-S. Pic, and C. Cabassud, "Determination of struvite crystallization mechanisms in urine using turbidity measurement.," *Water Res.*, vol. 46, no. 18, pp. 6084–94, Nov. 2012.

[124] C.-C. Wang, X.-D. Hao, G.-S. Guo, and M. C. M. van Loosdrecht, "Formation of pure struvite at neutral pH by electrochemical deposition," *Chem. Eng. J.*, vol. 159, pp. 280–283, May 2010.

[125] S. Moussa, G. Maurin, C. Gabrielli, and M. Ben Amor, "Electrochemical Precipitation of Struvite," *Electrochem. Solid-State Lett.*, vol. 9, no. 6, pp. 97–101, 2006.

[126] K. Rabaey, G. Lissens, S. D. Siciliano, and W. Verstraete, "A microbial fuel cell capable of converting glucose to electricity at high rate and efficiency," *Biotechnol. Lett.*, vol. 25, no. 18, pp. 1531–1535, Sep. 2003.

[127] Q. Ping, B. Cohen, C. Dosoretz, and Z. He, "Long-term investigation of fouling of cation and anion exchange membranes in microbial desalination cells," *Desalination*, vol. 325, pp. 48–55, Sep. 2013.

[128] B. E. Logan, "Scaling up microbial fuel cells and other bioelectrochemical systems.," *Appl. Microbiol. Biotechnol.*, vol. 85, no. 6, pp. 1665–1671, Mar. 2010.

[129] L. Gil-Carrera, A. Escapa, P. Mehta, G. Santoyo, S. R. Guiot, A. Morán, and B. Tartakovsky, "Microbial electrolysis cell scale-up for combined wastewater treatment and hydrogen production.," *Bioresour. Technol.*, vol. 130, pp. 584–591, Feb. 2013.

[130] E. S. Heidrich, J. Dolfing, K. Scott, S. R. Edwards, C. Jones, and T. P. Curtis, "Production of hydrogen from domestic wastewater in a pilot-scale microbial electrolysis cell," *Appl. Microbiol. Biotechnol.*, vol. 97, no. 15, pp. 6979–6989, Aug. 2013.

[131] D. J. Batstone, J. Keller, I. Angelidaki, S. V Kalyuzhnyi, S. G. Pavlostathis, a Rozzi, W. T. M. Sanders, H. Siegrist, and V. a Vavilin, "The IWA

Anaerobic Digestion Model No 1 (ADM1).," *Water Sci. Technol.*, vol. 45, no. 10, pp. 65–73, Jan. 2002.

[132] International Water Assocation, "Anaerobic digestion model No. 1 (ADM1)," 2002.

[133] S. Pavlostathis and E. Giraldo-Gomez, "Kinetics of anaerobic treatment," *Water Sci. Technol.*, vol. 24, no. 8, pp. 35–59, 1991.

[134] S. Pavlostathis, T. Miller, and M. Wolin, "Cellulose fermentation by continuous cultures of Ruminococcus albus and Methanobrevibacter smithii," *Appl. Microbiol. Biotechnol.*, vol. 33, pp. 109–116, 1990.

[135] A. Lawrence and P. McCarty, "Kinetics of methane fermentation in anaerobic treatment," *J. (Water Pollut. Control Fed.*, vol. 41, no. 2, pp. R1–R17, 1969.

[136] Y. Kim and B. E. Logan, "Simultaneous removal of organic matter and salt ions from saline wastewater in bioelectrochemical systems," *Desalination*, vol. 308, pp. 115–121, Jan. 2013.

[137] G. Chen, F. Zhang, B. E. Logan, and M. a. Hickner, "Poly(vinyl alcohol) separators improve the coulombic efficiency of activated carbon cathodes in microbial fuel cells," *Electrochem. commun.*, vol. 34, pp. 150–152, Sep. 2013.